

Supplementary Data

Inhibitor structure-guided design and synthesis of near-infrared fluorescent probe for Monoamine Oxidase A (MAO-A) and its application in living cells and *in vivo*

Zhengmin Yang,^{a,b} Wenxiu Li,^a Hua Chen,^a Qingyuan Mo,^a Jun Li,^{a*} Shulin Zhao,^a
Cheng Hou,^a Jiangke Qin,^{a*} Guifa Su^a

^a State Key Laboratory for the Chemistry and Molecular Engineering of Medicinal Resources, School of Chemistry and Pharmaceutical Sciences, Guangxi Normal University, Guilin 541004, PR China

^b Qiannan Medical College for Nationalities, Duyun, 558000, PR China

E-mail: lijun9593@163.com; jiangkeq@sina.com

Table of Contents

Experimental.....	S3
Syntheses of compounds.....	S5
Table S1.....	S13
Table S2.....	S15
Fig. S1.....	S16
Table S3.....	S17
Fig. S2.....	S17
Fig. S3.....	S18
Fig. S4.....	S18
Fig. S5.....	S19
Fig. S6.....	S19
Fig. S7.....	S20
Fig. S8.....	S20
Fig. S9.....	S21
Fig. S10.....	S22
Fig. S11.....	S22
Fig. S12.....	S23
Fig. S13.....	S24
Fig. S14.....	S24
Fig. S15.....	S25
Fig. S16.....	S25
Fig. S17.....	S26
¹ H-NMR, ¹³ C-NMR and ¹⁹ F-NMR spectra.....	S27
References.....	S53

Experimental

Apparatus and reagents

The ^1H , ^{13}C and ^{19}F -NMR spectra were recorded on a Bruker AVANCE III 400 WB spectrometer (Me_4Si as internal standard). HRMS spectra were recorded with Micromass QTOF2 Quadrupole/Time-of-Flight Tandem mass spectrometer using electron spray ionization. Absorption spectra were collected on a Varian Cary 500 spectrophotometer, and fluorescence spectra measurements were performed on a Varian Cary Eclipse fluorescence spectrophotometer. HPLC analysis was performed on an Agilent 1200 series. Confocal fluorescence images were taken on confocal laser scanning microscope (LSM710, Zeiss). Zebrafish fluorescence images were taken on BioTek Cytation5. *In vivo* tumor imaging was performed on a Kodak in vivo FX Pro imaging system (Bruker), the fluorescence images were analyzed using the Bruker Molecular Imaging (BMI) Software.

Unless special stated, all chemicals and solvents were commercially obtained from commercial suppliers and used without further purification. Vitamin B6, arginine, serine, glutamic acid, alanine, cysteine, glutathione, urea, creatinine, carboxylesterase, clorgyline, and 3-(4,5-dimethyl-2-thiazolyl)-2,5-diphenyl-2H-tetrazolium bromide (MTT), all kinds of metal salts, human recombinant Monoamine Oxidase A (M7316) and B (M7441) (5 mg/ml) purchased from Sigma-Aldrich. Acetone- d_6 ($\text{C}_3\text{D}_6\text{O}-d_6$), dimethyl sulfoxide- d_6 (DMSO- d_6) and reduced glutathione (GSH) were obtained from J&K Scientific Ltd. Phosphate buffered saline (PBS: 10 mM, pH 7.4) were purchased from Invitrogen. Reactive oxygen species (ROS) including NO_3^- , NO_2^- , TBHP, H_2O_2 , $\cdot\text{OH}$, O_2^- , ClO^- , benzoyl peroxide, GSNO and S^{2-} were prepared following the reported methods.¹ The cells lines (SH-SY5Y, HepG2 and NIH-3T3) were obtained from KeyGEN BioTECH Co., Ltd. (Nanjing, China). Zebrafishes were provided by Eze-Rinka (Nanjing). BALB/c nude mice were supplied by Hunan SJA Laboratory Animal Co., Ltd.

General spectral analysis for MAO

The stock solutions (1 mM) of probes were prepared in DMSO, which was diluted with PBS buffer (10 mM, pH 7.4) to required concentrations (10 μM) for absorbance or fluorescence spectra measurements. The absorbance and fluorescence spectrum changes of the reaction system (PBS/DMSO = 7:3 v:v, pH = 7.4, 37 °C) upon the addition of an appropriate volume of MAO (MAO-A or MAO-B) and/or other analytes were measured by an ultraviolet analyzer and a fluorimeter (excitation wavelength: 530 nm, excitation and emission slit widths: 10 nm). Data are expressed as mean standard deviation (SD) of three separate measurements.

Theoretical Calculations

All calculations were performed using Gaussian 16 program Rev. A.03; geometry optimizations were carried out with M06-2X/Def2-SVP level of theory.² The 3D optimized structure figures and molecular in this paper were displayed by IQmol visualization program.

Cell incubation, viability assay and imaging

SH-SY5Y, HepG2 and NIH-3T3 cells were incubated in complete medium

composed of DMEM medium (LO2) with 10% fetal bovine serum (FBS) and 1% penicillin & streptomycin at 37 °C in a humidified incubator containing 5% CO₂.

The cytotoxicity was investigated using an MTT assay. For the cytotoxicity experiment, SH-SY5Y, HepG2 and NIH-3T3 were seeded in 96-well plates and maintained at 37 °C for 24 h. The cells were incubated with the probe 3 or 3c with different concentrations of 0, 1, 3, 5, 7 and 10 μM (containing 1% DMSO) for another 24 hours, respectively. Then, MTT was added to each cell well, incubation for 4 h. An enzyme linked immunosorbent assay reader was employed to measure the absorbance of samples. In these experiments, the assays were performed in five replicates for each independent experiment.

For fluorescence imaging, the cells were incubated with 10 μM of probe 3 in FBS-free DMEM at 37 °C for 2 h, and then washed twice with DMEM to remove the free probe. Fluorescence imaging was conducted with an excitation wavelength of 530 nm and was collected in the range of 650-750 nm. The results are the mean standard deviation of three separate measurements.

Zebrafish viability assay and imaging

Zebrafish larvae (5 day postfertilization) were transferred to a 6-well microplate at the zebrafish larvae population of 20 larvae/well, and then the E3 media was substituted with fresh E3 media (2 mL) containing the probe 3 or 3c (concentration: 0, 1, 3, 5, 7, 10 μM) and incubated for 96 h at 28 °C. Tests were performed in triplicate and repeated twice (totally 120 larvae per concentration). The survival rate is expressed as the percentage of total number of survival larvae over total number of larvae after 96 h of incubation.

Zebrafish larvae (3-day-old or 5-day-old) were transferred to a 6-well microplate and incubated with E3 media which contained 20 μM of the probe 3 for 120 min at 28 °C, after that the media solution was discarded, and the larvae were washed with E3 media for three times. Finally the zebrafishes were subjected to fluorescence imaging.

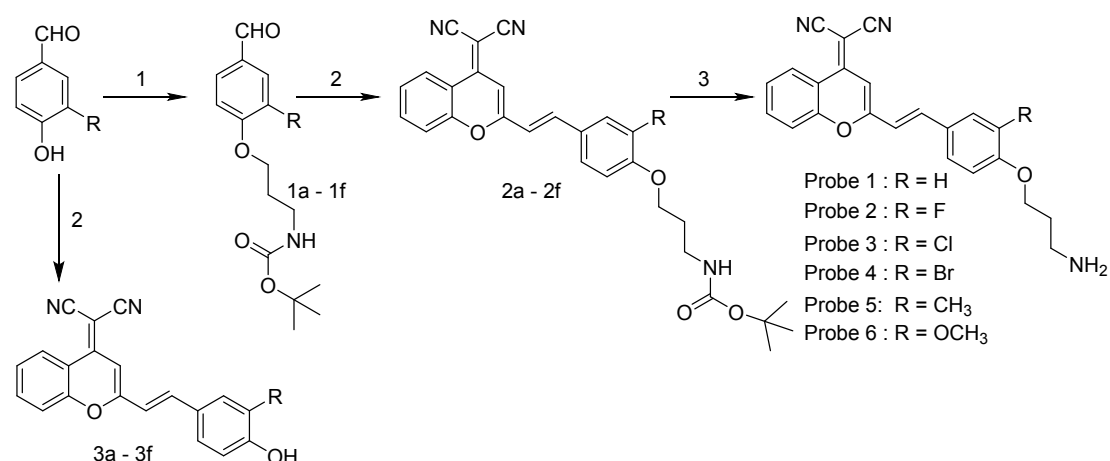
Tumour-bearing mice model

BALB/c nude mice were supplied by Hunan SJA Laboratory Animal Co., Ltd. All surgical procedures were conducted conforming with National Guidelines for the Care and Use of Laboratory Animals, and the experimental protocols were approved by the Animal Ethics Committee of Guangxi Normal University, Guilin, China. Approval Number: No. 20150325-XC. BALB/c nude mice (4-6 weeks) were chosen and given subcutaneous injection of 2×10⁶ SH-SY5Y cells on the right oxtar to construct the tumor model.

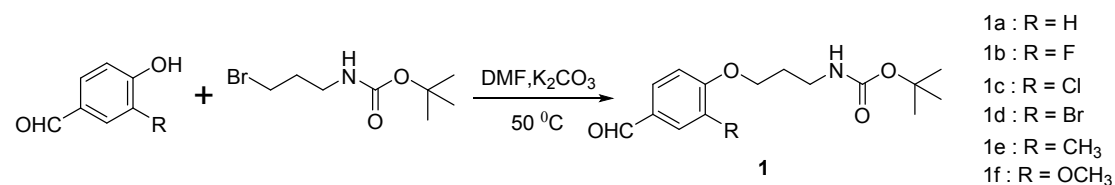
Fluorescent imaging of tumor and organs

By the time the tumor had grown for 2 weeks, the tumor-bearing mice were intratumorally injected with or without probe 3 (100 μM, 100μL). In the tumor site after in situ injection of probe 3 for different time, bright-field photos and fluorescent images were obtained by a fluorescence imaging system [Kodak in vivo FX Pro imaging system (Bruker)] with excitation filter of 530 nm and emission filter of 700 nm. After 2 h, the injected mice were sacrificed with CO₂, subsequently the tumor and other main organs were excised, then fluorescence imaging.

Syntheses of compounds



Scheme S1 Synthesis of probe 1-6. 1. Tert-butyl(3-bromopropyl) carbamate, DMF, K_2CO_3 , 50 °C; 2. 2-(2-methyl-4H-chromen-4-ylidene) malononitrile, toluene, piperidine and acetic acid, 110 °C; 3. Trifluoroacetic acid, 0 °C.



1a: A mixture of 4-hydroxybenzaldehyde (0.24 g, 2 mmol), K_2CO_3 (0.83 g, 6 mmol), tert-butyl(3-bromopropyl) carbamate (0.59 g, 2.5 mmol) in dry 5 mL DMF was stirred for 10 h at 50 °C under N_2 atmosphere. Then, the mixture was diluted with ethyl acetate (40 mL), and washed three times with water (40 mL). The organic layer was separated and dried over anhydrous Na_2SO_4 . The solvent was removed by evaporation under reduced pressure, and the residue was subjected to silica gel chromatography with AcOEt : PE (1 : 4) as eluent, obtaining **1a** as a white solid (0.46 g, yield 78%). The 1H -NMR and ^{13}C -NMR spectra of **1a** are shown below in Fig. S18 and S19, respectively. 1H -NMR (400 MHz, DMSO- d_6): δ 9.86 (s, 1H), 7.85 (d, J = 8.8 Hz, 2H), 7.10 (d, J = 8.8 Hz, 2H), 4.09 (t, J = 6.3 Hz, 2H), 3.09 (m, 2H), 1.85 (m, 2H), 1.36 (s, 9H). ^{13}C -NMR (100 MHz, DMSO- d_6): δ 191.7, 164.1, 132.3 (2C), 130.0, 115.4 (2C), 78.0, 66.3, 37.3, 29.5, 28.7 (2C). HRMS (ESI) m/z calcd for $C_{15}H_{21}NO_4$ ($M+Na$)⁺: 302.1368, Found: 302.1361.

1b: **1b**, prepared similarly as **1a** using 3-fluoro-4-hydroxybenzaldehyde (0.28 g, 2 mmol), K_2CO_3 (0.83 g, 6 mmol), and tert-butyl(3-bromopropyl) carbamate (0.59 g, 2.5 mmol), was obtained as a white solid (0.52 g, yield 87%). The 1H -NMR, ^{13}C -NMR and ^{19}F -NMR spectra of **1b** are shown below in Fig. S20, S21 and S22, respectively. 1H -NMR (400 MHz, DMSO- d_6): δ 9.86 (d, J = 2.0 Hz, 1H), 7.75 (t, J = 8.4 Hz, 1H), 7.67 (dd, J = 1.9, 11.3 Hz, 1H), 7.35 (t, J = 8.2 Hz, 1H), 6.91 (t, J = 5.3

Hz, 1H), 4.17 (t, $J = 6.2$ Hz, 2H), 3.10 (dd, $J = 6.6, 12.7$ Hz, 2H), 1.88 (t, $J = 6.5$ Hz, 2H), 1.36 (s, 9H). $^{13}\text{C-NMR}$ (100 MHz, $\text{DMSO-}d_6$): δ 191.3 (d, $J = 1.8$ Hz), 156.1, 153.4, 152.4 (d, $J = 10.9$ Hz), 150.9, 130.0 (d, $J = 5.0$ Hz), 128.8 (d, $J = 2.6$ Hz), 115.7 (d, $J = 18.1$ Hz), 114.9, 78.0, 67.3, 37.2, 29.4, 28.7 (3C). $^{19}\text{F-NMR}$ (400 MHz, $\text{DMSO-}d_6$): δ -133.76. HRMS (ESI) m/z calcd for $\text{C}_{15}\text{H}_{20}\text{FNO}_4$ ($\text{M}+\text{Na}$) $^+$: 320.1274, Found: 320.1266.

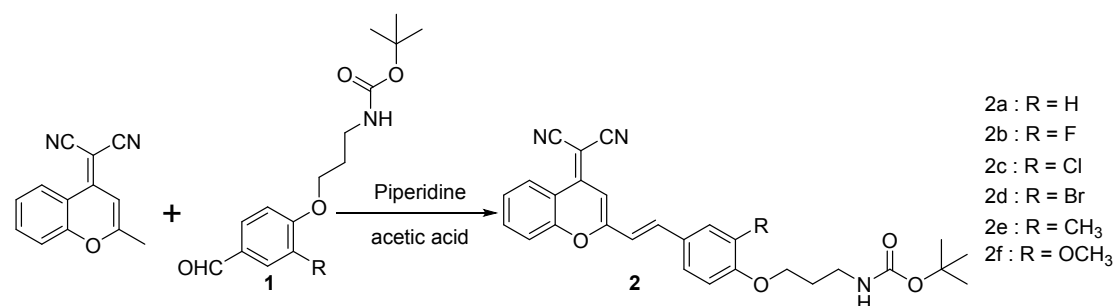
1c: 1c, prepared similarly as **1a** using 3-chloro-4-hydroxybenzaldehyde (0.31 g, 2 mmol), K_2CO_3 (0.83 g, 6 mmol), and tert-butyl(3-bromopropyl) carbamate (0.59 g, 2.5 mmol), was obtained as a white solid (0.51 g, yield 81%). The $^1\text{H-NMR}$, $^{13}\text{C-NMR}$ spectra of **1c** are shown below in Fig. S23 and S24, respectively. $^1\text{H-NMR}$ (400 MHz, $\text{DMSO-}d_6$): δ 9.86 (s, 1H), 7.94 (d, $J = 2.0$ Hz, 1H), 7.87 (dd, $J = 2.0, 8.5$ Hz, 1H), 7.33 (d, $J = 8.5$ Hz, 1H), 6.91 (t, $J = 5.6$ Hz, 1H), 4.19 (t, $J = 6.1$ Hz, 2H), 3.13 (dd, $J = 6.6, 12.6$ Hz, 2H), 1.89 (t, $J = 6.4$ Hz, 2H), 1.36 (s, 9H). $^{13}\text{C-NMR}$ (100 MHz, $\text{DMSO-}d_6$): δ 191.1, 159.1, 156.1, 131.1, 131.0, 130.5, 122.7, 114.1, 78.0, 67.6, 37.2, 29.4, 28.7(3C). HRMS (ESI) m/z calcd for $\text{C}_{15}\text{H}_{20}\text{ClNO}_4$ ($\text{M}+\text{Na}$) $^+$: 336.0973, Found: 336.0959.

1d: 1d, prepared similarly as **1a** using 3-bromo-4-hydroxybenzaldehyde (0.40 g, 2 mmol), K_2CO_3 (0.83 g, 6 mmol), and tert-butyl(3-bromopropyl) carbamate (0.59 g, 2.5 mmol), was obtained as a white solid (0.54 g, yield 76%). The $^1\text{H-NMR}$, $^{13}\text{C-NMR}$ spectra of **1d** are shown below in Fig. S25 and S26, respectively. $^1\text{H-NMR}$ (400 MHz, $\text{DMSO-}d_6$): δ 9.84 (s, 1H), 8.08 (d, $J = 3.6$ Hz, 1H), 7.90 (dd, $J = 2.0, 8.5$ Hz, 1H), 7.27 (d, $J = 8.5$ Hz, 1H), 6.90 (t, $J = 5.3$ Hz, 1H), 4.17 (t, $J = 6.1$ Hz, 2H), 3.13 (dd, $J = 6.6, 12.6$ Hz, 2H), 1.88 (t, $J = 6.4$ Hz, 2H), 1.36 (s, 9H). $^{13}\text{C-NMR}$ (100 MHz, $\text{DMSO-}d_6$): δ : 191.0, 160.0, 156.1, 134.4, 131.7, 130.9, 113.9, 112.2, 78.0, 67.6, 37.3, 29.4, 28.7 (3C). HRMS (ESI) m/z calcd for $\text{C}_{15}\text{H}_{20}\text{BrNO}_4$ ($\text{M}+\text{Na}$) $^+$: 380.1755, Found: 380.0473.

1e: 1e, prepared similarly as **1a** using 3-methyl-4-hydroxybenzaldehyde (0.27 g, 2 mmol), K_2CO_3 (0.83 g, 6 mmol), and tert-butyl(3-bromopropyl) carbamate (0.59 g, 2.5 mmol), was obtained as a white solid (0.43 g, yield 73%). The $^1\text{H-NMR}$, $^{13}\text{C-NMR}$ spectra of **1e** are shown below in Fig. S27 and S28, respectively. $^1\text{H-NMR}$ (400 MHz, $\text{DMSO-}d_6$): δ 9.82 (s, 1H), 7.74 (dd, $J = 2.0, 8.4$ Hz, 1H), 7.67 (s, 1H), 7.09 (d, $J = 8.4$ Hz, 1H), 6.90 (t, $J = 5.3$ Hz, 1H), 4.09 (t, $J = 6.1$ Hz, 2H), 3.13 (dd, $J = 6.6, 12.6$ Hz, 2H), 2.20 (s, 3H), 1.87 (t, $J = 6.4$ Hz, 2H), 1.36 (s, 9H). $^{13}\text{C-NMR}$ (100 MHz, $\text{DMSO-}d_6$): δ 191.8, 162.3, 156.1, 131.3, 131.2, 129.5, 127.3, 111.6, 78.0, 66.3, 37.4, 29.5, 28.7 (3 C), 16.3. HRMS (ESI) m/z calcd for $\text{C}_{16}\text{H}_{23}\text{NO}_4$ ($\text{M}+\text{Na}$) $^+$: 316.1525, Found: 316.1518.

1f: 1f, prepared similarly as **1a** using 3-methoxy-4-hydroxybenzaldehyde (0.30 g, 2 mmol), K_2CO_3 (0.83 g, 6 mmol), and tert-butyl(3-bromopropyl) carbamate (0.59 g, 2.5 mmol), was obtained as a white solid (0.45 g, yield 73%). The $^1\text{H-NMR}$, $^{13}\text{C-NMR}$ spectra of **1f** are shown below in Fig. S29 and S30, respectively. $^1\text{H-NMR}$ (400 MHz, $\text{DMSO-}d_6$): δ 9.83 (s, 1H), 7.54 (dd, $J = 2.3, 8.2$ Hz, 1H), 7.39 (d, $J = 1.9$ Hz, 1H), 7.14 (d, $J = 8.2$ Hz, 1H), 6.88 (t, $J = 5.3$ Hz, 1H), 4.08 (t, $J = 6.2$ Hz, 2H), 3.83 (s, 3H), 3.12 (dd, $J = 6.6, 12.6$ Hz, 2H), 1.86 (t, $J = 6.4$ Hz, 2H), 1.37 (s, 9H). $^{13}\text{C-NMR}$ (100 MHz, $\text{DMSO-}d_6$): δ 191.8, 156.1, 154.0, 149.7, 130.1, 126.5, 112.5, 110.1, 78.0,

67.0, 56.0, 37.6, 29.5, 28.7 (3C). HRMS (ESI) m/z calcd for $C_{16}H_{23}NO_5$ ($M+Na$) $^+$: 332.1474, Found: 332.1465.



2a: A mixture of 2-(2-Methyl-4H-chromen-4-ylidene) malononitrile (0.21 g, 1 mmol), **1a** (0.28 g, 1 mmol) in dry 30 mL toluene. After adding piperidine (1.0 mL) and acetic acid (1.0 mL), the solution was stirred for 12 h at 110 °C under N_2 atmosphere. The mixture was cooled to room temperature and the solvent removed under vacuum. The residue was subjected to silica gel chromatography with CH_2Cl_2 : CH_3OH (30 : 1) as eluent, obtaining **2a** as a red solid (0.32 g, yield 68%). The 1H -NMR and ^{13}C -NMR spectra of **2a** are shown below in Fig. S31 and S32, respectively. 1H -NMR (400 MHz, $DMSO-d_6$): δ 8.70 (dd, $J = 8.4, 1.2$ Hz, 1H), 7.90 (t, $J = 7.8$ Hz, 1H), 7.76 (d, $J = 8.5$ Hz, 1H), 7.70 (d, $J = 8.8$ Hz, 2H), 7.58 (dd, $J = 7.6, 6.6$ Hz, 1H), 7.32 (d, $J = 16.0$ Hz, 1H), 7.00 (d, $J = 8.8$ Hz, 2H), 6.94 (s, 1H), 4.04 (t, $J = 6.3$ Hz, 2H), 3.10 (d, $J = 6.1$ Hz, 2H), 1.93 – 1.77 (m, 2H), 1.38 (s, 9H). ^{13}C -NMR (100 MHz, $DMSO-d_6$): δ 161.1, 159.1, 156.2, 153.3, 152.5, 139.2, 135.8, 130.5 (2C), 128.0, 126.5, 125.1, 119.5, 117.8, 117.6, 117.4, 116.4, 115.5 (2C), 106.5, 78.1, 66.1, 60.0, 37.4, 29.6, 28.8 (3C). HRMS (ESI) m/z calcd for $C_{28}H_{28}N_3O_4$ ($M+H$) $^+$: 470.2074, Found: 470.2079.

2b: **2b** prepared similarly as **2a** using 2-(2-Methyl-4H-chromen-4-ylidene) malononitrile (0.21 g, 1 mmol), **1b** (0.28 g, 1 mmol) was obtained as a red solid (0.34 g, yield 70%). The 1H -NMR, ^{13}C -NMR and ^{19}F -NMR spectra of **2b** are shown below in Fig. S33, S34 and S35, respectively. 1H -NMR (400 MHz, $DMSO-d_6$): δ 8.62 (dd, $J = 8.4, 1.3$ Hz, 1H), 7.86 (dd, $J = 8.5, 1.4$ Hz, 1H), 7.65 (dd, $J = 8.4, 1.0$ Hz, 1H), 7.59 (dd, $J = 12.7, 1.9$ Hz, 1H), 7.54 (d, $J = 5.0$ Hz, 1H), 7.51 (s, 1H), 7.41 (d, $J = 8.5$ Hz, 1H), 7.27 (d, $J = 16.0$ Hz, 1H), 7.13 (t, $J = 8.7$ Hz, 1H), 6.83 (s, 1H), 4.08 (t, $J = 6.2$ Hz, 2H), 3.10 (q, $J = 6.6$ Hz, 2H), 1.87 (m, 2H), 1.38 (s, 9H). ^{13}C -NMR (100 MHz, $DMSO-d_6$): δ 158.5, 156.1, 153.4, 153.0, 152.3, 150.9, 148.8 (d, $J = 10.9$ Hz), 137.8, 135.8, 128.6 (d, $J = 6.9$ Hz), 126.5, 125.0, 119.4, 118.9, 117.5, 117.4, 116.2, 115.0 (d, $J = 4.3$ Hz), 114.8, 106.8, 78.00, 67.0, 60.5, 37.3, 29.5, 28.7 (3C). ^{19}F -NMR (400 MHz, $DMSO-d_6$): δ -134.11. HRMS (ESI) m/z calcd for $C_{28}H_{27}FN_3O_4$ ($M+H$) $^+$: 488.1980, Found: 488.1985.

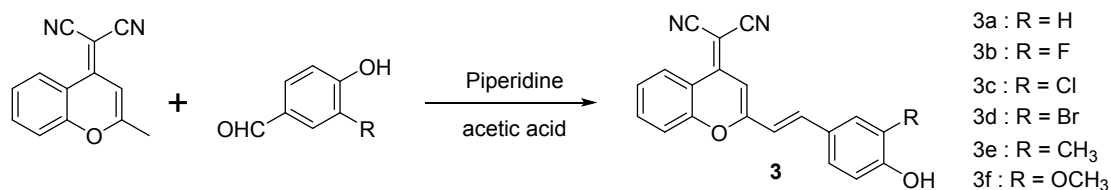
2c: **2c** prepared similarly as **2a** using 2-(2-Methyl-4H-chromen-4-ylidene) malononitrile (0.21 g, 1 mmol), **1c** (0.31 g, 1 mmol) was obtained as a red solid (0.35 g, yield 70%). The 1H -NMR and ^{13}C -NMR spectra of **2c** are shown below in Fig. S36 and S37, respectively. 1H -NMR (400 MHz, $DMSO-d_6$): δ 8.65 (dd, $J = 8.4, 1.2$ Hz, 1H), 7.91 – 7.84 (m, 1H), 7.82 (d, $J = 1.9$ Hz, 1H), 7.67 (dd, $J = 8.4, 0.9$ Hz, 1H), 7.58 (t, $J = 9.9$ Hz, 2H), 7.53 (s, 1H), 7.34 (d, $J = 16.0$ Hz, 1H), 7.13 (d, $J = 8.7$ Hz, 1H),

6.87 (s, 1H), 4.11 (t, $J = 6.1$ Hz, 2H), 3.13 (dd, $J = 12.6, 6.6$ Hz, 2H), 1.93 – 1.81 (m, 2H), 1.38 (s, 9H). ^{13}C -NMR (100 MHz, DMSO- d_6): δ 158.5, 156.1, 155.8, 153.1, 152.3, 137.5, 135.8, 129.5, 129.4, 129.0, 126.5, 125.0, 122.7, 119.4, 118.9, 117.6, 117.5, 116.2, 114.2, 106.9, 78.0, 67.2, 60.5, 37.4, 29.5, 28.7 (3C). HRMS (ESI) m/z calcd for $\text{C}_{28}\text{H}_{26}\text{ClN}_3\text{O}_4$ (M+Na) $^+$: 526.1504, Found: 526.1486.

2d: **2d** prepared similarly as **2a** using 2-(2-Methyl-4H-chromen-4-ylidene) malononitrile (0.21 g, 1 mmol), **1d** (0.36 g, 1 mmol) was obtained as a red solid (0.38 g, yield 69%). The ^1H -NMR and ^{13}C -NMR spectra of **2d** are shown below in Fig. S38 and S39, respectively. ^1H -NMR (400 MHz, DMSO- d_6): δ 8.67 (dd, $J = 8.4, 1.2$ Hz, 1H), 8.00 (d, $J = 2.0$ Hz, 1H), 7.93 – 7.85 (m, 1H), 7.69 (dd, $J = 8.4, 1.0$ Hz, 1H), 7.65 (dd, $J = 8.7, 1.9$ Hz, 1H), 7.61 – 7.54 (m, 2H), 7.37 (d, $J = 16.0$ Hz, 1H), 7.12 (d, $J = 8.7$ Hz, 1H), 6.90 (s, 1H), 4.11 (t, $J = 6.1$ Hz, 2H), 3.14 (dd, $J = 12.6, 6.6$ Hz, 2H), 1.92 – 1.84 (m, 2H), 1.39 (s, 9H). ^{13}C -NMR (100 MHz, DMSO- d_6): δ 158.6, 156.7, 156.1, 153.2, 152.4, 137.4, 135.8, 132.5, 130.1, 129.5, 126.5, 125.1, 119.4, 118.8, 117.6, 117.5, 116.3, 114.0, 112.4, 106.9, 78.0, 67.3, 60.5, 37.4, 29.5, 28.7 (3C). HRMS (ESI) m/z calcd for $\text{C}_{28}\text{H}_{26}\text{BrN}_3\text{O}_4$ (M+Na) $^+$: 570.0999, Found: 570.0971.

2e: **2e** prepared similarly as **2a** using 2-(2-Methyl-4H-chromen-4-ylidene) malononitrile (0.21 g, 1 mmol), **1e** (0.29 g, 1 mmol) was obtained as a red solid (0.31 g, yield 64%). The ^1H -NMR and ^{13}C -NMR spectra of **2e** are shown below in Fig. S40 and S41, respectively. ^1H -NMR (400 MHz, DMSO- d_6): δ 8.66 (dd, $J = 8.4, 1.3$ Hz, 1H), 7.88 (dd, $J = 8.5, 1.4$ Hz, 1H), 7.71 (dd, $J = 8.4, 1.0$ Hz, 1H), 7.58 (d, $J = 4.1$ Hz, 1H), 7.55 (t, $J = 3.6$ Hz, 1H), 7.54 – 7.52 (m, 1H), 7.47 (dd, $J = 8.5, 1.8$ Hz, 1H), 7.22 (d, $J = 15.9$ Hz, 1H), 6.93 (d, $J = 8.6$ Hz, 1H), 6.86 (s, 1H), 4.03 (t, $J = 6.1$ Hz, 2H), 3.13 (q, $J = 6.6$ Hz, 2H), 2.15 (s, 3H), 1.94 – 1.82 (m, 2H), 1.38 (s, 9H). ^{13}C -NMR (100 MHz, DMSO- d_6): δ 159.3, 159.1, 156.1, 153.1, 152.4, 139.3, 135.6, 130.3, 128.9, 127.4, 127.05, 126.4, 125.0, 119.4, 117.8, 117.5, 117.0, 116.4, 111.8, 106.3, 77.9, 66.0, 59.7, 37.4, 29.6, 28.7(3C), 16.4. HRMS (ESI) m/z calcd for $\text{C}_{29}\text{H}_{29}\text{N}_3\text{O}_4$ (M+Na) $^+$: 506.2056, Found: 506.2047.

2f: **2f** prepared similarly as **2a** using 2-(2-Methyl-4H-chromen-4-ylidene) malononitrile (0.21 g, 1 mmol), **1f** (0.31 g, 1 mmol) was obtained as a red solid (0.29 g, yield 58%). The ^1H -NMR and ^{13}C -NMR spectra of **2f** are shown below in Fig. S42 and S43, respectively. ^1H -NMR(400 MHz, DMSO- d_6): δ 8.70 (d, $J = 8.3$ Hz, 1H), 7.90 (t, $J = 7.8$ Hz, 1H), 7.75 (d, $J = 8.4$ Hz, 1H), 7.66 (d, $J = 15.9$ Hz, 1H), 7.58 (t, $J = 7.8$ Hz, 1H), 7.42 – 7.31 (m, 2H), 7.24 (d, $J = 8.3$ Hz, 1H), 6.99 (d, $J = 8.4$ Hz, 1H), 6.91 (s, 1H), 4.03 (t, $J = 6.2$ Hz, 2H), 3.11 (dd, $J = 12.6, 6.5$ Hz, 2H), 1.91 – 1.81 (m, 2H), 1.39 (s, 9H). ^{13}C -NMR (100 MHz, DMSO- d_6): δ 159.1, 156.1, 153.3, 152.5, 150.9, 149.7, 139.6, 135.8, 128.3, 126.5, 125.1, 123.8, 119.4, 117.8, 117.6, 117.5, 116.5, 113.0, 110.5, 106.4, 78.0, 66.8, 59.9, 56.1, 37.6, 29.6, 28.7 (3C). HRMS (ESI) m/z calcd for $\text{C}_{29}\text{H}_{29}\text{N}_3\text{O}_5$ (M+Na) $^+$: 522.2005, Found: 522.1996.



3a: A mixture of 2-(2-Methyl-4H-chromen-4-ylidene) malononitrile (208 mg, 1 mmol), 4-hydroxybenzaldehyde (0.12 g, 1 mmol) in dry 30 mL toluene. After adding piperidine (1.0 mL) and acetic acid (1.0 mL), the solution was stirred for 12 h at 110 °C under N₂ atmosphere. The mixture was cooled to room temperature and the solvent removed under vacuum. The residue was subjected to silica gel chromatography with CH₂Cl₂ : CH₃OH (30 : 1) as eluent, obtaining **3a** as a red solid (0.17 g, yield 55%). The ¹H-NMR and ¹³C-NMR spectra of **3a** are shown below in Fig. S44 and S45, respectively. ¹H-NMR (400 MHz, Acetone): δ 9.02 (s, 1H), 8.85 (dd, *J* = 8.4, 1.3 Hz, 1H), 7.90 (ddd, *J* = 8.5, 7.2, 1.4 Hz, 1H), 7.79 – 7.72 (m, 2H), 7.66 (d, *J* = 8.6 Hz, 2H), 7.61 – 7.56 (m, 1H), 7.19 (d, *J* = 16.0 Hz, 1H), 6.94 (d, *J* = 8.6 Hz, 2H), 6.89 (s, 1H). ¹³C-NMR (100 MHz, Acetone): δ 207.1, 161.7, 160.6, 154.7, 154.3, 141.0, 136.8, 132.0 (2C), 128.8, 127.6, 126.9, 120.7, 119.4, 118.8, 117.8 (2C), 117.4, 107.5, 62.6. HRMS (ESI) *m/z* calcd for C₂₀H₁₂N₂O₂⁻ (M-H)⁻: 311.0826, Found: 311.0809.

3b: **3b**, prepared similarly as **3a** using 2-(2-Methyl-4H-chromen-4-ylidene) malononitrile (0.21 g, 1 mmol), 3-fluoro-4-hydroxybenzaldehyde (0.14 g, 1 mmol), piperidine (1.0 mL) and acetic acid (1.0 mL), was obtained as a red solid (0.22 g, yield 66%). The ¹H-NMR, ¹³C-NMR and ¹⁹F-NMR spectra of **3b** are shown below in Fig. S46, S47 and S48, respectively. ¹H-NMR (400 MHz, DMSO-*d*₆): δ 8.65 (dd, *J* = 8.4, 1.3 Hz, 1H), 7.86 (td, *J* = 8.5, 1.4 Hz, 1H), 7.69 (dd, *J* = 8.5, 1.1 Hz, 2H), 7.52-7.59 (m, 3H), 7.33 (dd, *J* = 8.5, 1.1 Hz, 1H), 7.12 (d, *J* = 15.9 Hz, 1H), 6.93 (d, *J* = 8.6 Hz, 2H), 6.84 (s, 1H). ¹³C-NMR (100 MHz, DMSO-*d*₆): δ 158.8, 153.1, 152.9, 152.4, 150.5, 148.0 (d, *J* = 12.4 Hz), 138.4, 135.7, 127.4 (d, *J* = 6.5 Hz), 126.6 (d, *J* = 6.4 Hz), 125.0, 119.4, 118.4 (d, *J* = 3.5 Hz), 117.9, 117.6, 117.5, 116.3, 115.6 (d, *J* = 18.6 Hz), 106.6, 60.19. ¹⁹F-NMR(400MHz, DMSO-*d*₆): δ -135.49. HRMS (ESI) *m/z* calcd for C₂₀H₁₁FN₂O₂⁻ (M-H)⁻: 329.0732, Found: 329.0714.

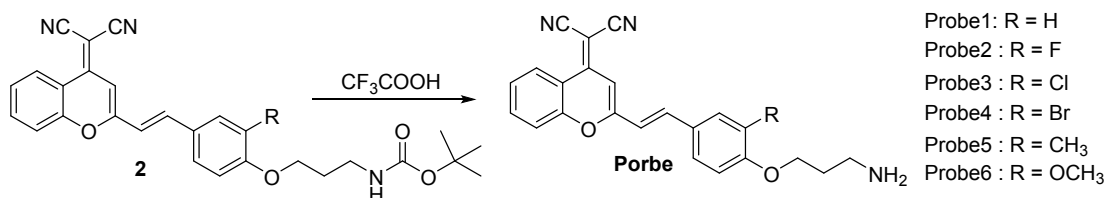
3c: **3c**, prepared similarly as **3a** using 2-(2-Methyl-4H-chromen-4-ylidene) malononitrile (0.21 g, 1 mmol) and 3-chloro-4-hydroxybenzaldehyde (0.16 g, 1 mmol) was obtained as a red solid (0.25 g, yield 72%). The ¹H-NMR and ¹³C-NMR spectra of **3c** are shown below in Fig. S49 and S50, respectively. ¹H-NMR (400 MHz, DMSO-*d*₆): δ 10.86 (s, 1H), 8.70 (d, *J* = 8.0 Hz, 1H), 7.89 (t, *J* = 7.3 Hz, 1H), 7.82 (s, 1H), 7.73 (d, *J* = 8.0 Hz, 1H), 7.51-7.63 (m, 3H), 7.36 (d, *J* = 15.9 Hz, 1H), 7.02 (d, *J* = 8.3 Hz, 1H), 6.93 (s, 1H). ¹³C-NMR (100 MHz, DMSO-*d*₆): δ 158.8, 155.7, 153.1, 152.4, 138.0, 135.7, 129.9, 129.3, 127.8, 126.5, 125.0, 121.1, 119.4, 117.9, 117.7, 117.5, 117.3, 116.3, 106.6, 60.2. HRMS (ESI) *m/z* calcd for C₂₀H₁₂ClN₂O₂⁻ (M-H)⁻: 345.0436, Found: 345.0418.

3d: **3d**, prepared similarly as **3a** using 2-(2-Methyl-4H-chromen-4-ylidene) malononitrile (0.21 g, 1 mmol) and 3-bromo-4-hydroxybenzaldehyde (0.20 g, 1 mmol) was obtained as a red solid (0.26 g, yield 67%). The ¹H-NMR and ¹³C-NMR spectra of **3d** are shown below in Fig. S51 and S52, respectively. ¹H-NMR (400 MHz, DMSO-*d*₆): δ 10.86 (s, 1H), 8.70 (d, *J* = 8.0 Hz, 1H), 7.89 (t, *J* = 7.3 Hz, 1H), 7.82 (s, 1H), 7.73 (d, *J* = 8.0 Hz, 1H), 7.51-7.63 (m, 3H), 7.36 (d, *J* = 15.9 Hz, 1H), 7.02 (d, *J* = 8.3 Hz, 1H), 6.93 (s, 1H). ¹³C-NMR (100 MHz, DMSO-*d*₆): δ 158.8, 156.7, 153.2, 152.4, 137.9, 135.8, 133.0, 130.0, 128.3, 126.5, 125.1, 119.4, 117.9, 117.7, 117.5, 117.1, 116.4, 110.8, 106.7, 60.2. HRMS (ESI) *m/z* calcd for C₂₀H₁₁BrN₂O₂⁻ (M-H)⁻:

388.9931, Found: 388.9915.

3e: **3e**, prepared similarly as **3a** using 2-(2-Methyl-4H-chromen-4-ylidene) malononitrile (0.21 g, 1 mmol) and 3-methyl-4-hydroxybenzaldehyde (0.14 g, 1 mmol) was obtained as a red solid (0.21 g, yield 64%). The ¹H-NMR and ¹³C-NMR spectra of **3e** are shown below in Fig. S53 and S54, respectively. ¹H-NMR (400 MHz, DMSO-*d*₆): δ 10.05 (s, 1H), 8.67 (d, *J* = 7.7 Hz, 1H), 7.86 (t, *J* = 7.3 Hz, 1H), 7.71 (t, *J* = 8.0 Hz, 1H), 7.57 (d, *J* = 6.2 Hz, 1H), 7.54 (d, *J* = 6.2 Hz, 1H), 7.49 (s, 1H), 7.38 (d, *J* = 8.3 Hz, 1H), 7.18 (d, *J* = 15.9 Hz, 1H), 6.84 (s, 1H), 6.82 (d, *J* = 8.3 Hz, 1H), 2.13 (s, 3H). ¹³C-NMR (100 MHz, DMSO-*d*₆): δ 159.4, 158.8, 153.2, 152.4, 139.9, 135.6, 131.2, 128.7, 126.4, 126.4, 125.3, 125.0, 119.4, 117.9, 117.5, 116.5, 116.0, 115.5, 106.0, 59.4, 16.4. HRMS (ESI) *m/z* calcd for C₂₁H₁₄N₂O₂⁻ (M-H)⁻: 325.0983, Found: 327.0965.

3f: **3f**, prepared similarly as **3a** using 2-(2-Methyl-4H-chromen-4-ylidene) malononitrile (0.21 g, 1 mmol) and 3-methoxy-4-hydroxybenzaldehyde (0.14 g, 1 mmol) was obtained as a red solid (0.21 g, yield 64%). The ¹H-NMR and ¹³C-NMR spectra of **3f** are shown below in Fig. S55 and S56, respectively. ¹H-NMR (400 MHz, DMSO-*d*₆): δ 9.75 (s, 1H), 8.70 (dd, *J* = 1.1, 8.4 Hz, 1H), 7.88 (t, *J* = 8.4 Hz, 1H), 7.75 (d, *J* = 8.4 Hz, 1H), 7.65 (d, *J* = 15.9 Hz, 1H), 7.57 (t, *J* = 8.4 Hz, 1H), 7.39 (d, *J* = 1.6 Hz, 1H), 7.29 (d, *J* = 15.9 Hz, 1H), 7.16 (dd, *J* = 1.7, 8.2 Hz, 1H), 6.88 (s, 1H), 6.84 (d, *J* = 8.2 Hz, 1H), 3.85 (s, 3H). ¹³C-NMR (100 MHz, DMSO-*d*₆): δ 159.4, 153.3, 152.5, 150.2, 148.6, 140.1, 135.7, 127.1, 126.5, 125.1, 124.2, 119.4, 117.9, 117.6, 116.6, 116.5, 116.2, 111.1, 106.1, 59.5, 56.1. HRMS (ESI) *m/z* calcd for C₂₁H₁₄N₂O₃⁻ (M-H)⁻: 341.0932, Found: 341.0915.



Probe 1: To a solution of intermediate **2a** (0.23g, 0.5 mmol) in anhydrous CH₂Cl₂ (5 mL) at 0 °C was added a solution of trifluoroacetic acid (1.0 mL) in anhydrous CH₂Cl₂ (3 mL) dropwise. The resulting mixture was stirred at 0 °C for 2 h, and then the solvent was removed by evaporation under reduced pressure. The residue was subjected to silica chromatography with CH₂Cl₂ : CH₃OH (20 : 1) as eluent, obtaining **probe 1** as a orange solid (0.16 g, yield 86%). The ¹H-NMR and ¹³C-NMR spectra of **probe 1** are shown below in Fig. S57 and S58, respectively. ¹H-NMR (400 MHz, DMSO-*d*₆): δ 8.66 (dd, *J* = 8.3, 0.9 Hz, 1H), 7.88 (d, *J* = 8.4 Hz, 3H), 7.71 (d, *J* = 8.5 Hz, 1H), 7.65 (dd, *J* = 18.6, 12.4 Hz, 3H), 7.57 – 7.51 (m, 1H), 7.27 (d, *J* = 16.0 Hz, 1H), 7.00 (d, *J* = 8.7 Hz, 2H), 6.88 (s, 1H), 4.12 (t, *J* = 6.0 Hz, 2H), 2.99 (dd, *J* = 13.0, 6.7 Hz, 2H), 2.08 – 2.00 (m, 2H). ¹³C-NMR (100 MHz, DMSO-*d*₆): δ 160.7, 159.2, 159.0, 158.8, 153.2, 152.5, 139.0, 135.8, 130.5, 128.3, 126.5, 125.1, 119.5, 117.8, 117.6, 116.4, 115.6, 114.8, 106.5, 65.4, 60.1, 36.8, 27.3. HRMS (ESI) *m/z* calcd for C₂₃H₂₀N₃O₂⁺ (M+H)⁺: 370.1550, Found: 370.1546.

Probe 2: **probe 2** prepared similarly as **Probe 1** using **2b** (0.24g, 0.5 mmol) was obtained as a orange solid (0.18 g, yield 93%). The $^1\text{H-NMR}$, $^{13}\text{C-NMR}$ and $^{19}\text{F-NMR}$ spectra of **probe 2** are shown below in Fig. S59, S60 and S61, respectively. $^1\text{H-NMR}$ (400 MHz, $\text{DMSO-}d_6$): δ 8.66 (d, $J = 8.1$ Hz, 1H), 7.92 (d, $J = 9.0$ Hz, 3H), 7.87 (d, $J = 7.4$ Hz, 1H), 7.69 (d, $J = 8.3$ Hz, 1H), 7.62 (d, $J = 9.9$ Hz, 1H), 7.58 – 7.56 (m, 1H), 7.47 (d, $J = 8.4$ Hz, 1H), 7.33 (d, $J = 16.0$ Hz, 1H), 7.20 (t, $J = 8.7$ Hz, 1H), 6.88 (s, 1H), 4.20 (t, $J = 5.8$ Hz, 2H), 2.99 (d, $J = 6.1$ Hz, 2H), 2.07 (m, 2H). $^{13}\text{C-NMR}$ (100 MHz, $\text{DMSO-}d_6$): δ 158.5, 153.2, 152.4, 151.0, 148.5 (d, $J = 10.8$ Hz), 137.8, 135.9, 128.9 (d, $J = 6.9$ Hz), 126.6, 125.1, 119.4, 119.1, 117.6, 117.5, 116.3, 115.3, 115.1, 114.9, 107.0, 66.3, 60.6, 36.7, 27.2. $^{19}\text{F-NMR}$ (400MHz, $\text{DMSO-}d_6$): δ -74.36, -134.15. HRMS (ESI)m/z calcd for $\text{C}_{23}\text{H}_{19}\text{FN}_3\text{O}_2^+$ (M+H) $^+$: 388.1456, Found: 388.1451.

Probe 3: **probe 3** prepared similarly as **Probe 1** using **2c** (0.25g, 0.5 mmol) was obtained as a orange solid (0.17 g, yield 85%). The $^1\text{H-NMR}$ and $^{13}\text{C-NMR}$ spectra of **probe 3** are shown below in Fig. S62 and S63, respectively. $^1\text{H-NMR}$ (400 MHz, $\text{DMSO-}d_6$): δ 8.66 (dd, $J = 8.4, 1.2$ Hz, 1H), 7.90 (dd, $J = 7.1, 1.3$ Hz, 3H), 7.87 (d, $J = 2.1$ Hz, 1H), 7.69 (dd, $J = 8.4, 0.9$ Hz, 1H), 7.64 (dd, $J = 8.8, 2.0$ Hz, 1H), 7.59 (dd, $J = 11.6, 8.3$ Hz, 2H), 7.38 (d, $J = 16.0$ Hz, 1H), 7.18 (d, $J = 8.7$ Hz, 1H), 6.90 (s, 1H), 4.21 (s, 2H), 3.02 (d, $J = 6.5$ Hz, 2H), 2.19 – 1.94 (m, 2H). $^{13}\text{C-NMR}$ (100 MHz, $\text{DMSO-}d_6$): δ 158.5, 155.5, 153.2, 152.4, 137.4, 135.9, 129.5, 129.4, 129.3, 126.6, 125.1, 122.7, 119.4, 119.1, 117.6, 117.5, 116.3, 114.4, 107.0, 66.4, 60.6, 36.7, 27.2. HRMS (ESI) m/z calcd for $\text{C}_{23}\text{H}_{19}\text{ClN}_3\text{O}_2^+$ (M+H) $^+$: 404.1160, Found: 404.1157.

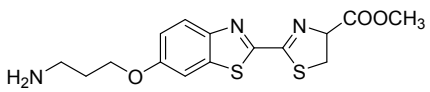
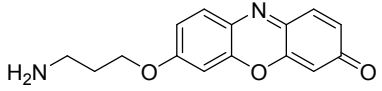
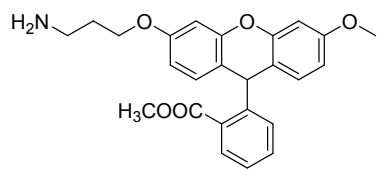
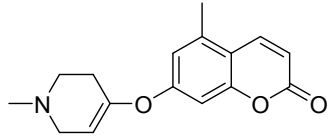
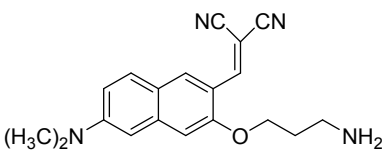
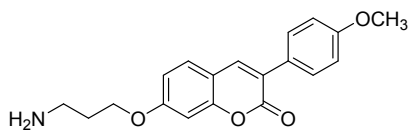
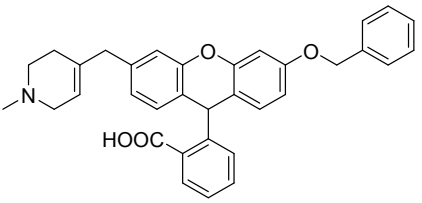
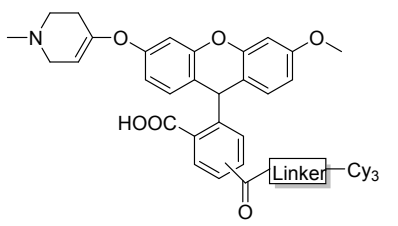
Probe 4: **probe 4** prepared similarly as **Probe 1** using **2d** (0.27g, 0.5 mmol) was obtained as a orange solid (0.20 g, yield 90%). The $^1\text{H-NMR}$ and $^{13}\text{C-NMR}$ spectra of **probe 4** are shown below in Fig. S64 and S65, respectively. $^1\text{H-NMR}$ (400 MHz, $\text{DMSO-}d_6$): δ 8.68 (dd, $J = 8.4, 1.2$ Hz, 1H), 8.04 (d, $J = 2.0$ Hz, 1H), 8.00 – 7.87 (m, 3H), 7.73 – 7.66 (m, 2H), 7.65 – 7.60 (m, 1H), 7.60 – 7.53 (m, 1H), 7.40 (d, $J = 16.0$ Hz, 1H), 7.16 (d, $J = 8.7$ Hz, 1H), 6.92 (s, 1H), 4.22 (t, $J = 5.9$ Hz, 2H), 3.04 (d, $J = 6.8$ Hz, 2H), 2.14 – 2.04 (m, 2H). $^{13}\text{C-NMR}$ (100 MHz, $\text{DMSO-}d_6$): δ 158.5, 156.4, 153.2, 152.4, 137.3, 135.9, 132.5, 130.2, 129.8, 126.6, 125.1, 119.4, 119.1, 117.6, 117.5, 116.3, 114.2, 112.4, 107.0, 66.4, 60.6, 36.7, 27.2. HRMS (ESI) m/z calcd for $\text{C}_{23}\text{H}_{19}\text{BrN}_3\text{O}_2^+$ (M+H) $^+$: 448.0655, Found: 448.0653.

Probe 5: **probe 5** prepared similarly as **Probe 1** using **2e** (0.24g, 0.5 mmol) was obtained as a orange solid (0.18 g, yield 94%). The $^1\text{H-NMR}$ and $^{13}\text{C-NMR}$ spectra of **probe 5** are shown below in Fig. S66 and S67, respectively. $^1\text{H-NMR}$ (400 MHz, $\text{DMSO-}d_6$): δ 8.64 (dd, $J = 8.4, 1.1$ Hz, 1H), 7.95 (s, 3H), 7.89 – 7.83 (m, 1H), 7.70 (d, $J = 7.7$ Hz, 1H), 7.57 (d, $J = 2.0$ Hz, 1H), 7.53 (d, $J = 2.3$ Hz, 1H), 7.48 (d, $J = 8.5$ Hz, 1H), 7.22 (d, $J = 15.9$ Hz, 1H), 6.94 (d, $J = 8.6$ Hz, 1H), 6.84 (s, 1H), 4.11 (t, $J = 5.9$ Hz, 2H), 3.02 (dd, $J = 12.8, 6.6$ Hz, 2H), 2.15 (s, 3H), 2.11 – 2.02 (m, 2H). $^{13}\text{C-NMR}$ (100 MHz, $\text{DMSO-}d_6$): δ 159.0, 158.9, 153.1, 152.4, 139.2, 135.7, 130.4, 128.9, 127.7, 127.3, 126.5, 125.0, 119.4, 117.8, 117.5, 117.2, 116.4, 111.9, 106.4, 65.2, 59.8, 36.8, 27.4, 16.4. HRMS (ESI) m/z calcd for $\text{C}_{24}\text{H}_{22}\text{N}_3\text{O}_2^+$ (M+H) $^+$: 384.1707, Found: 384.1700.

Probe 6: **probe 6** prepared similarly as **Probe 1** using **2f** (0.25g, 0.5 mmol) was

obtained as a orange solid (0.18 g, yield 90%). The ^1H -NMR and ^{13}C -NMR spectra of **probe 6** are shown below in Fig. S68 and S69, respectively. ^1H -NMR (400 MHz, $\text{DMSO-}d_6$): δ 8.67 (d, $J = 8.2$ Hz, 1H), 7.89 (d, $J = 7.0$ Hz, 3H), 7.72 (d, $J = 8.3$ Hz, 1H), 7.63 (d, $J = 15.9$ Hz, 1H), 7.56 (t, $J = 7.7$ Hz, 1H), 7.39 (s, 1H), 7.32 (d, $J = 15.9$ Hz, 1H), 7.23 (d, $J = 7.8$ Hz, 1H), 7.00 (d, $J = 8.3$ Hz, 1H), 6.88 (s, 1H), 4.11 (t, $J = 5.7$ Hz, 2H), 3.84 (s, 3H), 2.99 (d, $J = 5.9$ Hz, 2H), 2.10 – 1.98 (m, 2H). ^{13}C -NMR (100 MHz, $\text{DMSO-}d_6$): δ 159.0, 153.2, 152.5, 150.5, 149.7, 139.5, 135.8, 128.6, 126.5, 125.1, 123.7, 119.4, 117.7, 117.7, 117.5, 116.5, 113.2, 110.5, 106.5, 65.9, 60.0, 56.1, 36.9, 27.3. HRMS (ESI) m/z calcd for $\text{C}_{24}\text{H}_{22}\text{N}_3\text{O}_3^+$ (M+H) $^+$: 400.1656, Found 400.1644.

Table S1 Current fluorescent probes for MAOs

Probe structure	$\lambda_{\text{abs}}(\text{nm})$	$\lambda_{\text{em}}(\text{nm})$	Km(μm)	Limit of detection	selectivity	references
	NO	NO	6.4 (MAO-B) 15 (MAO-A)	NO	NO	3
	544	590	7.6 (MAO-A) 1.8 (MAO-B)	NO	NO	4
	470	535	11.4 (MAO-A) 7.7 (MAO-B)	NO	NO	5
	360	460	59.63(MAO-B)	NO	MAO-B	6
	448	600	70(MAO-A) 75(MAO-B)	NO	NO	7
	345	465	NO	NO	NO	8
	470	515	246.2(MAO-A) 44.6(MAO-B)	NO	MAO-B	9
	475	570	647.2(MAO-A) 157.1(MAO-B)	NO	MAO-B	10

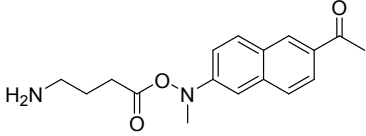
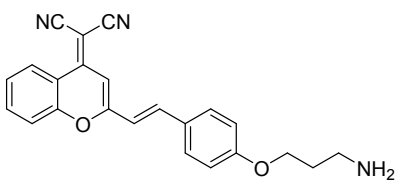
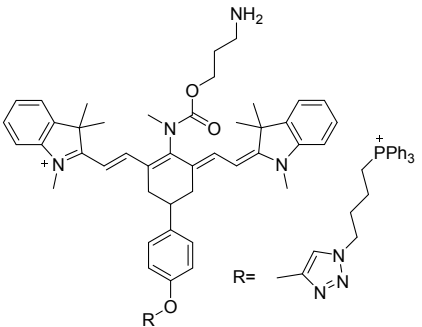
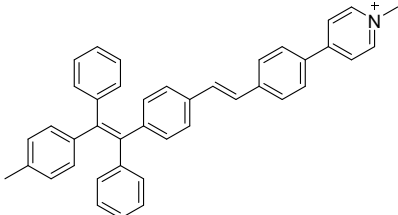
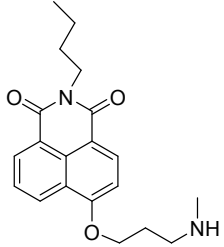
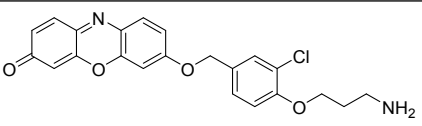
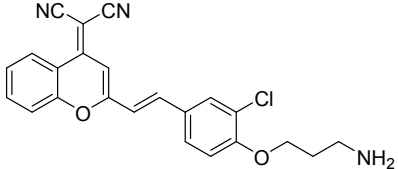
	304	449	8.33 (MAO-B)	NO	MAO-B	11
	420	664	270 (MAO-B)	1.2 µg/mL	NO	12
	650 730	720 790	10.1 (MAO-B)	NO	MAO-B	13
	360	530	17.1 (MAO-A) 101.8 (MAO-B)	7.1 µg/mL	MAO-A	14
	454	550	NO	1.1 ng/mL	MAO-A	15
	550	586	2.9 (MAO-A)	2.7 ng/mL	MAO-A	16
	530	675	4.5 (MAO-A)	2.6 ng/mL	MAO-A (our work)	

Table S2 Photophysical data of all the 3a-e and probe1-6 in PBS/DMSO solution (7:3, v/v, pH = 7.4)

Compound	$\lambda_{\max}^a(\epsilon_{\max}^b)$	λ_{\max}^c	$\Delta \nu^d$	Φ^e
3a	530 (3.1)	675	135	0.09
3b	530 (4.4)	675	135	0.10
3c	530 (4.6)	675	135	0.10
3d	530 (4.5)	675	135	0.10
3e	460 (3.5)	580	120	0.09
3f	460 (3.4)	590	130	0.09
prboe 1	430 (0.35)	675		0.002
prboe 2	430 (0.44)	675		0.002
prboe 3	430 (0.51)	675		0.002
prboe 4	430 (0.50)	675		0.002
prboe 5	430 (0.37)	580		0.002
prboe 6	430 (0.37)	590		0.002

[a] Peak position of the longest absorption band. [b] Maximum molar absorbance in $10^4 \text{ mol}^{-1} \text{ L cm}^{-1}$. [c] Peak position of emission, excited at the absorption maximum. [d] Stokes' shift in nm. [e] Fluorescence quantum yield (Φ) was measured using rhodamine B ($\Phi = 0.69$ in EtOH) as a standard.

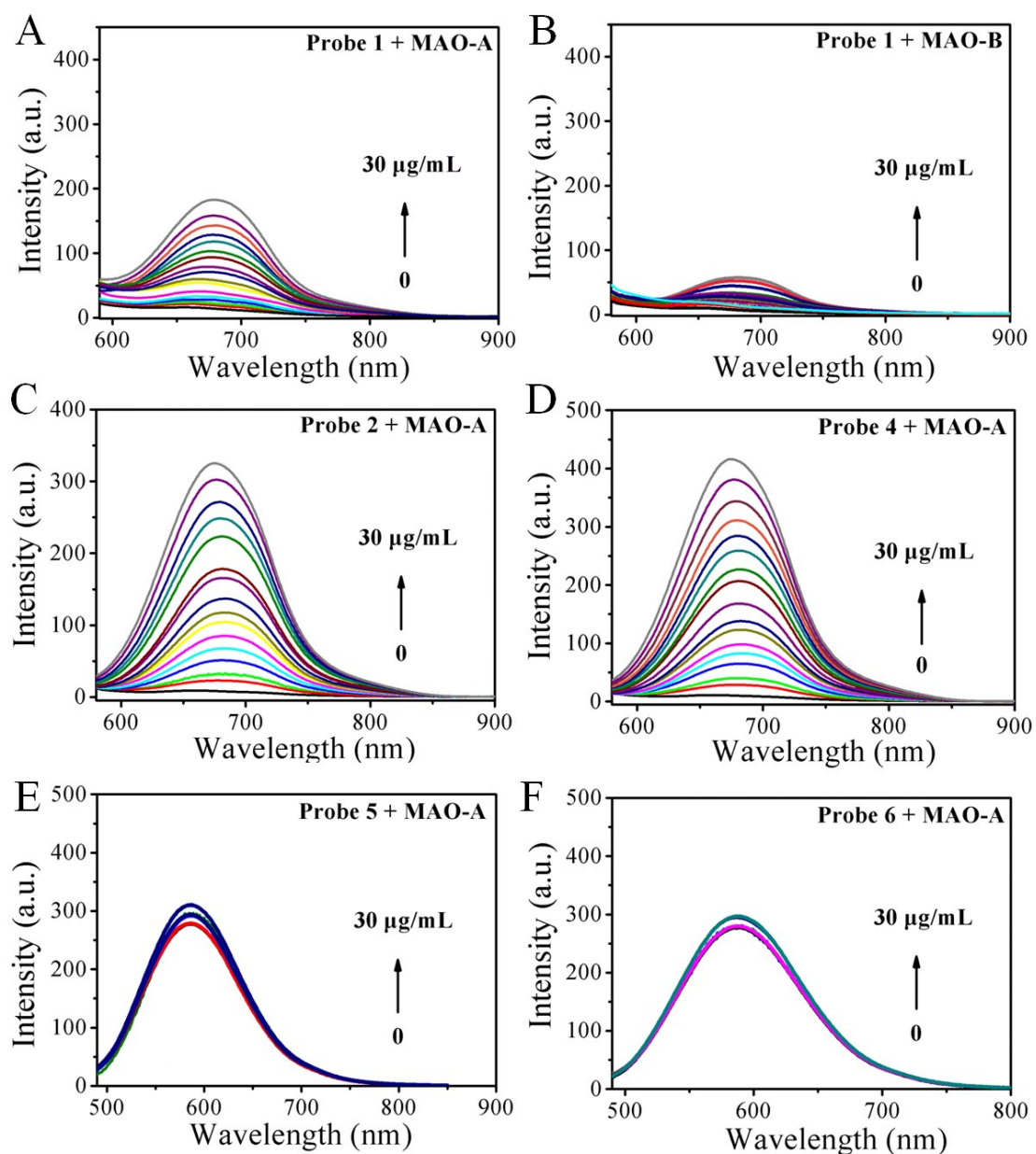


Fig. S1. Fluorescence responses of 10 μM of probes (1, 2, 4, 5 and 6) to MAO-A (A, C, D, E and F) and probe 1 to MAO-B (B) at different concentrations (0-30 $\mu\text{g/mL}$), respectively. $\lambda_{\text{ex/em}} = 530/675$ nm.

Table S3. Kinetic parameters of probes 1-6 for MAO-A

probe	MAO-A		
	K_m (μM)	k_{cat} (s^{-1})	k_{cat} / K_m ($\text{s}^{-1} \text{M}^{-1}$)
1	11.4 ± 0.3	16.2 ± 0.3	1.4×10^6
2	5.4 ± 0.3	30.9 ± 0.2	5.7×10^6
3	4.5 ± 0.2	34.3 ± 0.3	7.6×10^6
4	5.0 ± 0.2	32.1 ± 0.2	6.4×10^6
5	NO	NO	NO
6	NO	NO	NO

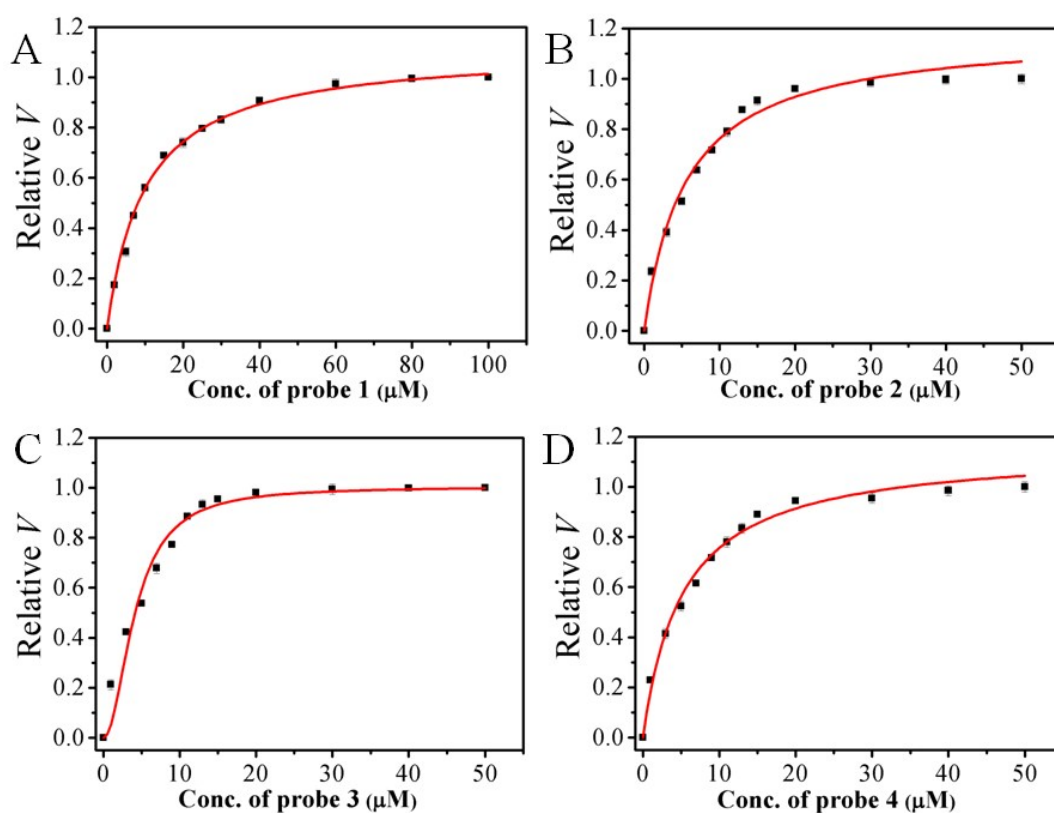


Fig. S2. Reaction kinetics of probes 1-4 with 20 $\mu\text{g/mL}$ of MAO-A. Relative reaction rate (V) of probes 1-4 in their corresponding concentration ranges. Data are expressed as the mean SD ($n = 3$). $\lambda_{\text{ex/em}} = 530/675$ nm.

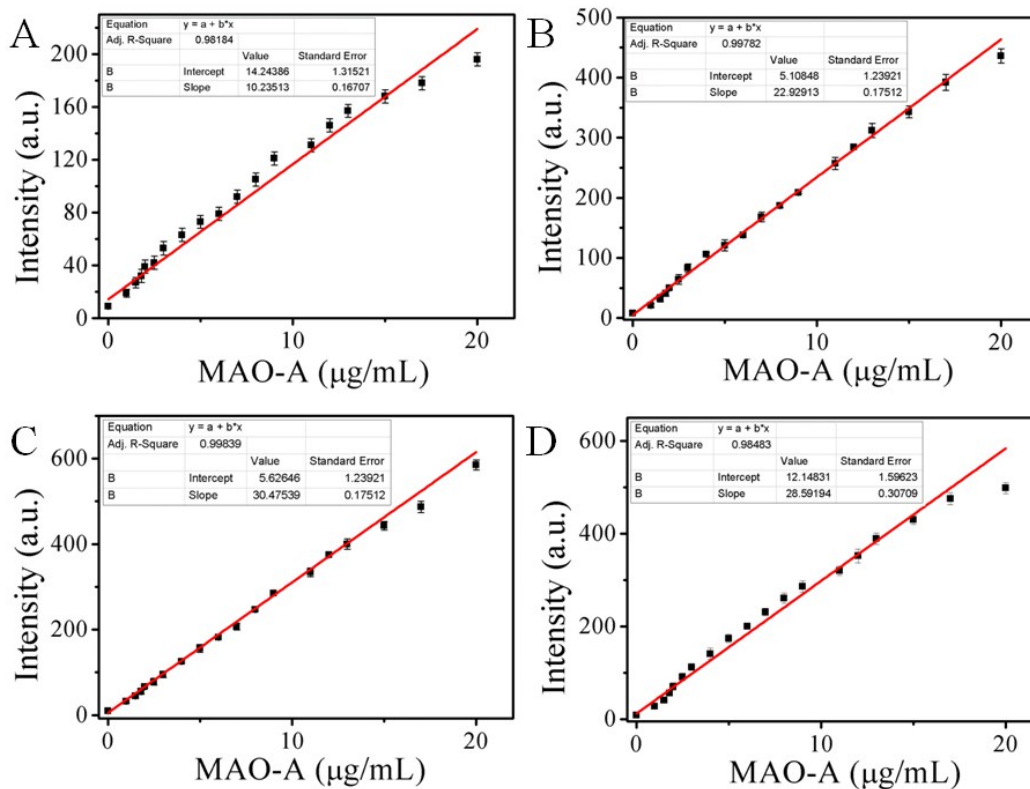


Fig. S3. Fluorescence intensity as a function of MAO-A level (A, B, C, D were probe 1-4, respectively).

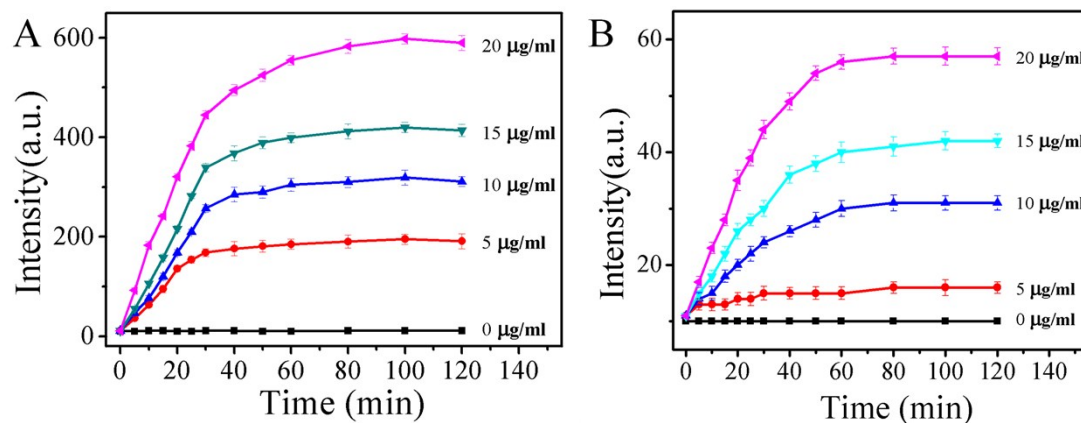


Fig. S4. Fluorescence response of probe 3 (10 μM) towards different concentrations MAO-A (0-20 $\mu\text{g/mL}$) in aqueous solution (A: PBS/DMSO = 7:3 v:v; B: PBS/DMSO = 99:1 v:v, pH = 7.4, 37 $^{\circ}\text{C}$) for 2 h. $\lambda_{\text{ex/em}}$ = 530/675 nm.

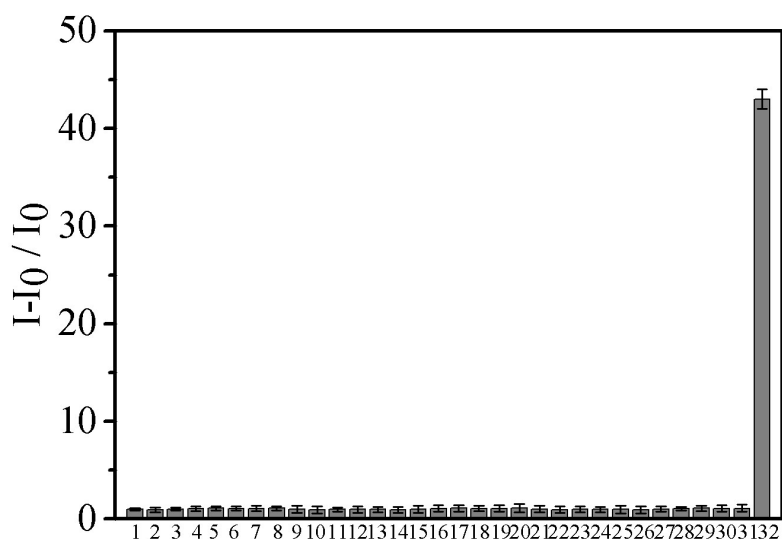


Fig. S5. Fluorescence response of probe 3 (10 μM) after 120 min of incubation with various analytes: 1. blank, 2-10. Mg^{2+} , Cd^{2+} , Ca^{2+} , Mn^{2+} , Zn^{2+} , Hg^{2+} , Fe^{2+} , Fe^{3+} , Cu^{2+} (1 mM), 11-20. NO_3^- , NO_2^- , TBHP, H_2O_2 , $\cdot\text{OH}$, O_2^- , ClO^- , benzoyl peroxide, GSNO and S^{2-} (1 mM), 21-31. vitamin B6, arginine, serine, glutamic acid, alanine, cysteine, glutathione, urea, creatinine, carboxylesterase (1 mM), MAO-B (20 $\mu\text{g}/\text{mL}$), 32. MAO-A (20 $\mu\text{g}/\text{mL}$). The results are expressed as the mean SD ($n = 3$). $\lambda_{\text{ex}}/\text{em} = 530/675 \text{ nm}$.

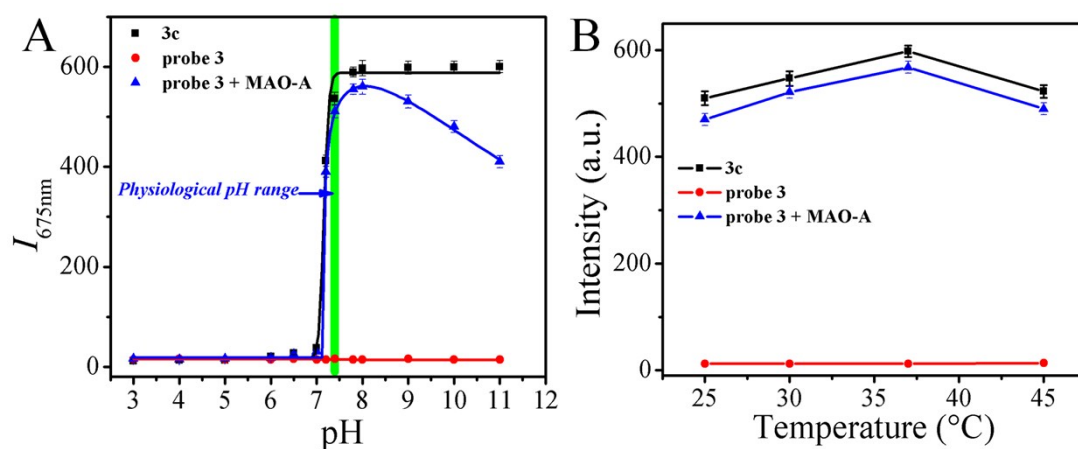


Fig. S6. Effects of (A) pH and (B) temperature on the fluorescence intensity of 3c (black curve), probe 3 (red curve) and probe 3 (10 μM) reacting with MAO-A (20 $\mu\text{g}/\text{ml}$) in aqueous solution (PBS/DMSO = 7:3 v:v), monitored at 675 nm and $\lambda_{\text{ex}} = 530 \text{ nm}$. The results are expressed as the mean SD ($n = 3$).

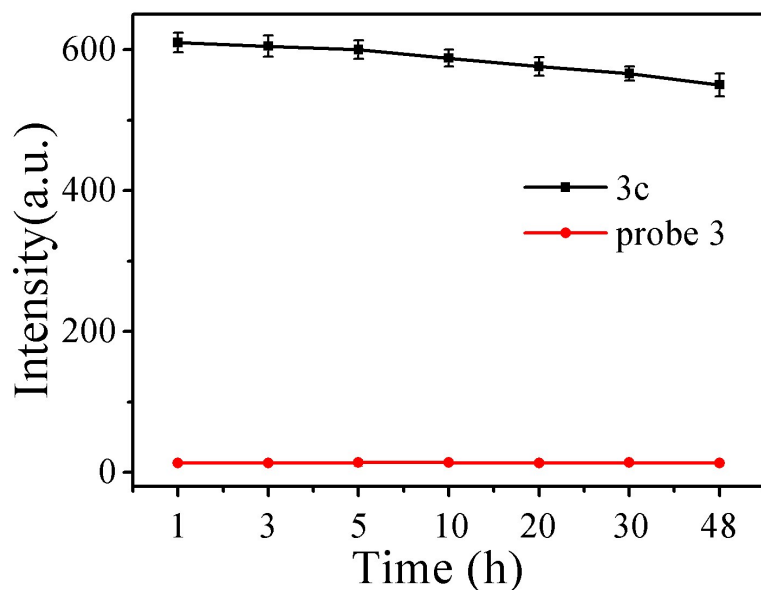


Fig. S7. The stability of probe 3 and 3c (10 μ M) in 10% FBS investigated by determining its fluorescent intensity changes, monitored at 675 nm and λ_{ex} = 530 nm. The results are expressed as the mean SD (n = 3).

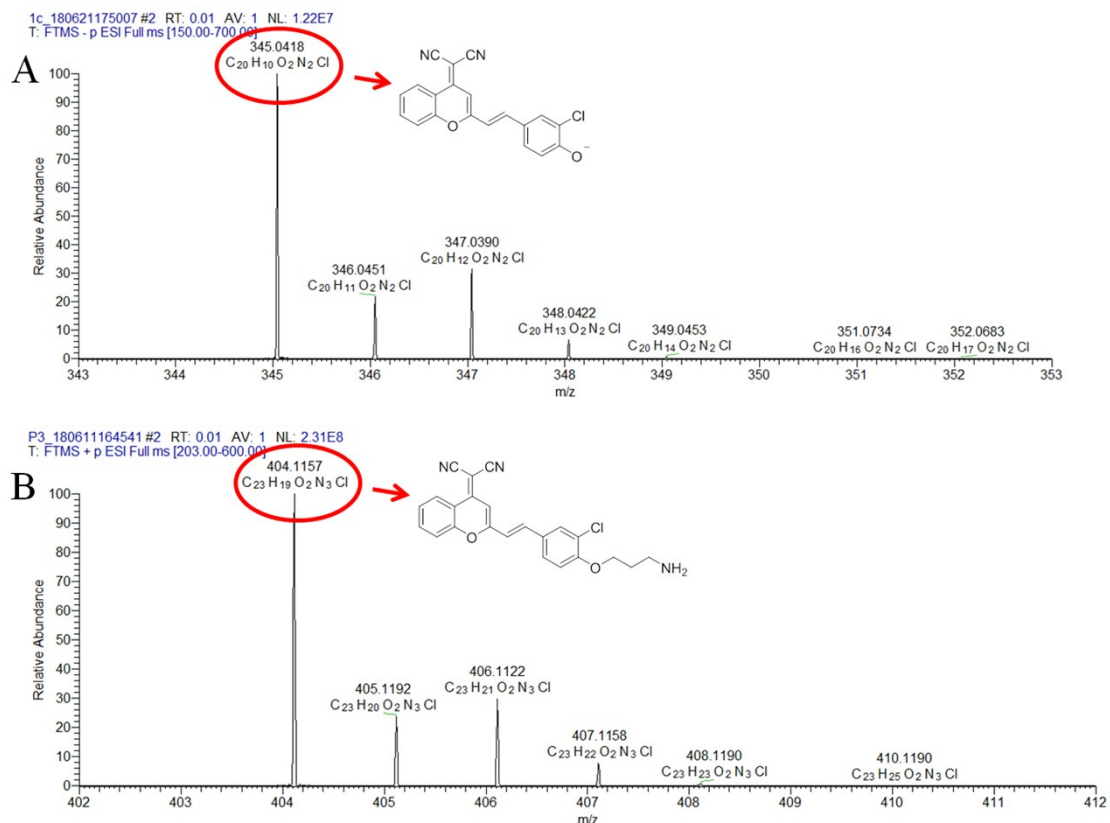


Fig. S8. (A) and (B) are the ESI mass spectra of the purified product from the reaction of probe 3 (100 μ M) towards MAO-A and MAO-B in PBS (pH = 7.4, 37 $^{\circ}$ C) , respectively.

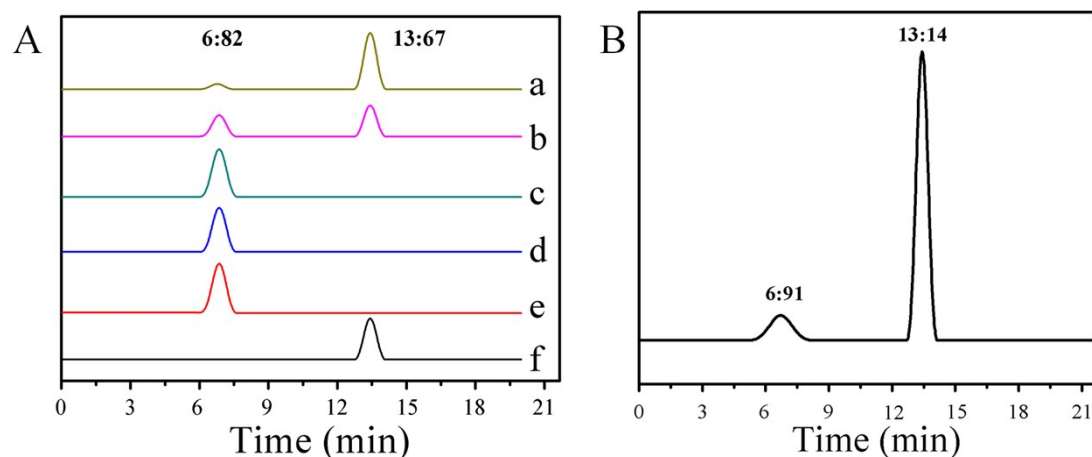


Fig. S9. (A) HPLC kinetic profiles of MAO-A and MAO-B in pH 7.4 phosphate buffered saline (PBS)/dimethyl sulfoxide (DMSO) (7:3 = v:v), respectively. a and b) Probe 3 (100 μM) reacting with 100 $\mu\text{g}/\text{mL}$ of MAO-A for 120 and 30 min, respectively; c) Probe 3 (100 μM) ($t_{\text{R}}=6.82$ min); d) The reaction solutions of probe 3 with MAO-B for 120 min; e) Probe 3 (100 μM) and clorgyline (5 μM) with MAO-A (100 $\mu\text{g}/\text{mL}$) reacting with 120 min, f) 100 μM 3c ($t_{\text{R}} = 13.67$ min). (B) Probe 3 (100 μM) reacting with 100 $\mu\text{g}/\text{mL}$ of MAO-A for 60 min in pH 7.4 phosphate-buffered saline (PBS)/dimethyl sulfoxide (DMSO) (99:1 = v:v) at 37 $^{\circ}\text{C}$, 3c ($t_{\text{R}} = 13.14$ min), probe 3 ($t_{\text{R}} = 6.91$ min). The peaks eluting from the column were monitored at 400 nm. The column was eluted with methanol/water (1 : 1, v/v). The flow rate was set at 0.7 mL min^{-1} . Because of the different operating time of the instrument (HPLC), the t_{R} is different in A and B.

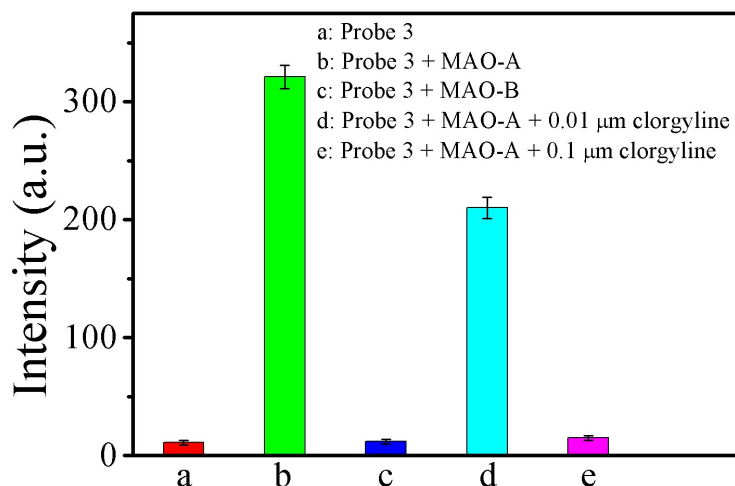


Fig. S10. Fluorescence intensity of different reaction systems. (a) 10 μM probe 3 only; (b): system (a) + MAO-A (15 $\mu\text{g}/\text{mL}$); (c): system (a) + MAO-B (50 $\mu\text{g}/\text{mL}$); (d): system (b) + clorgyline (0.01 μM); (e): system (b) + clorgyline (0.1 μM). $\lambda_{\text{exc/em}}$ = 530/675 nm.

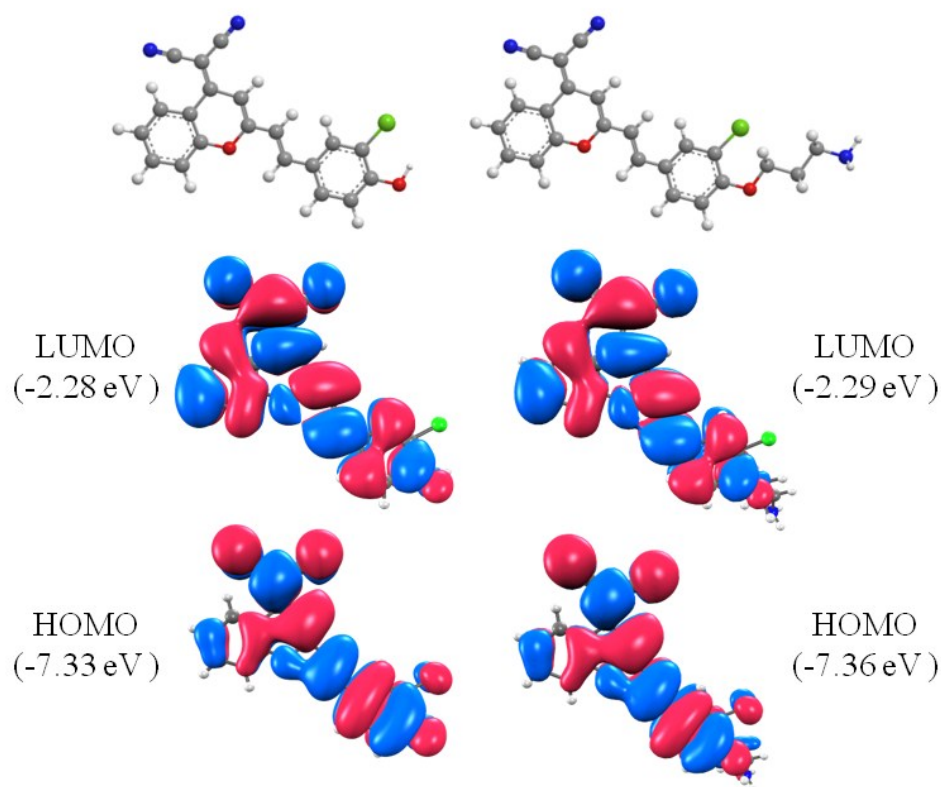


Fig. S11. The frontier molecular orbitals (FMOs) and corresponding energy levels of 3c (left) and probe 3 (right) are calculated based density functional theory (DFT). In the ball-and-stick representation, carbon, nitrogen, oxygen and chlorine atoms are colored in gray, blue, red and green respectively.

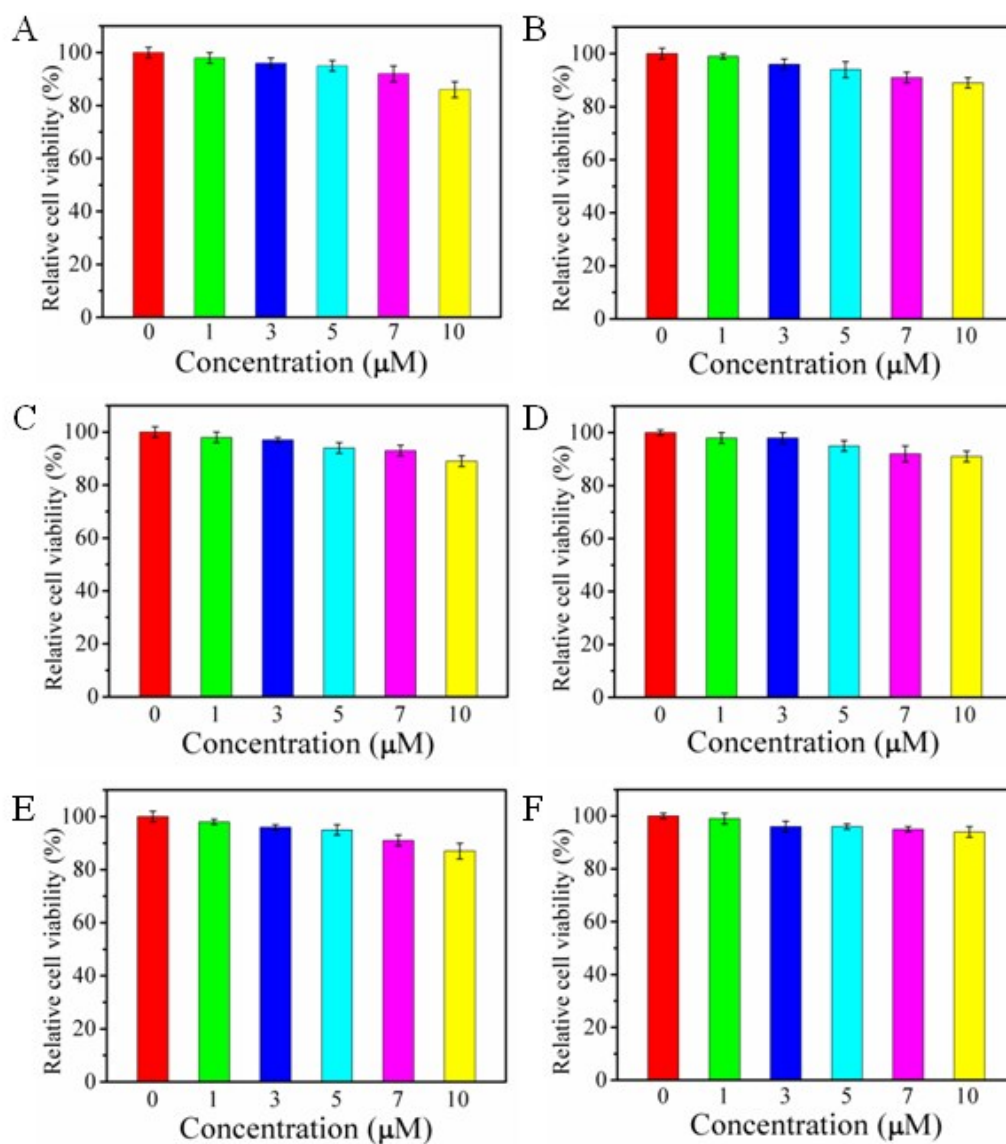


Fig. S12. Relative viability of SH-SY5Y (A-B), HepG2 (C-D) and NIH-3T3 (E-F) cells *in vitro* after incubation for 24 h with probe 3 (A, C and E) and 3c (B, D and F) at various concentrations. Note: both probe 3 and its hydrolysate 3c have minimal toxicity. The results are expressed as the mean SD (n = 5).

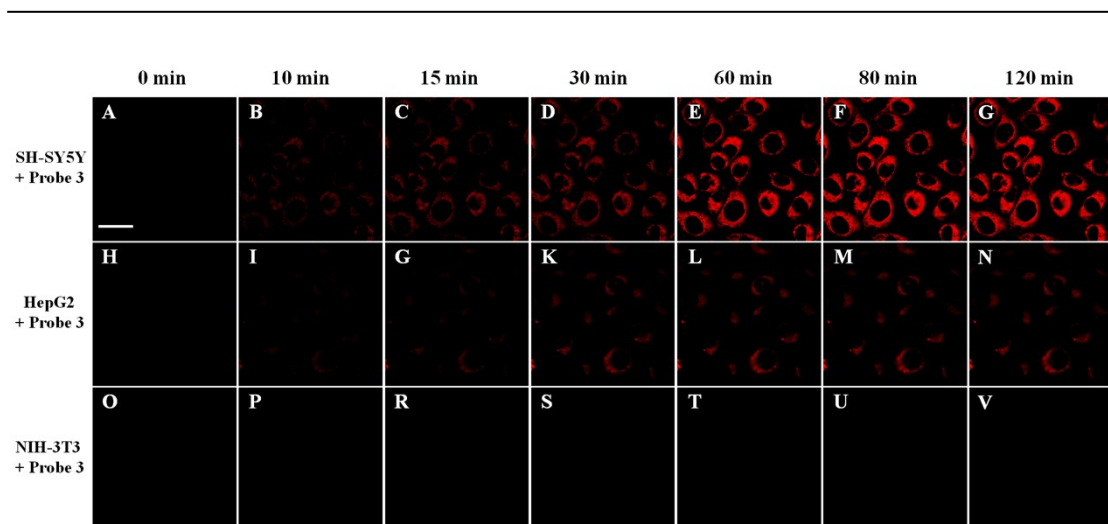


Fig. S13. The fluorescence images of SH-SY5Y, HepG2 and NIH-3T3 cells incubated with different periods of time (0, 10, 15, 30, 60, 80 and 120 min) of probe 3 (10 μ M). Scale bar: 50 μ m.

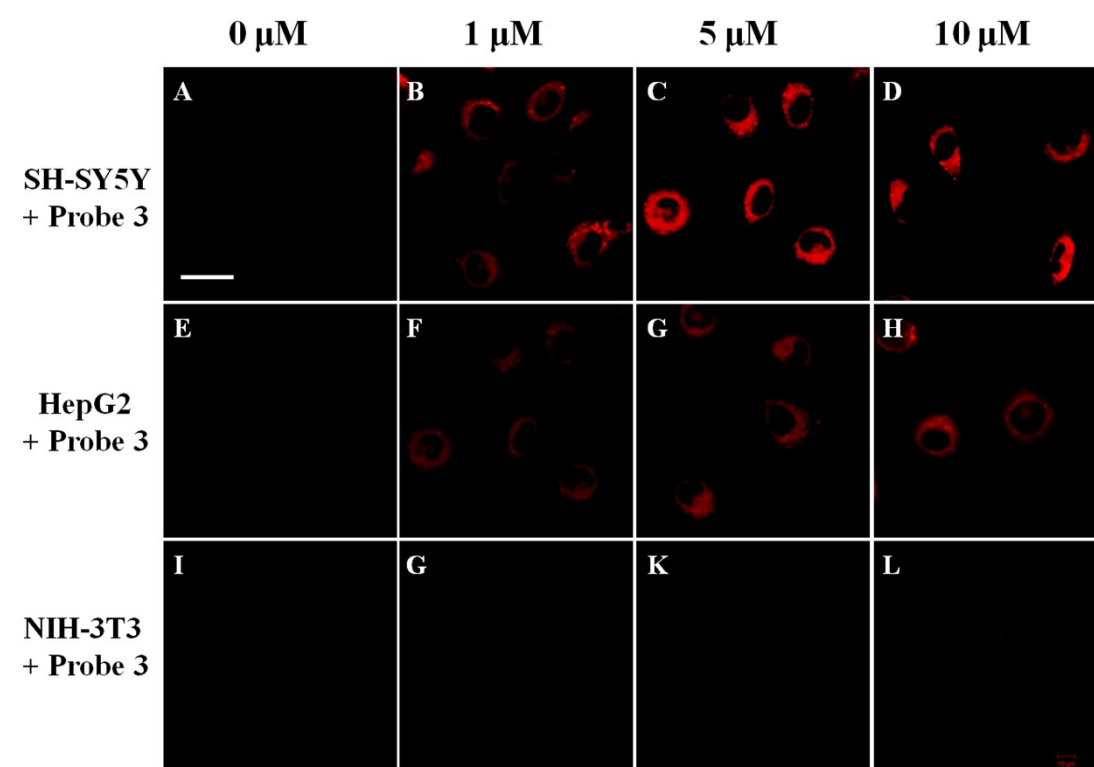


Fig. S14. The fluorescence images of SH-SY5Y, HepG2 and NIH-3T3 cells incubated with different concentrations of probe 3 (0, 1, 5 and 10 μ M). Scale bar: 50 μ m.

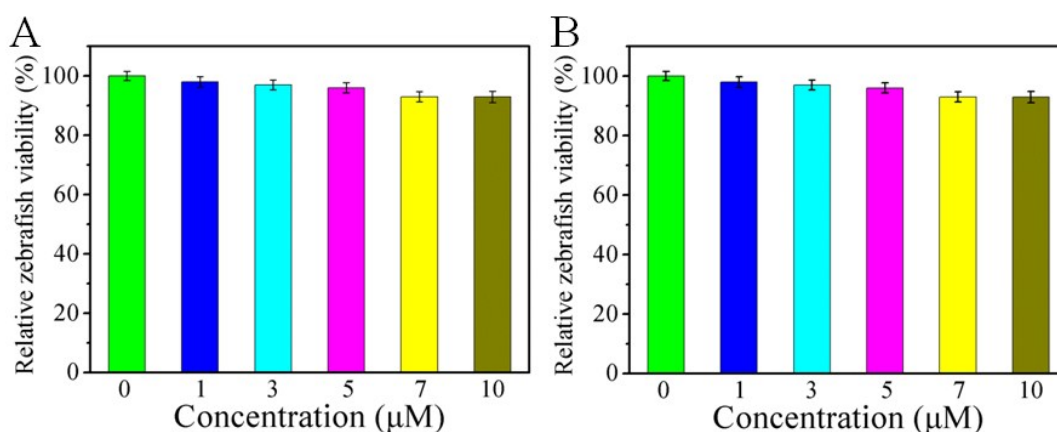


Fig. S15. Relative viability of the 5-day-old zebrafish *in vitro* after incubation for 96 h with probe 3 (A) and 3c (B) at various concentrations. Note: both probe 3 and its hydrolysate 3c have minimal toxicity. The results are expressed as the mean SD (n = 3).

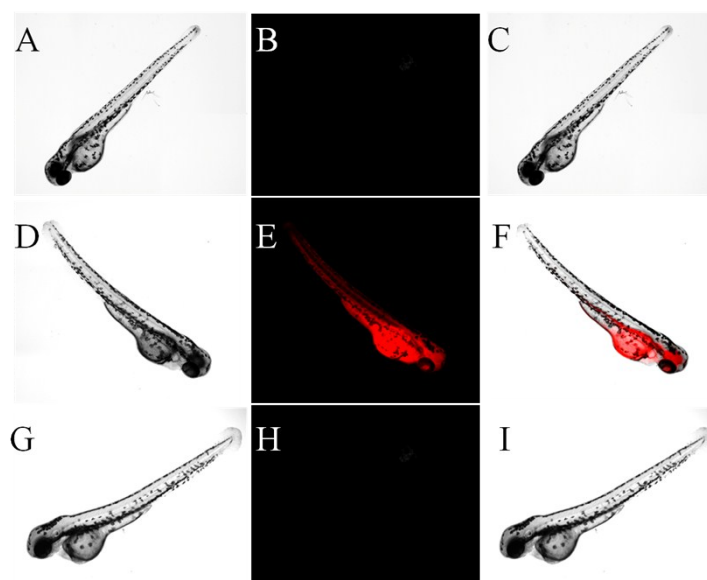


Fig. S16. Fluorescence images of MAO-A in 5-day-old zebrafish larvae. (A) Control bright field, (B) Control reg channel, (C) Overlay of images A and B; (D) Bright field, (E) Fluorescence image of zebrafish incubated with probe 3 (20 μM) for 120 min from red channel, (F) Overlay of images D and E. (G) Bright field, (H) Fluorescence image of zebrafish pre-incubated with clorgyline (5 μM) for 30 min and then with the probe 3 (20 μM) for 120 min from red channel; (I) Overlay of images G and H.

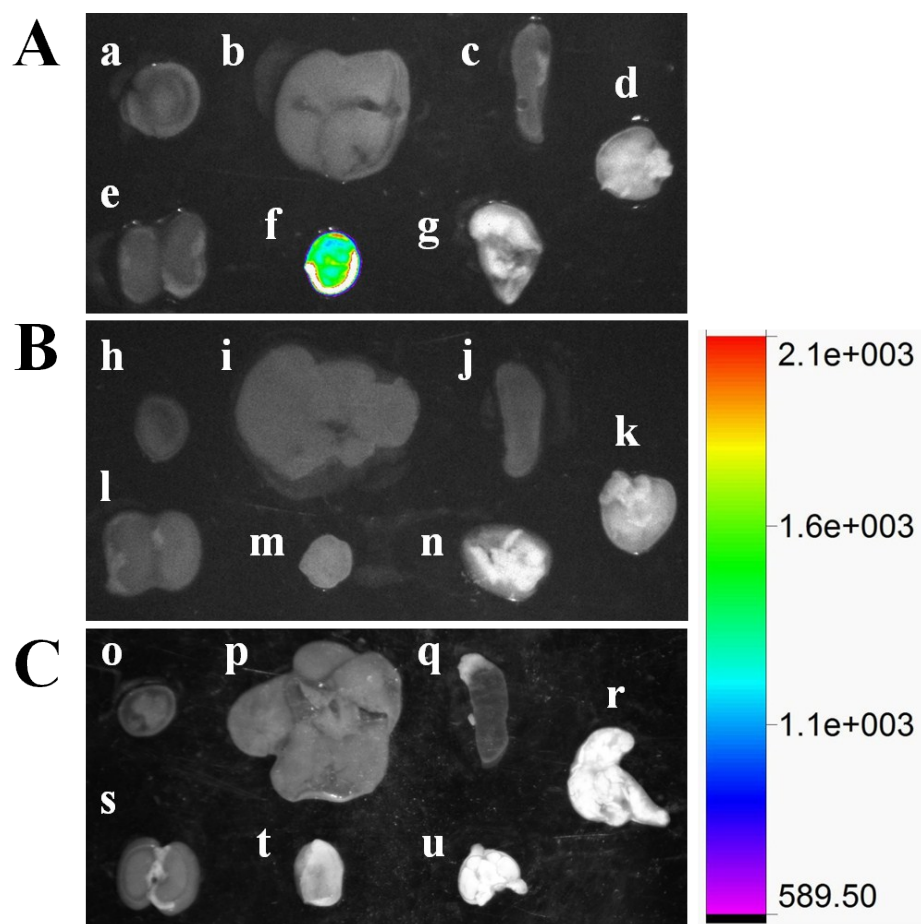


Fig. S17. Fluorescence images of MAO-A in tumor and other normal organs. (A) Tumor-bearing mice treated with probe 3 (100 μ M, 100 μ L) for 2 h. (B) The mice treated with PBS buffer for 2 h as the control. (C) Tumor-bearing mice pre-incubated with clorgyline (50 μ M, 100 μ L) for 30 min and then with the probe 3 for 120 min. a, h and o: heart; b, i and p: liver; c, j and q: spleen; d, k and r: lung; e, l and s: kidney; f, m and t: tumor; g, n and u: brain.

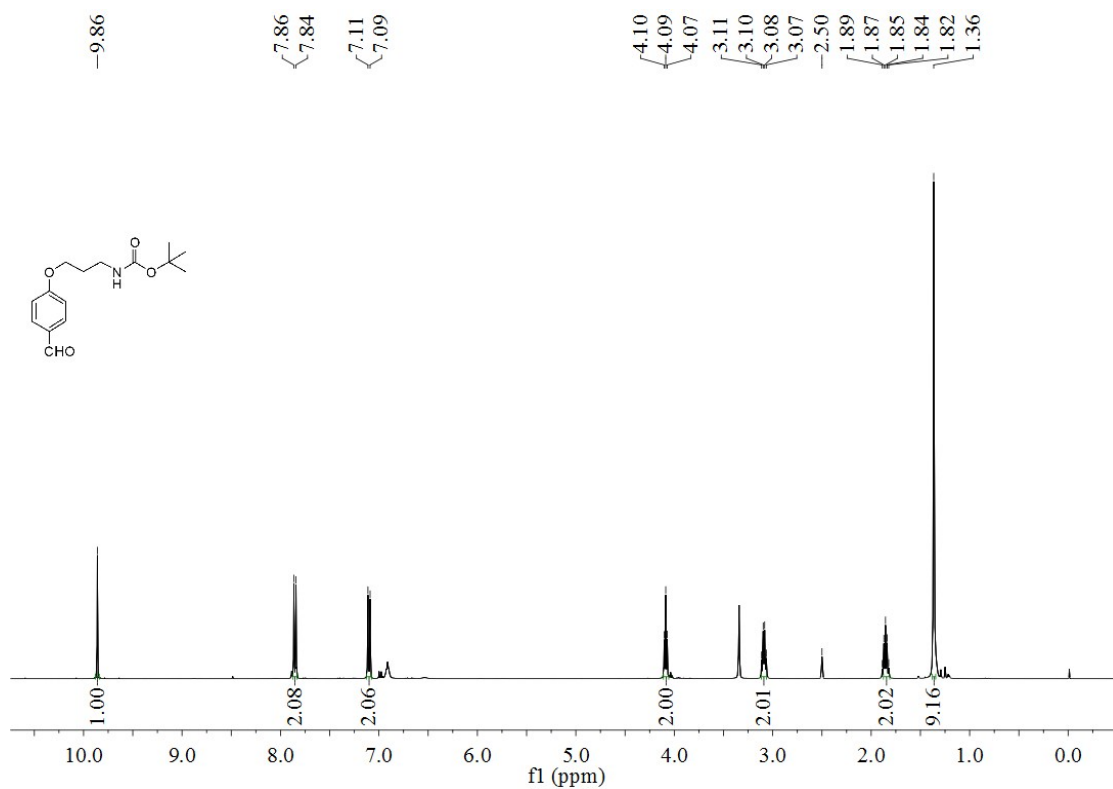


Fig. S18. ¹H-NMR spectrum of **1a** (400 MHz, DMSO-*d*₆).

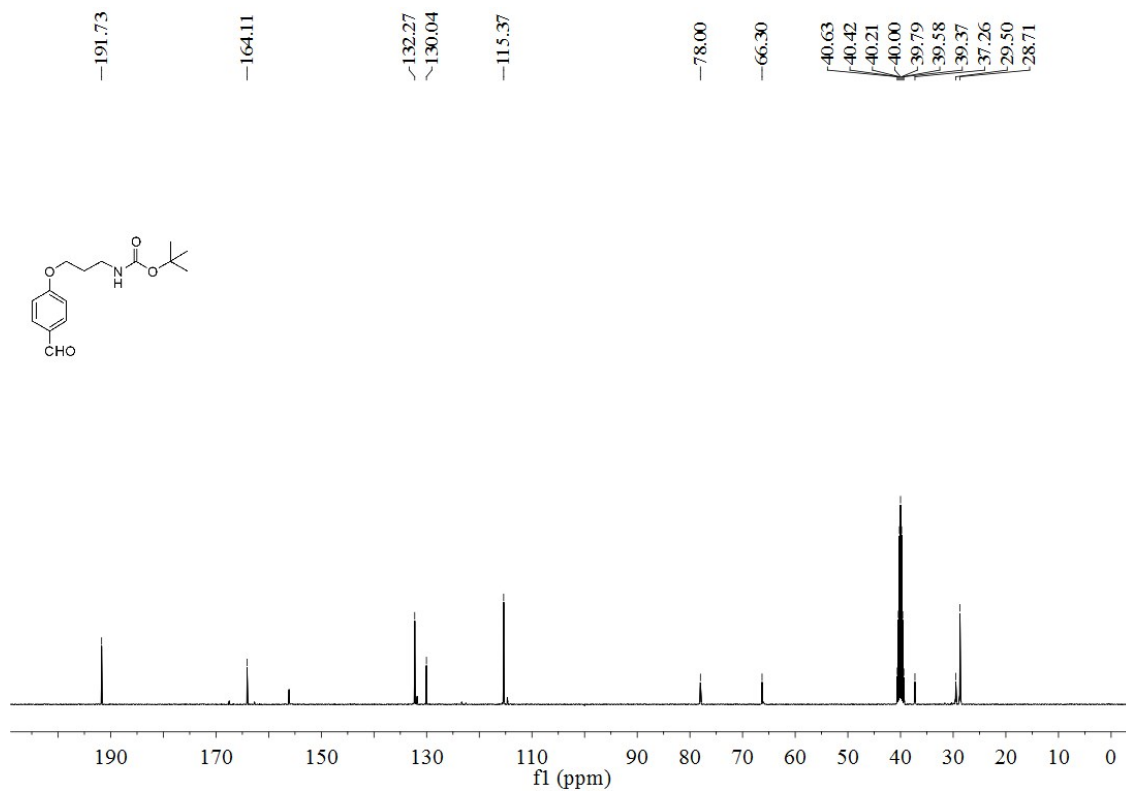


Fig. S19. ¹³C-NMR spectrum of **1a** (100 MHz, DMSO-*d*₆).

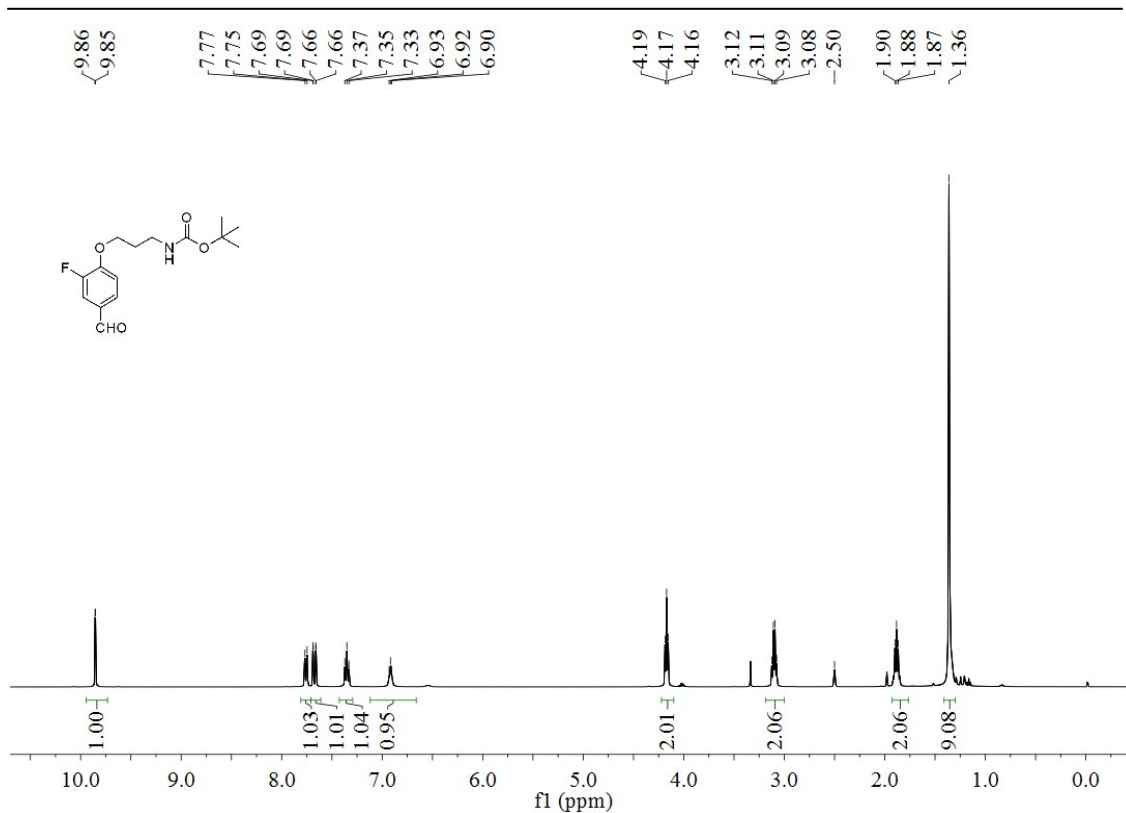


Fig. S20. ¹H-NMR spectrum of 1b (400 MHz, DMSO-d₆).

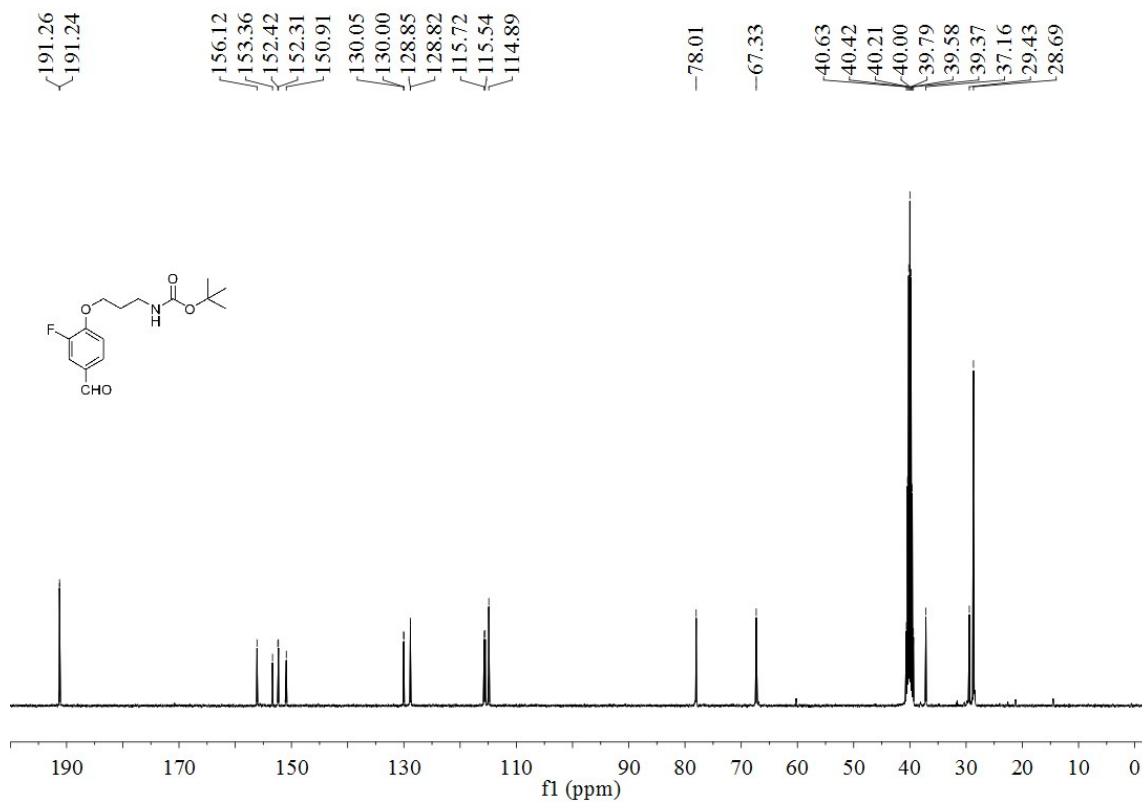


Fig. S21. ¹³C-NMR spectrum of 1b (100 MHz, DMSO-d₆).

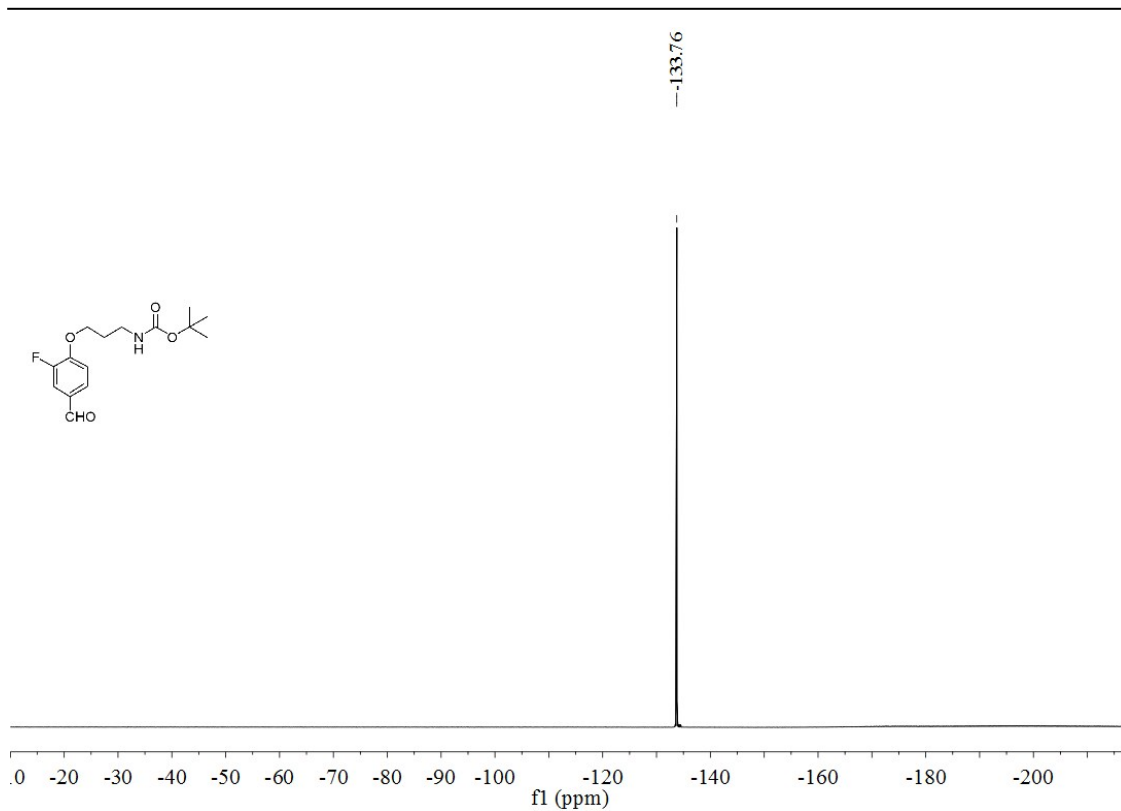


Fig. S22. ^{19}F -NMR spectrum of **1b** (400 MHz, $\text{DMSO-}d_6$).

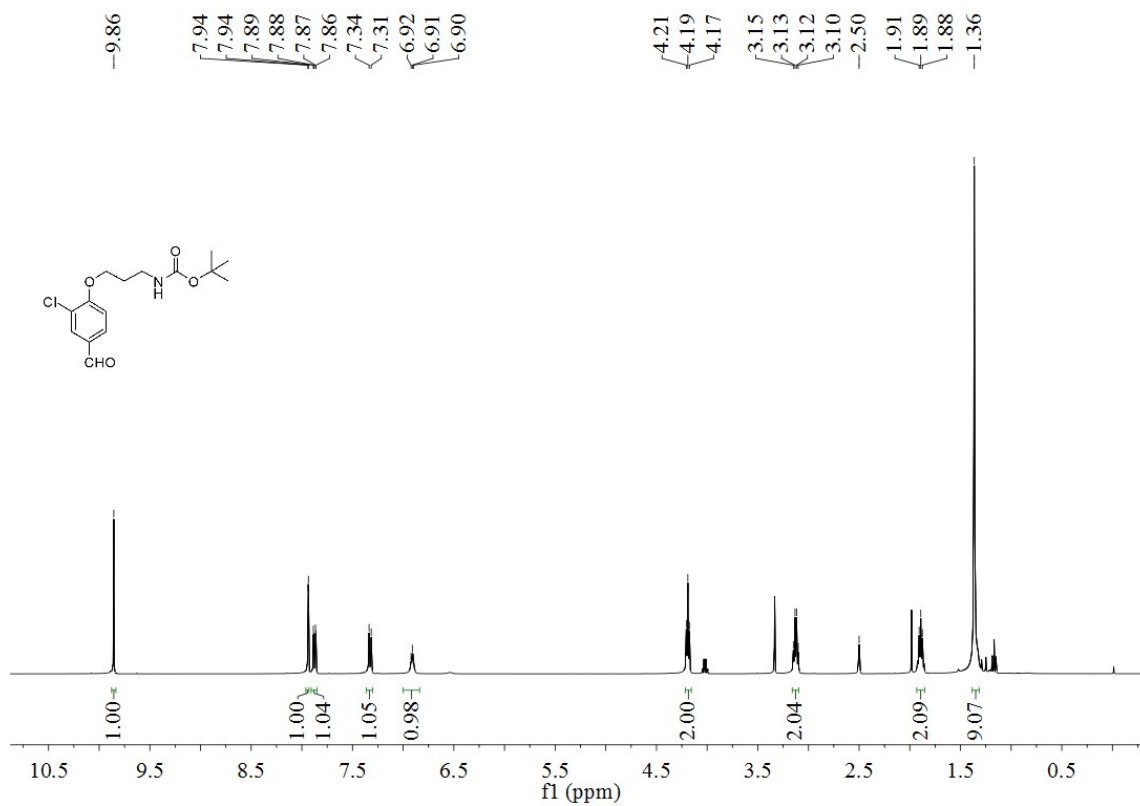


Fig. S23. ^1H -NMR spectrum of **1c** (400 MHz, $\text{DMSO-}d_6$).

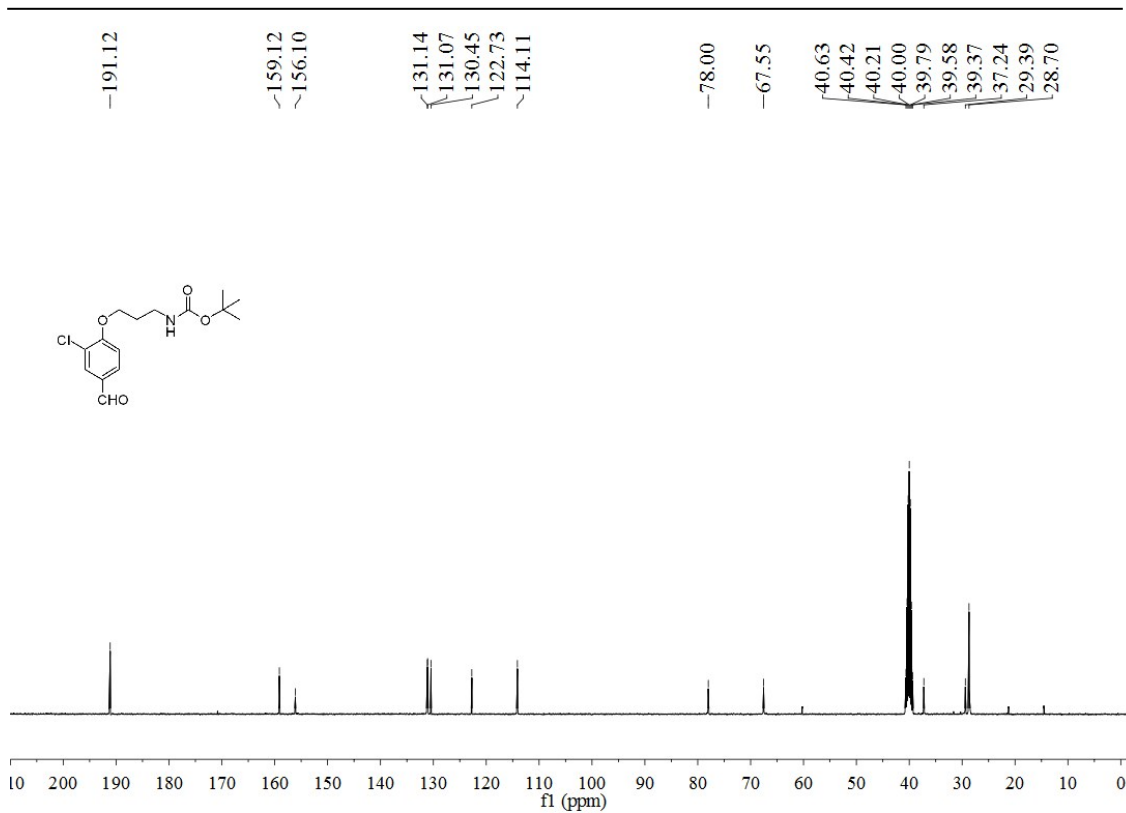


Fig. S24. ^{13}C -NMR spectrum of **1c** (100 MHz, $\text{DMSO-}d_6$).

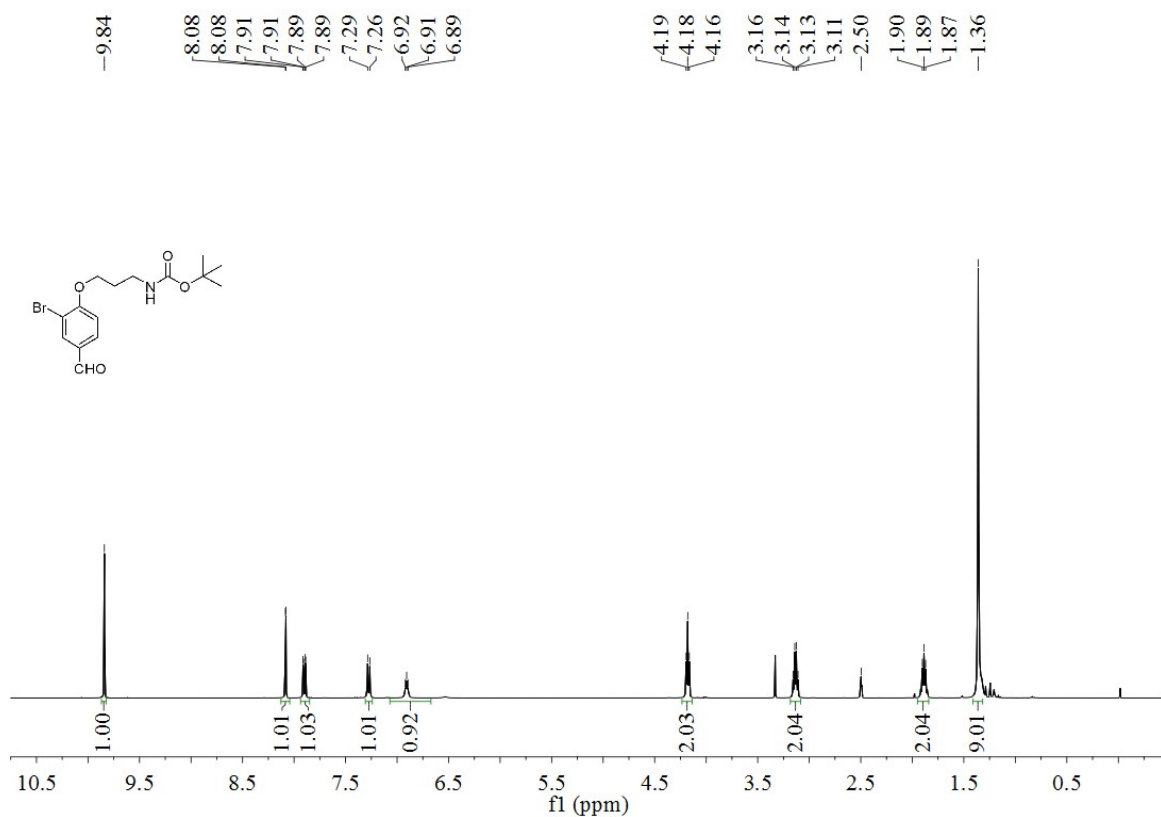


Fig. S25. ^1H -NMR spectrum of **1d** (400 MHz, $\text{DMSO-}d_6$).

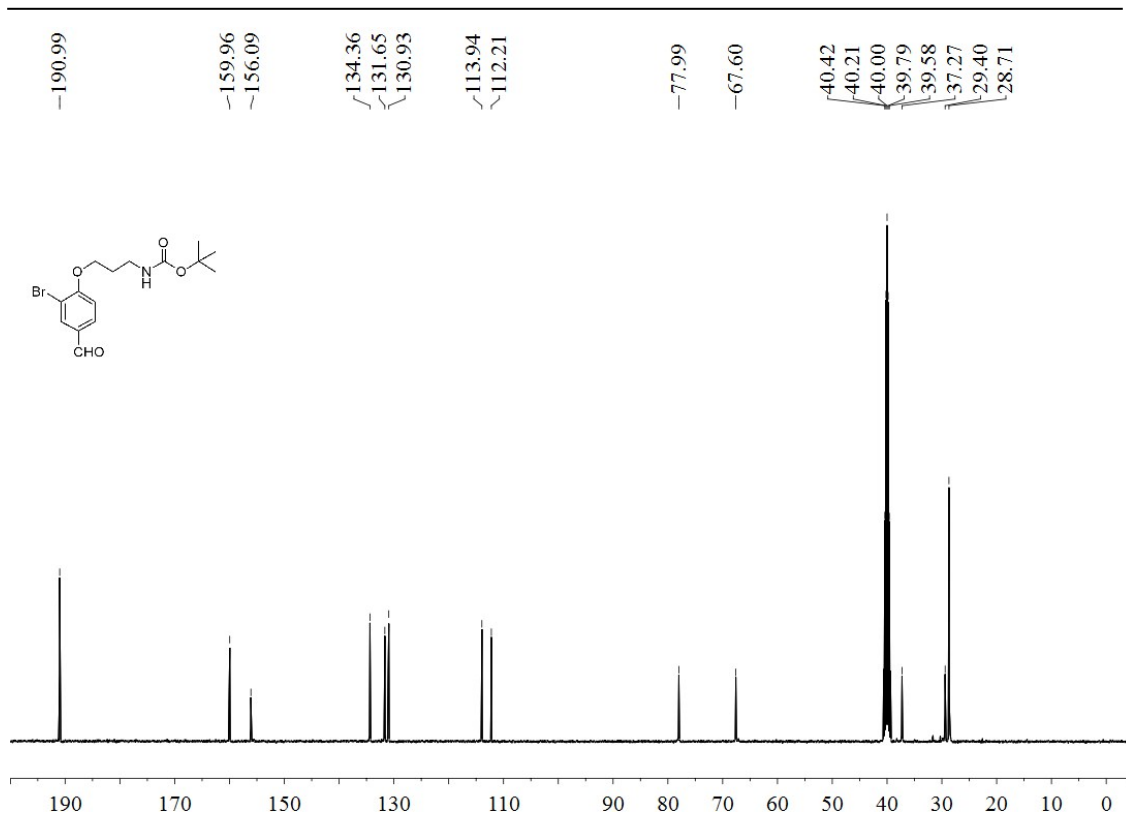


Fig. S26. ^{13}C -NMR spectrum of **1d** (100 MHz, $\text{DMSO-}d_6$).

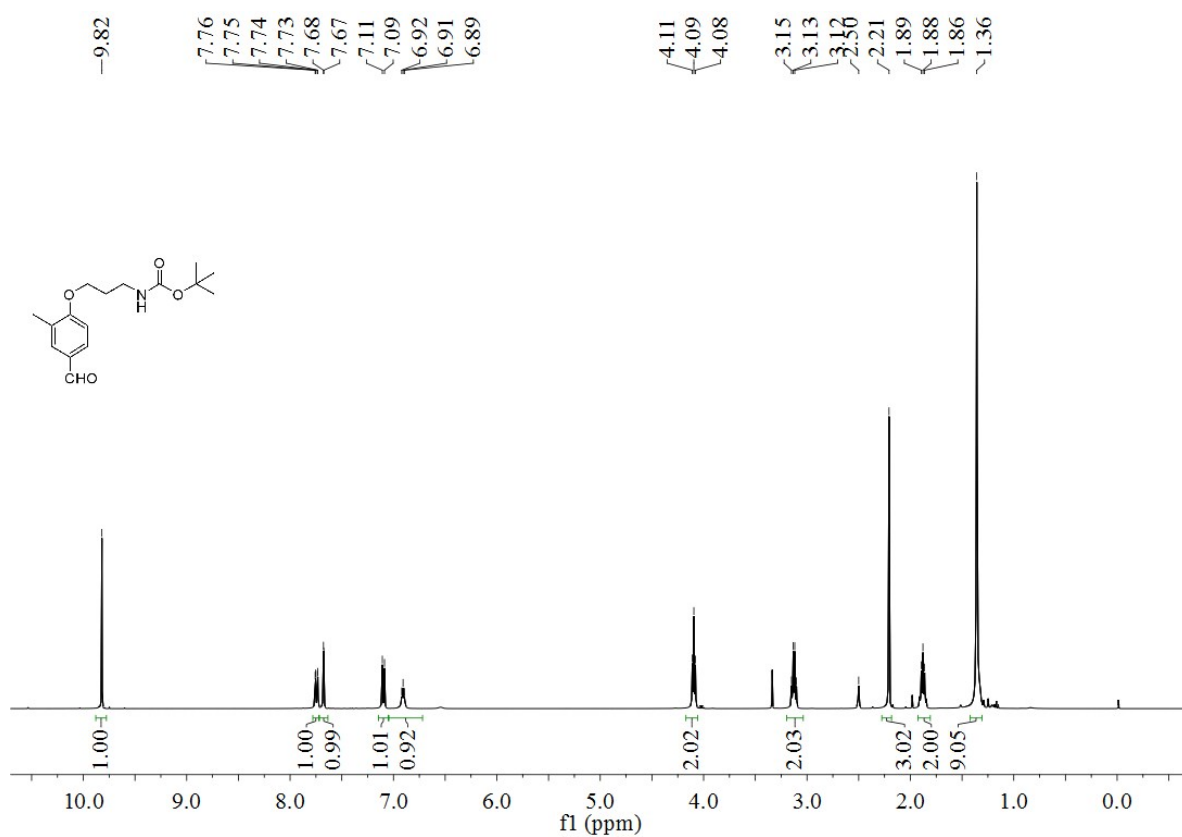


Fig. S27. ^1H -NMR spectrum of **1e** (400 MHz, $\text{DMSO-}d_6$).

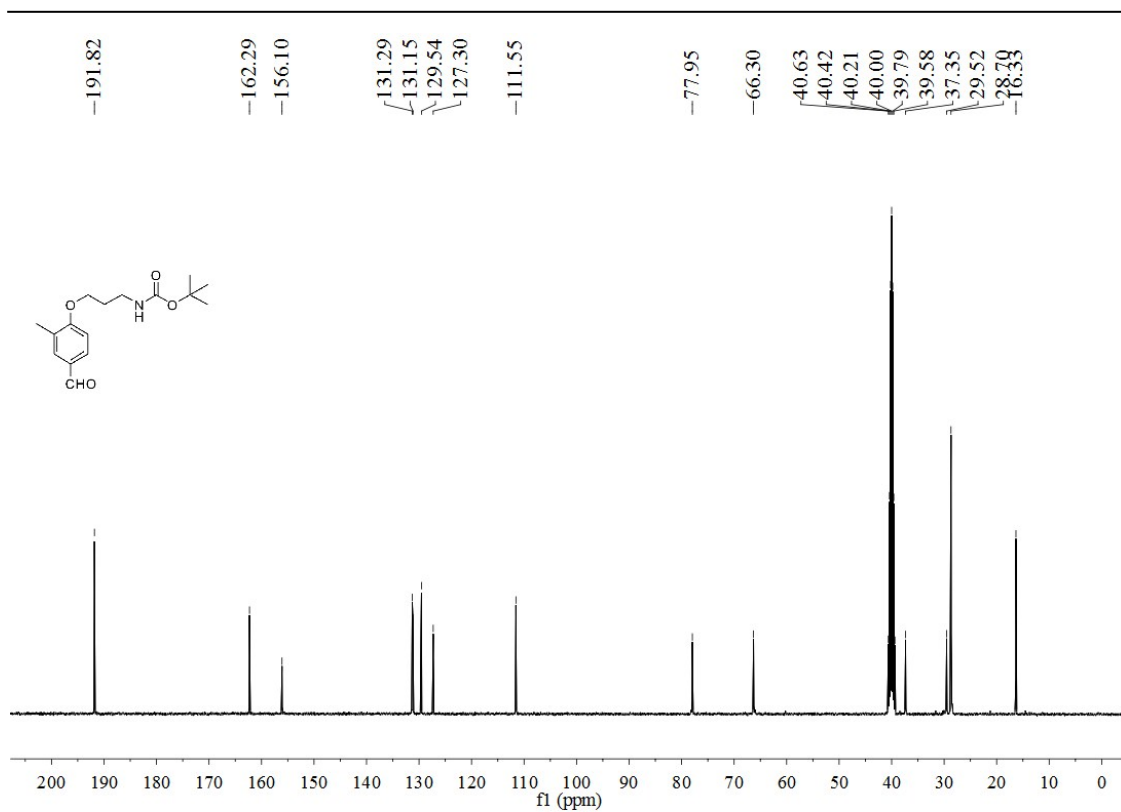


Fig. S28. $^{13}\text{C-NMR}$ spectrum of **1e** (100 MHz, $\text{DMSO-}d_6$).

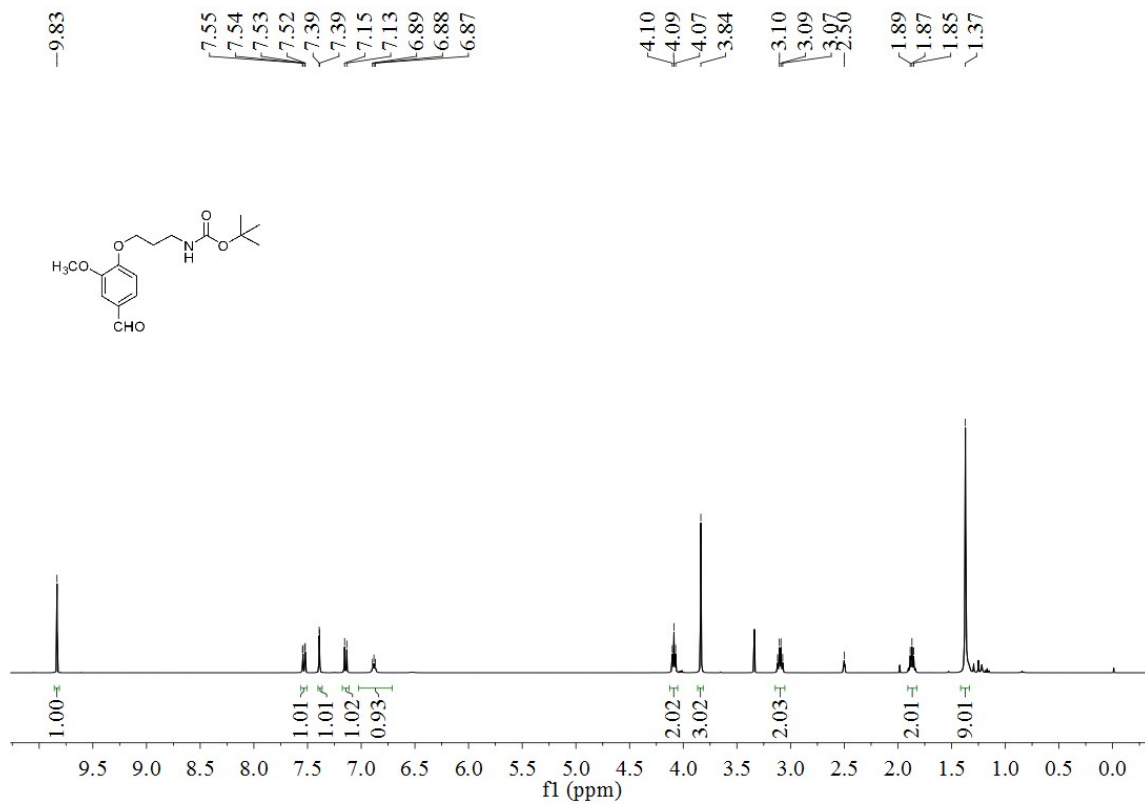


Fig. S29. $^1\text{H-NMR}$ spectrum of **1f** (400 MHz, $\text{DMSO-}d_6$).

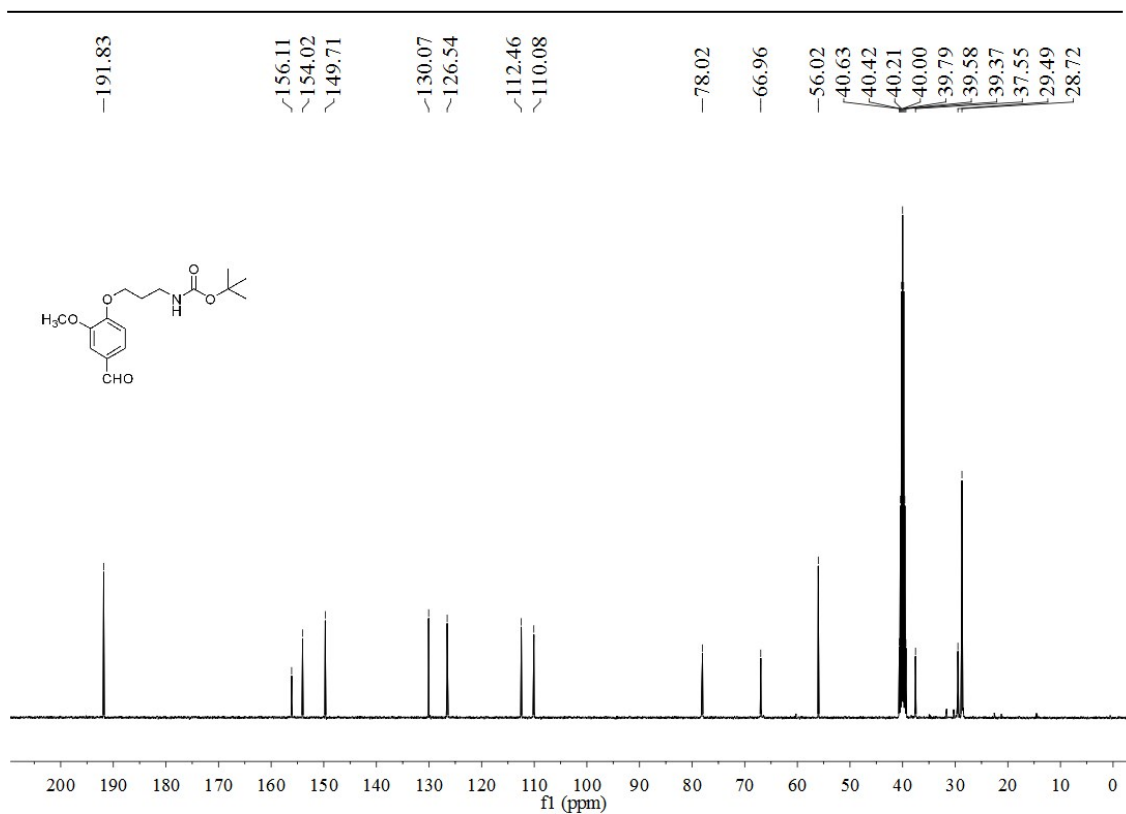


Fig. S30. ¹³C-NMR spectrum of **1f** (100 MHz, DMSO-*d*₆).

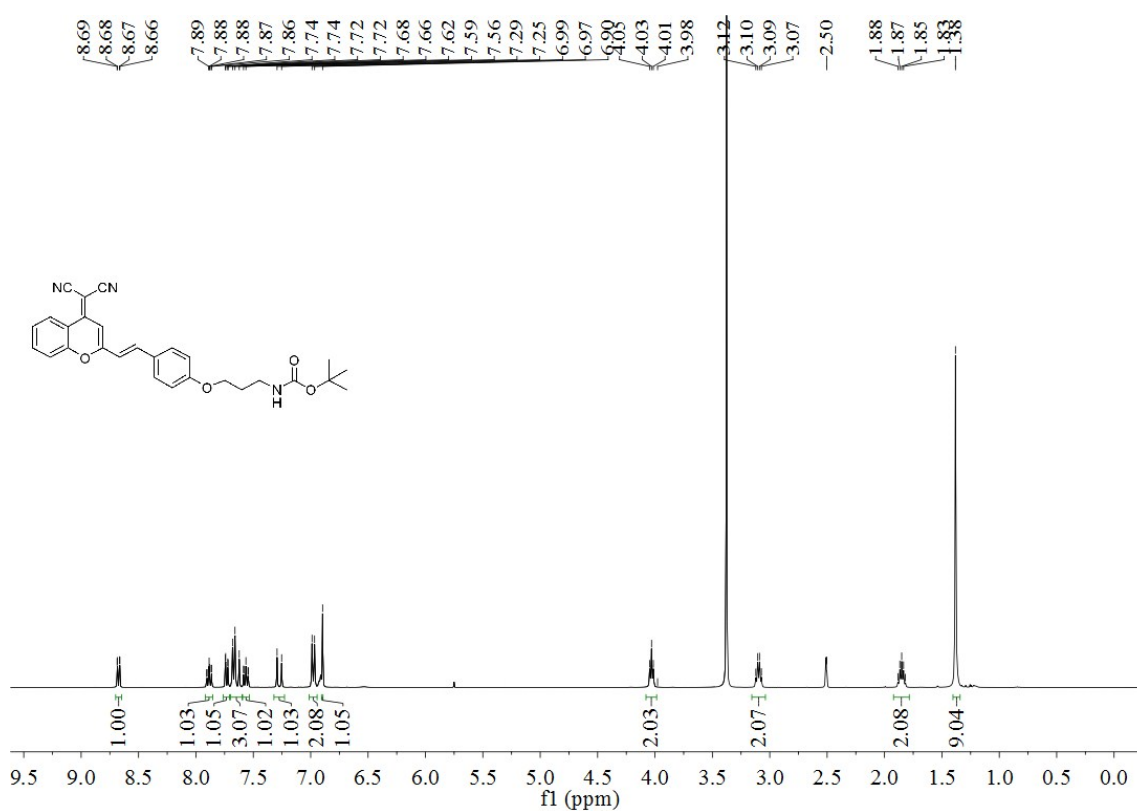


Fig. S31. ¹H-NMR spectrum of **2a** (400 MHz, DMSO-*d*₆).

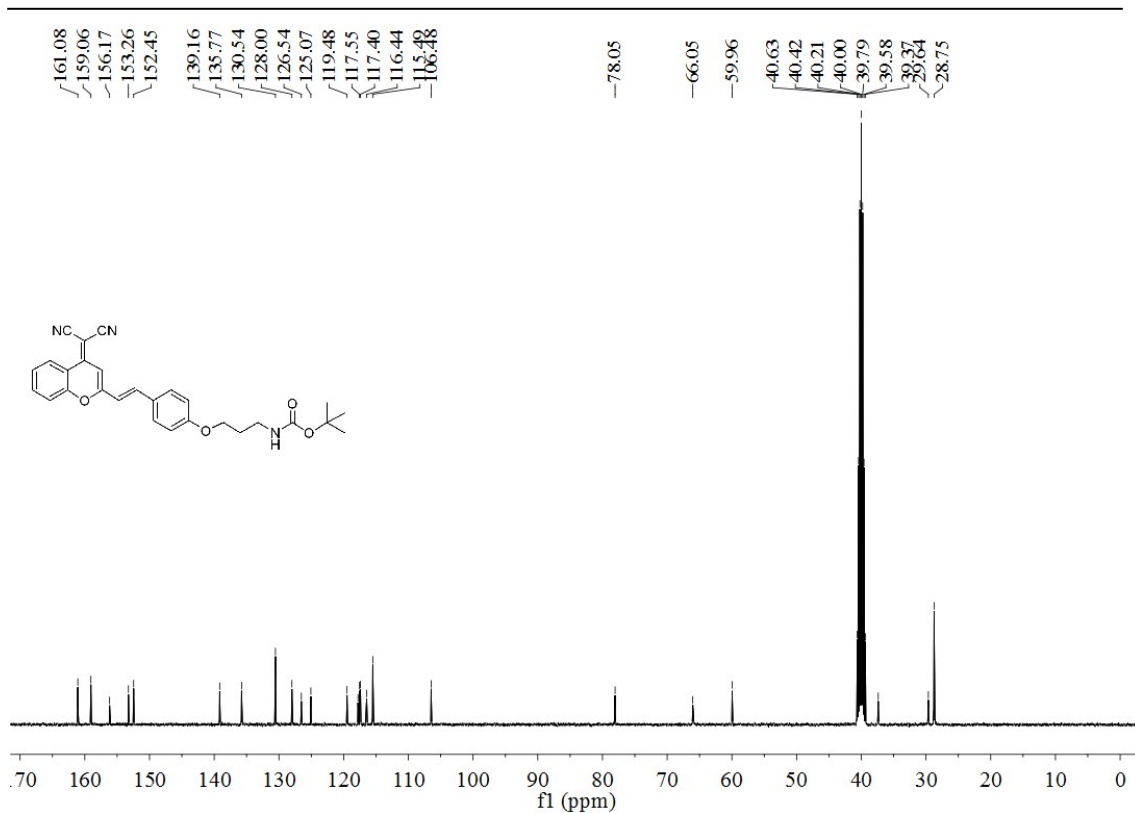


Fig. S32. $^{13}\text{C-NMR}$ spectrum of **2a** (100 MHz, $\text{DMSO-}d_6$).

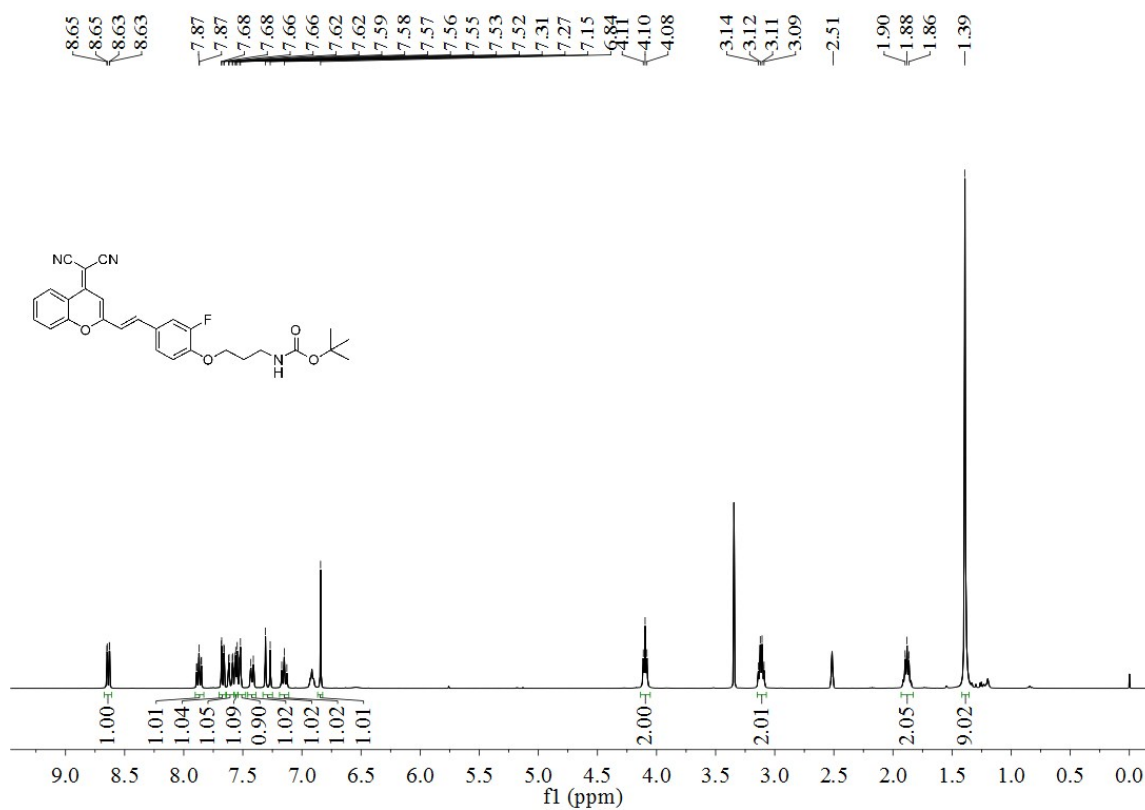


Fig. S33. $^1\text{H-NMR}$ spectrum of **2b** (400 MHz, $\text{DMSO-}d_6$).

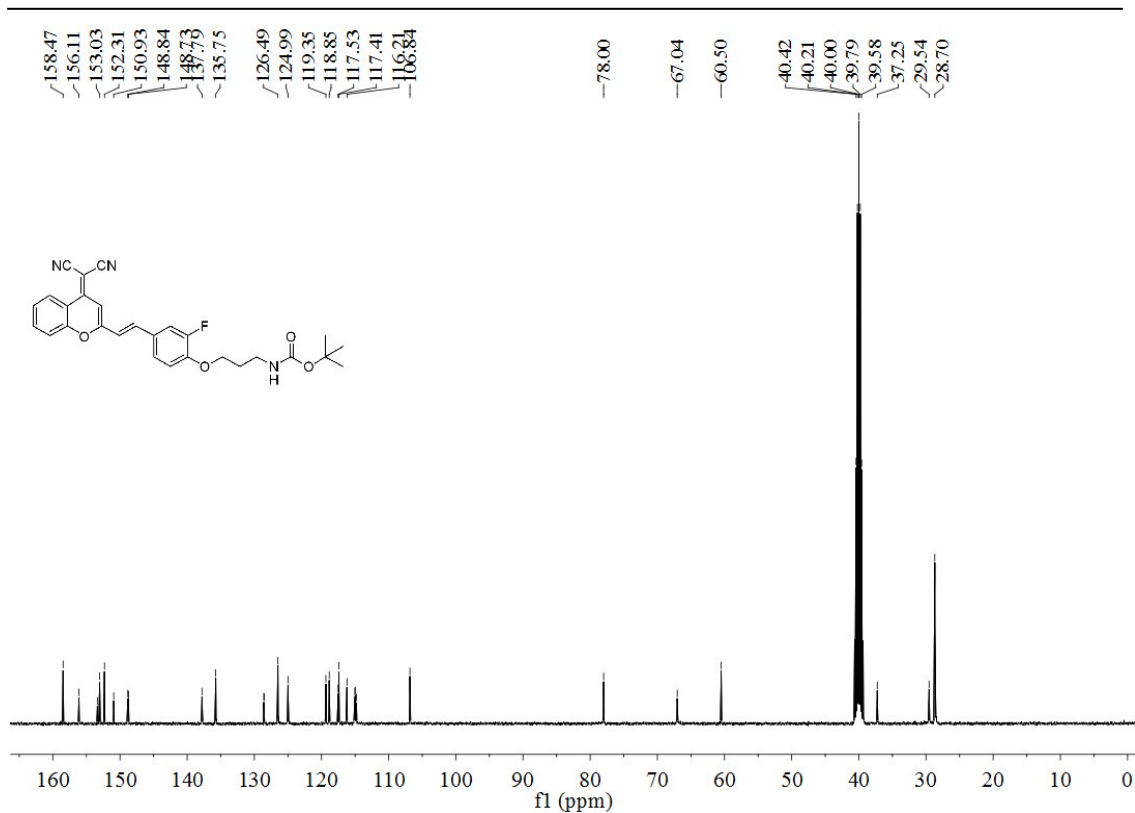


Fig. S34. ¹³C-NMR spectrum of **2b** (100 MHz, DMSO-*d*₆).

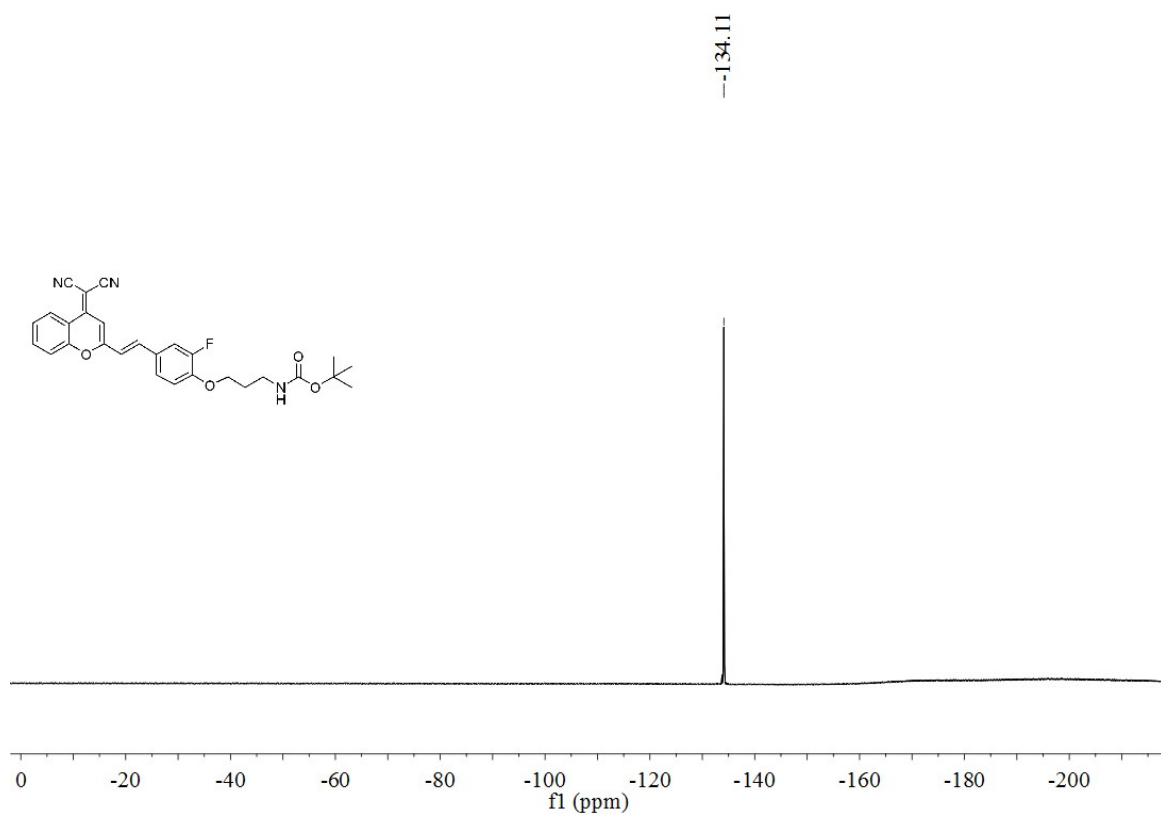


Fig. S35. ¹⁹F-NMR spectrum of **2b** (400 MHz, DMSO-*d*₆).

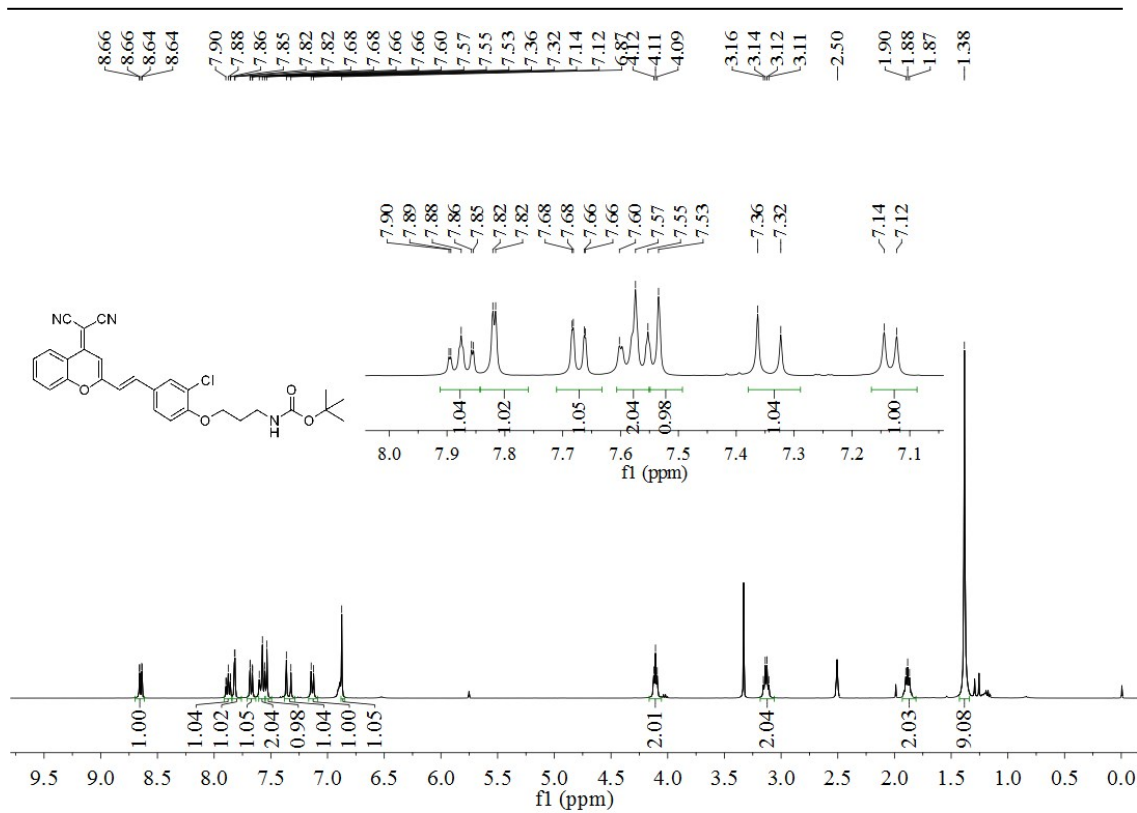


Fig. S36. $^1\text{H-NMR}$ spectrum of **2c** (400 MHz, $\text{DMSO-}d_6$).

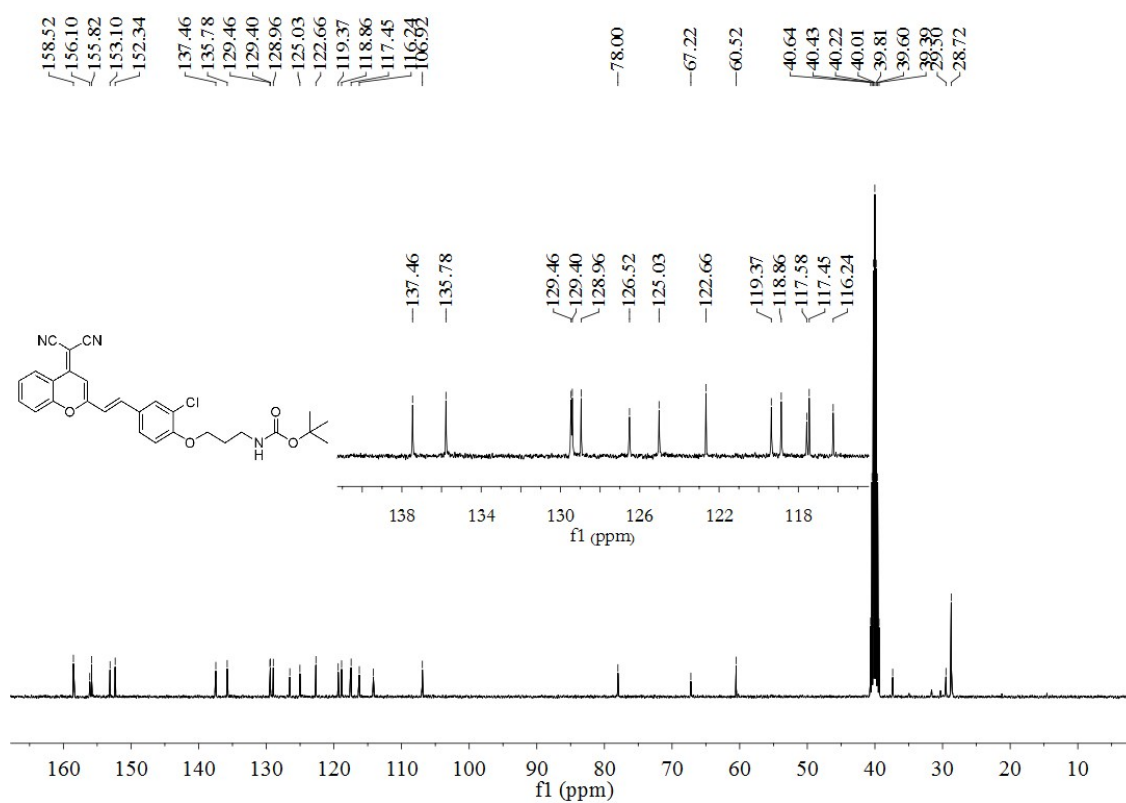


Fig. S37. $^{13}\text{C-NMR}$ spectrum of **2c** (100 MHz, $\text{DMSO-}d_6$).

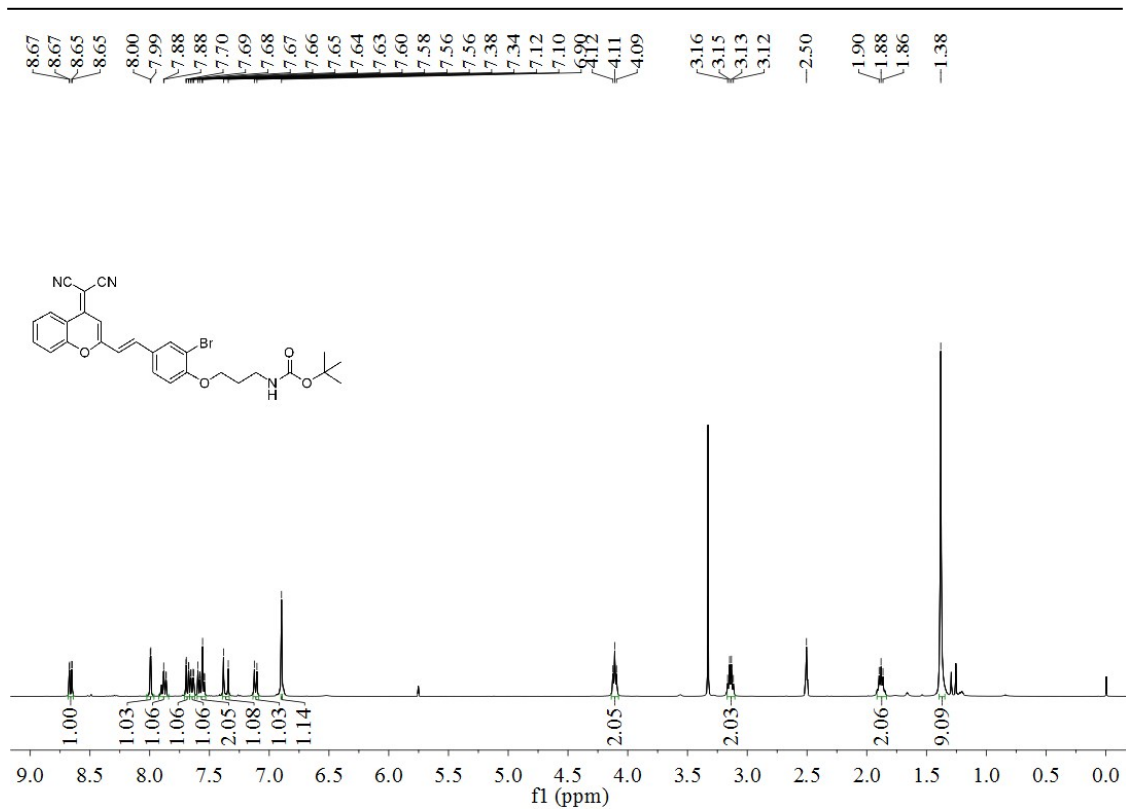


Fig. S38. ¹H-NMR spectrum of **2d** (400 MHz, DMSO-*d*₆).

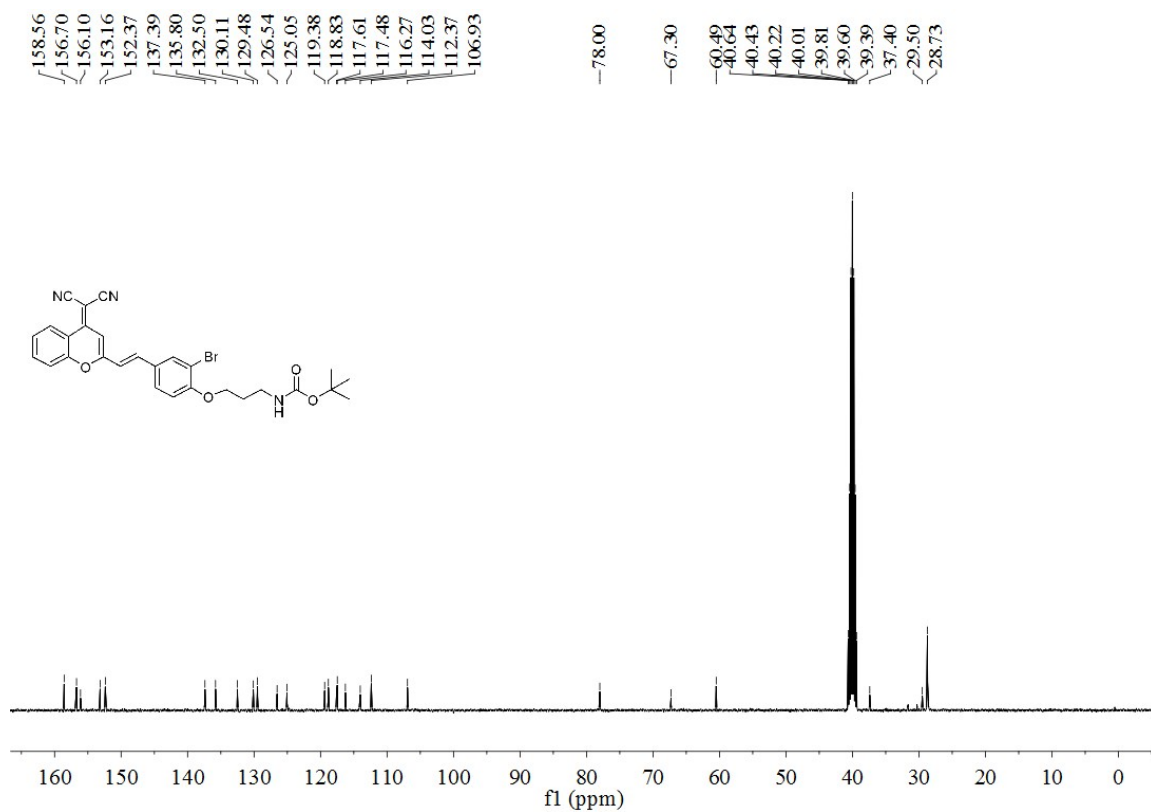


Fig. S39. ¹³C-NMR spectrum of **2d** (100 MHz, DMSO-*d*₆).

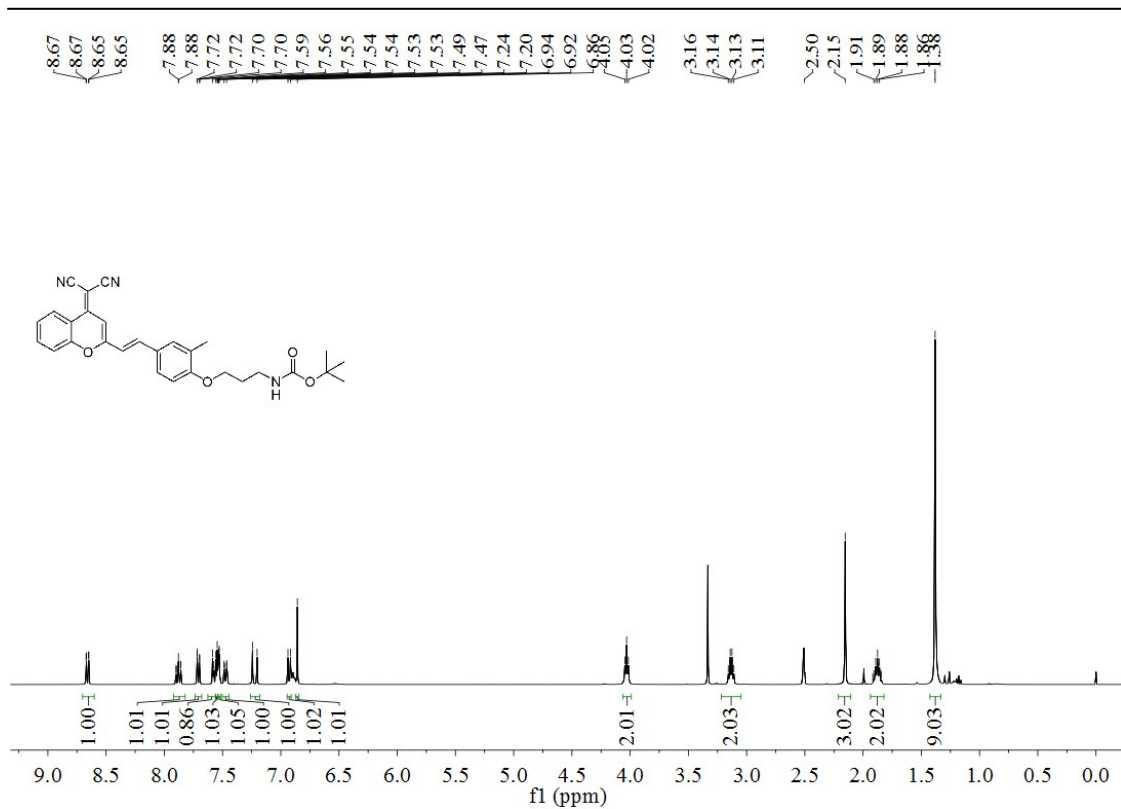


Fig. S40. ¹H-NMR spectrum of **2e** (400 MHz, DMSO-*d*₆).

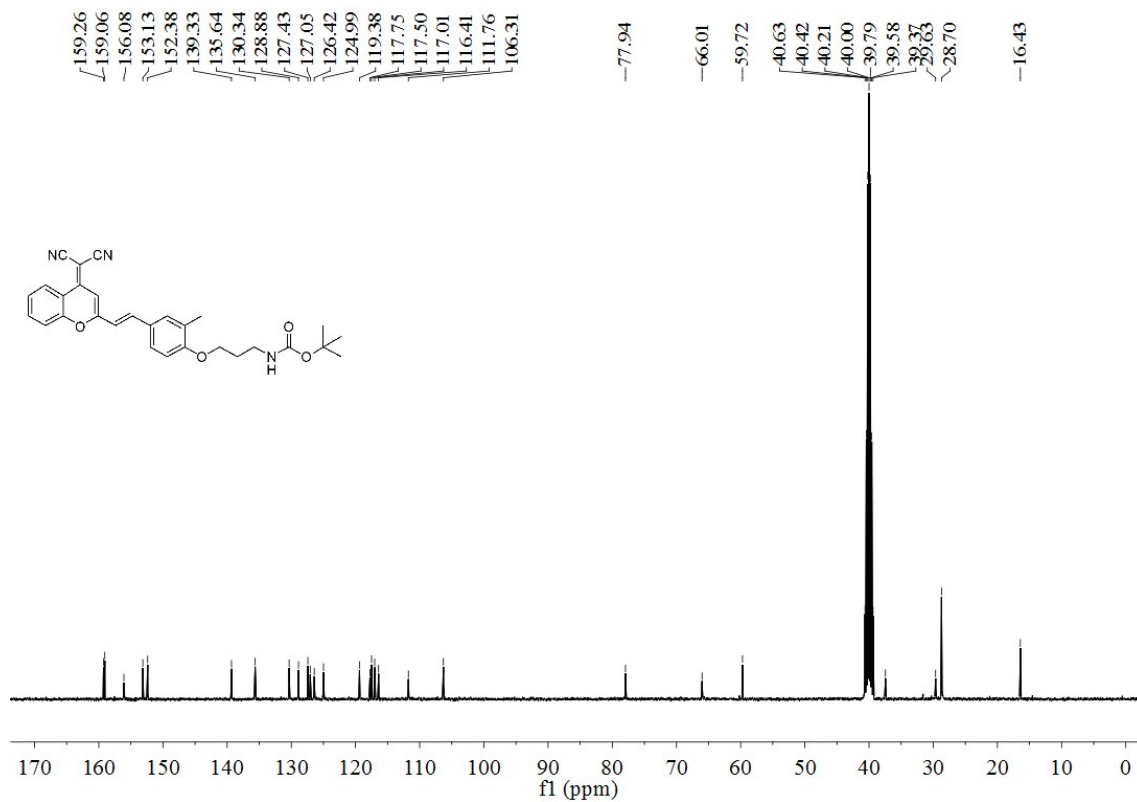


Fig. S41. ¹³C-NMR spectrum of **2e** (100 MHz, DMSO-*d*₆).

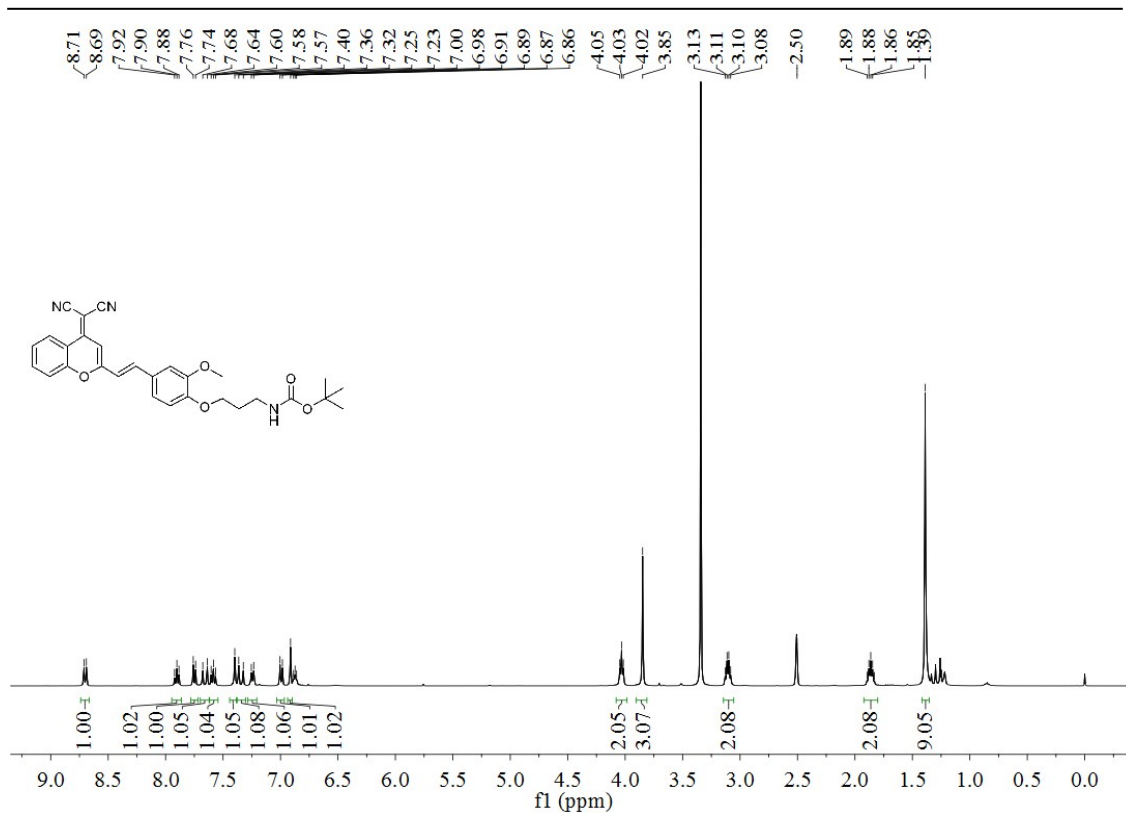


Fig. S42. ¹H-NMR spectrum of **2f** (400 MHz, DMSO-*d*₆).

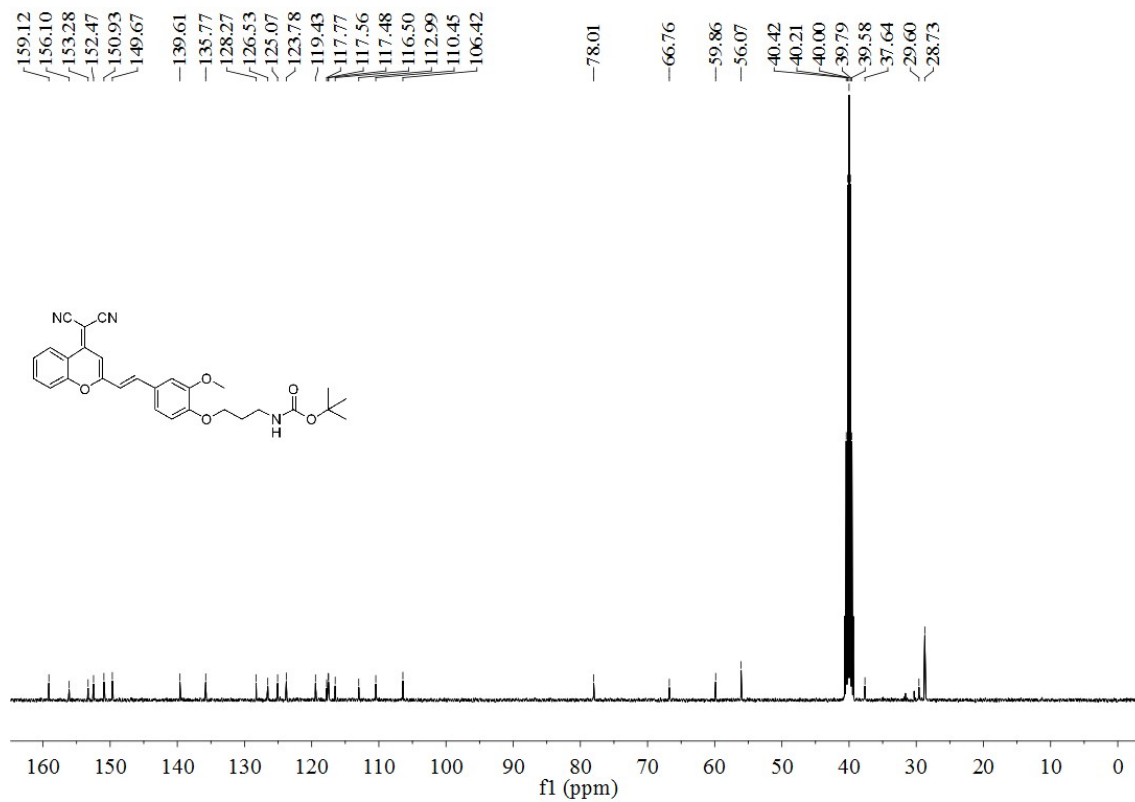


Fig. S43. ¹³C-NMR spectrum of **2f** (100 MHz, DMSO-*d*₆).

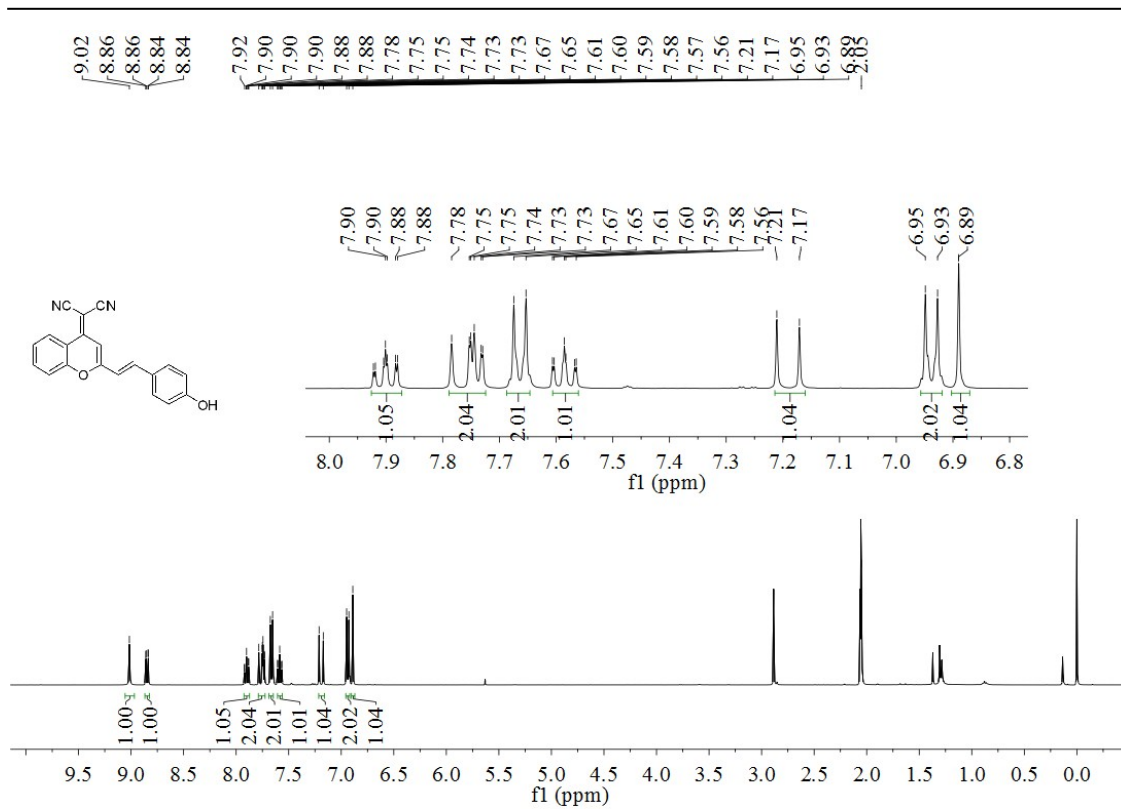


Fig. S44. ¹H-NMR spectrum of **3a** (400 MHz, Acetone).

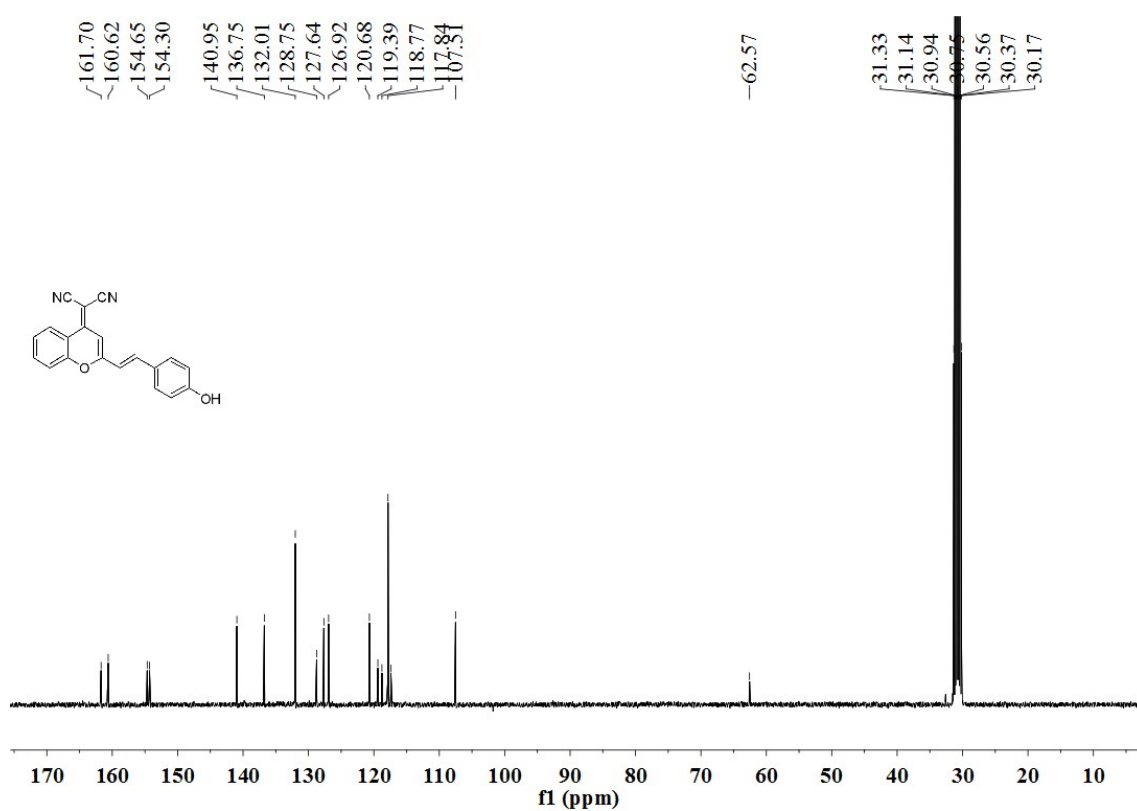


Fig. S45. ¹³C-NMR spectrum of **3a** (100 MHz, Acetone).

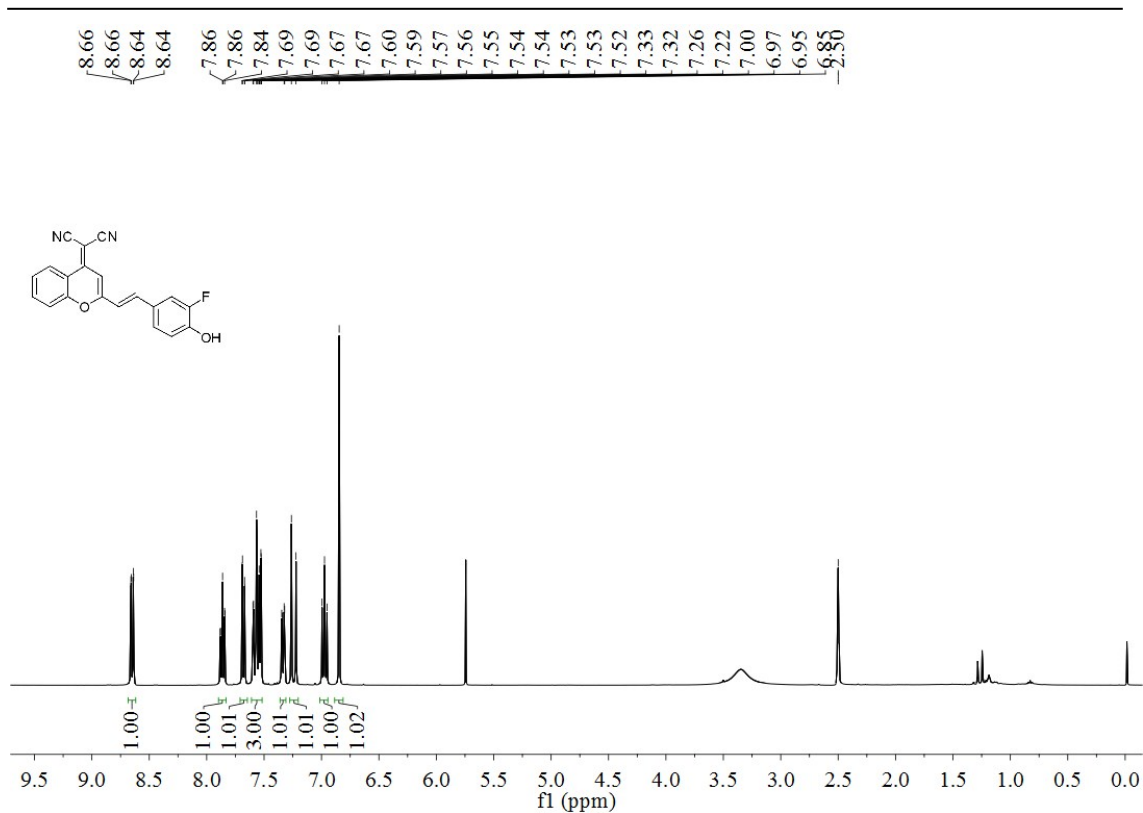


Fig. S46. ¹H-NMR spectrum of **3b** (400 MHz, DMSO-*d*₆).

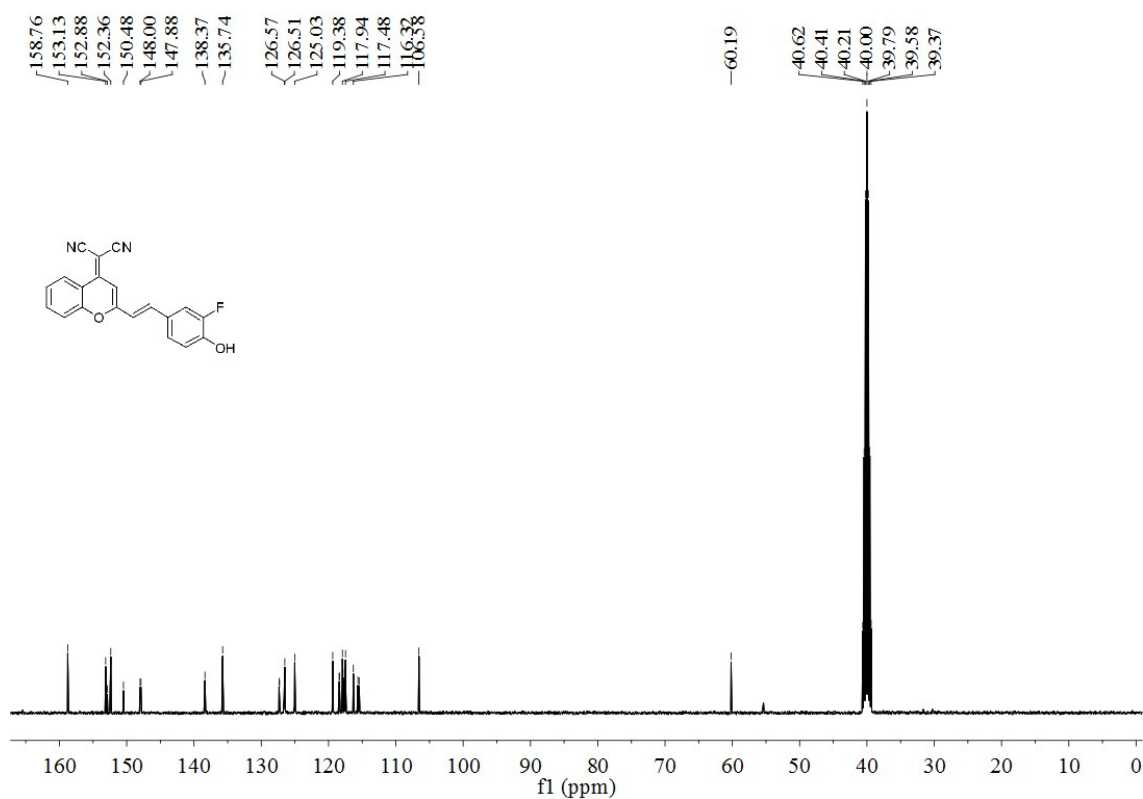


Fig. S47. ¹³C-NMR spectrum of **3b** (100 MHz, DMSO-*d*₆).

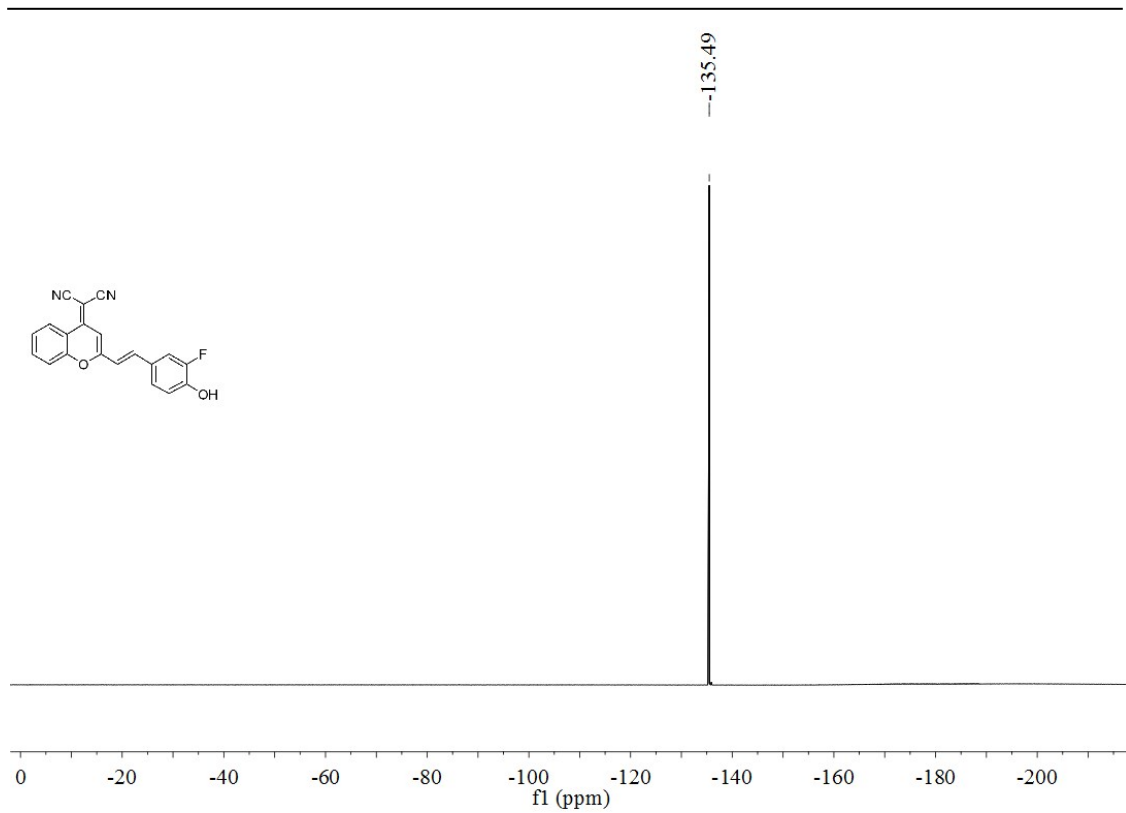


Fig. S48. ^{19}F -NMR spectrum of **3b** (400 MHz, $\text{DMSO-}d_6$).

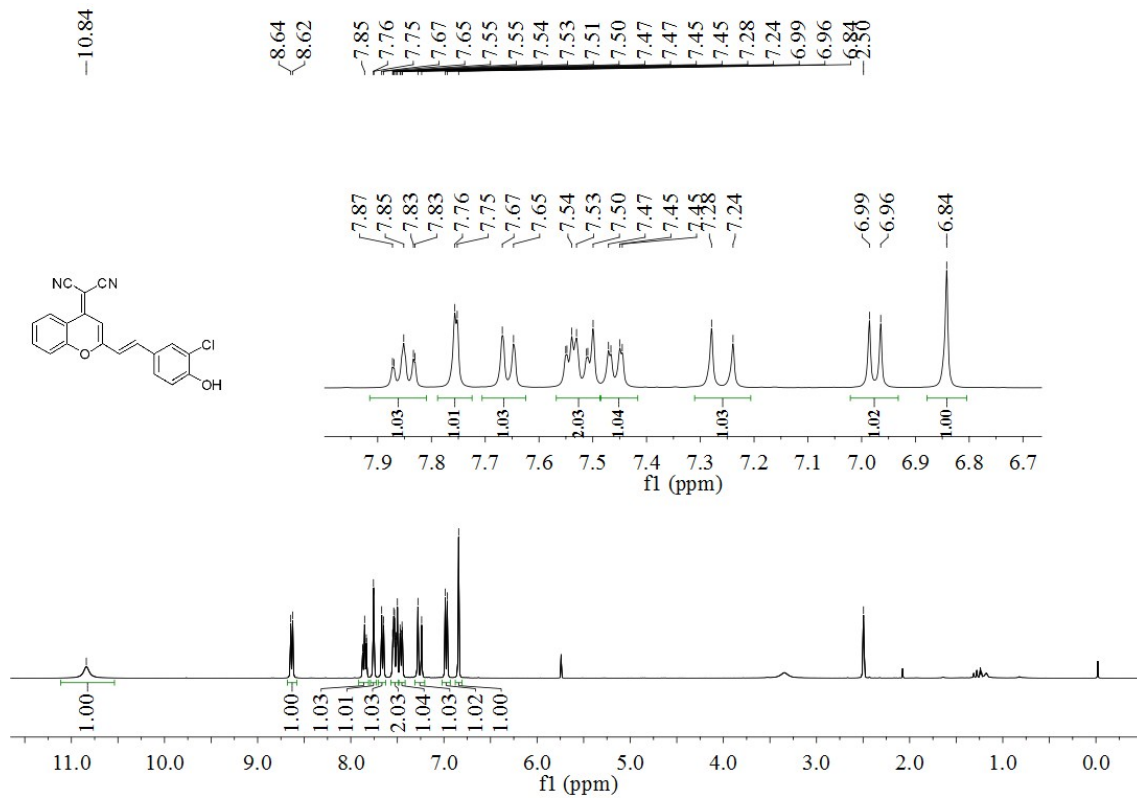


Fig. S49. ^1H -NMR spectrum of **3c** (400 MHz, $\text{DMSO-}d_6$).

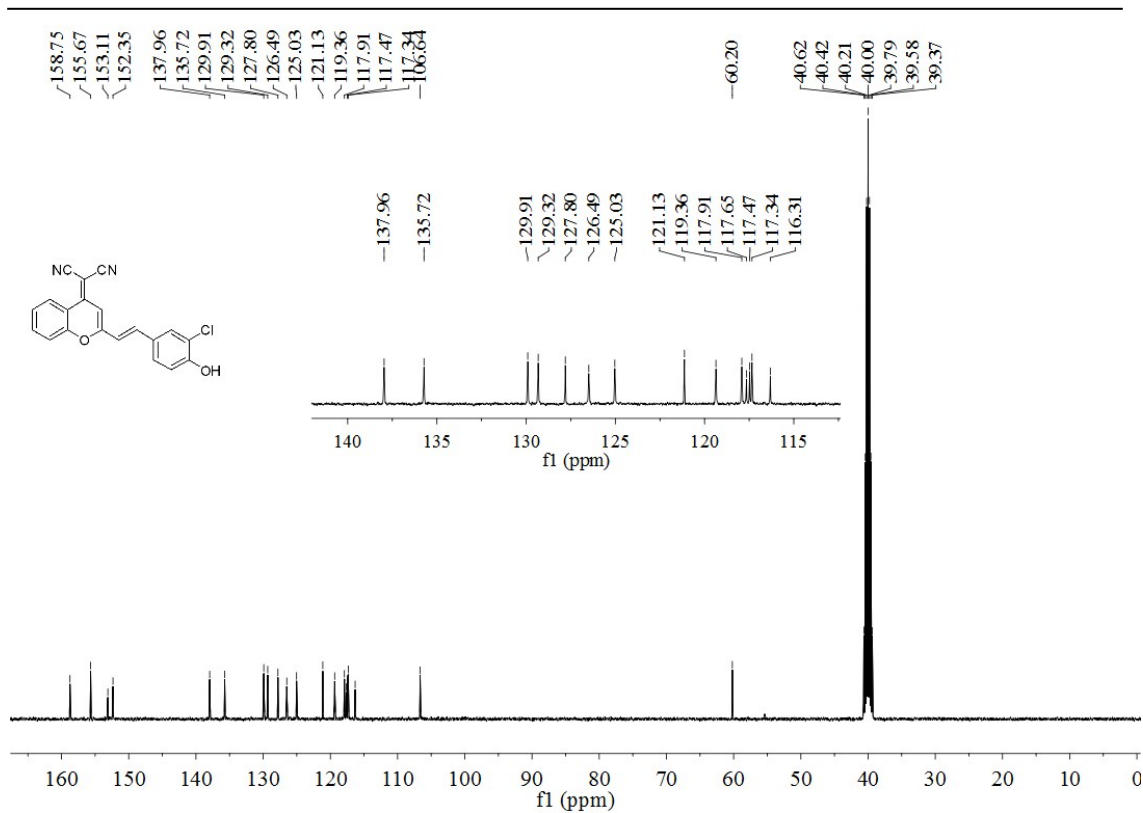


Fig. S50. ^{13}C -NMR spectrum of **3c** (100 MHz, $\text{DMSO-}d_6$).

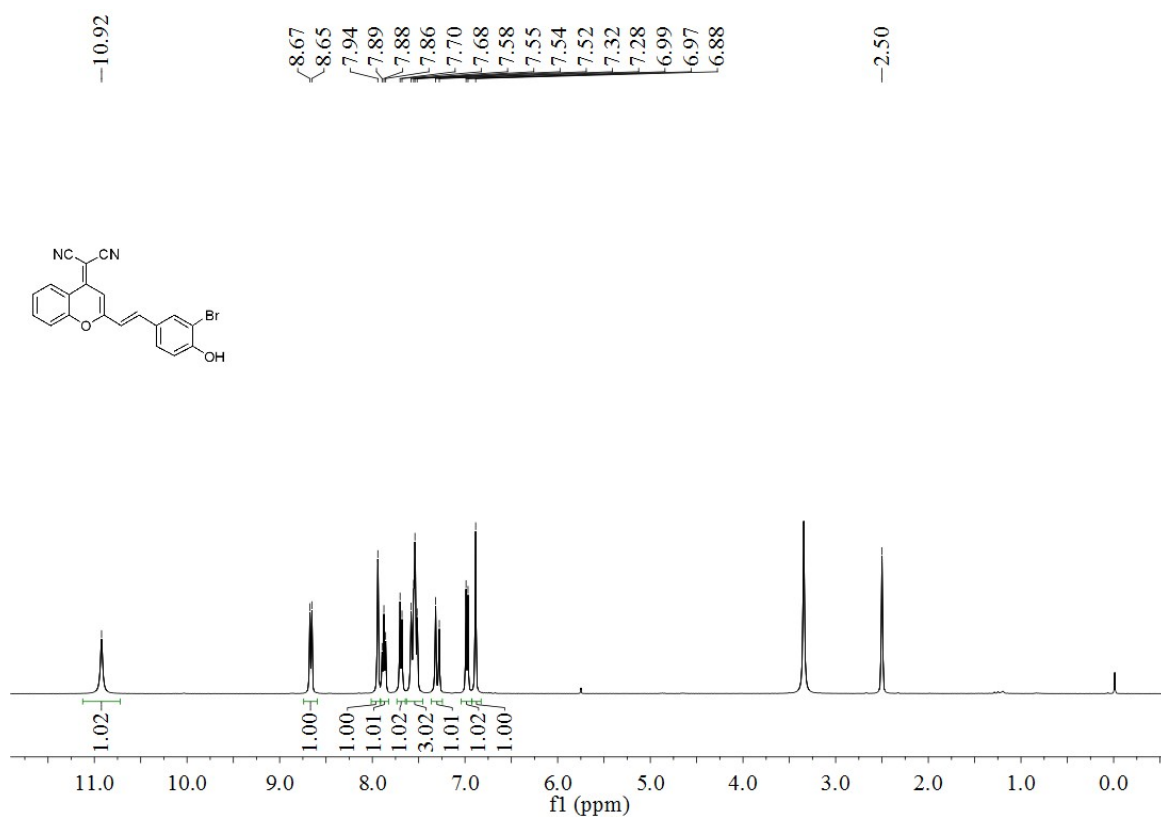


Fig. S51. ^1H -NMR spectrum of **3d** (400 MHz, $\text{DMSO-}d_6$).

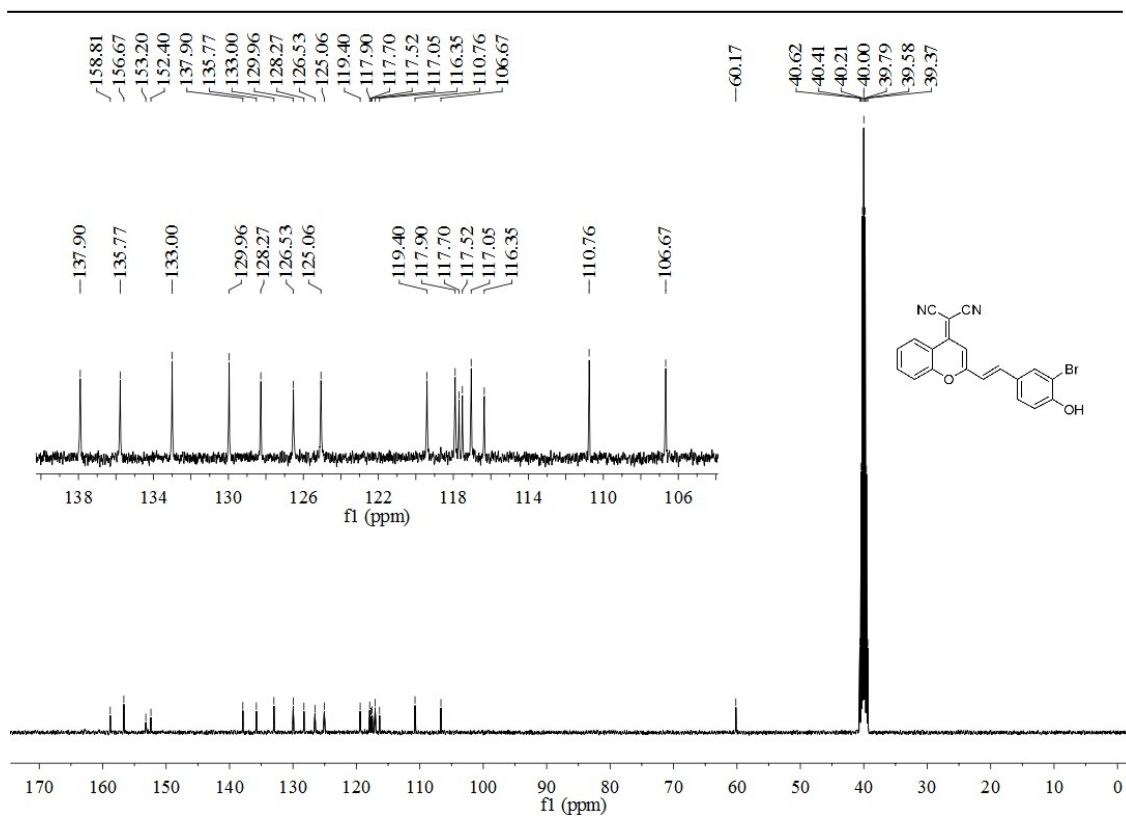


Fig. S52. ¹³C-NMR spectrum of **3d** (100 MHz, DMSO-*d*₆).

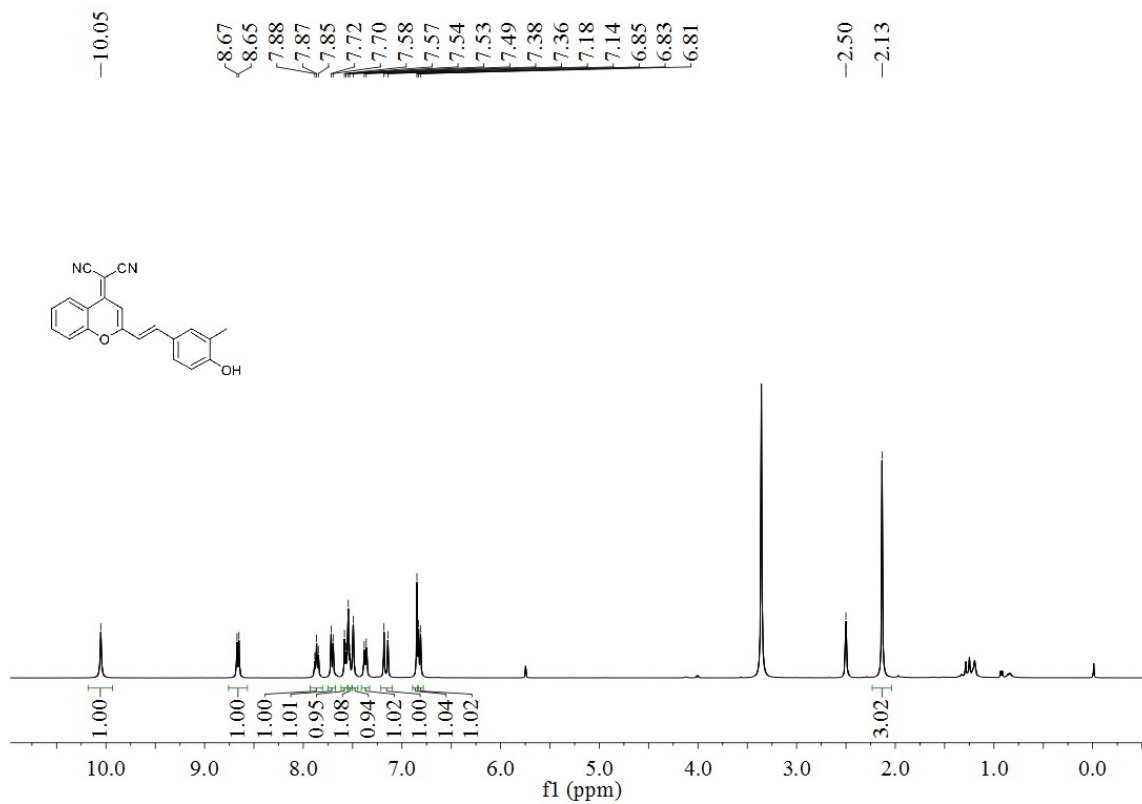


Fig. S53. ¹H-NMR spectrum of **3e** (400 MHz, DMSO-*d*₆).

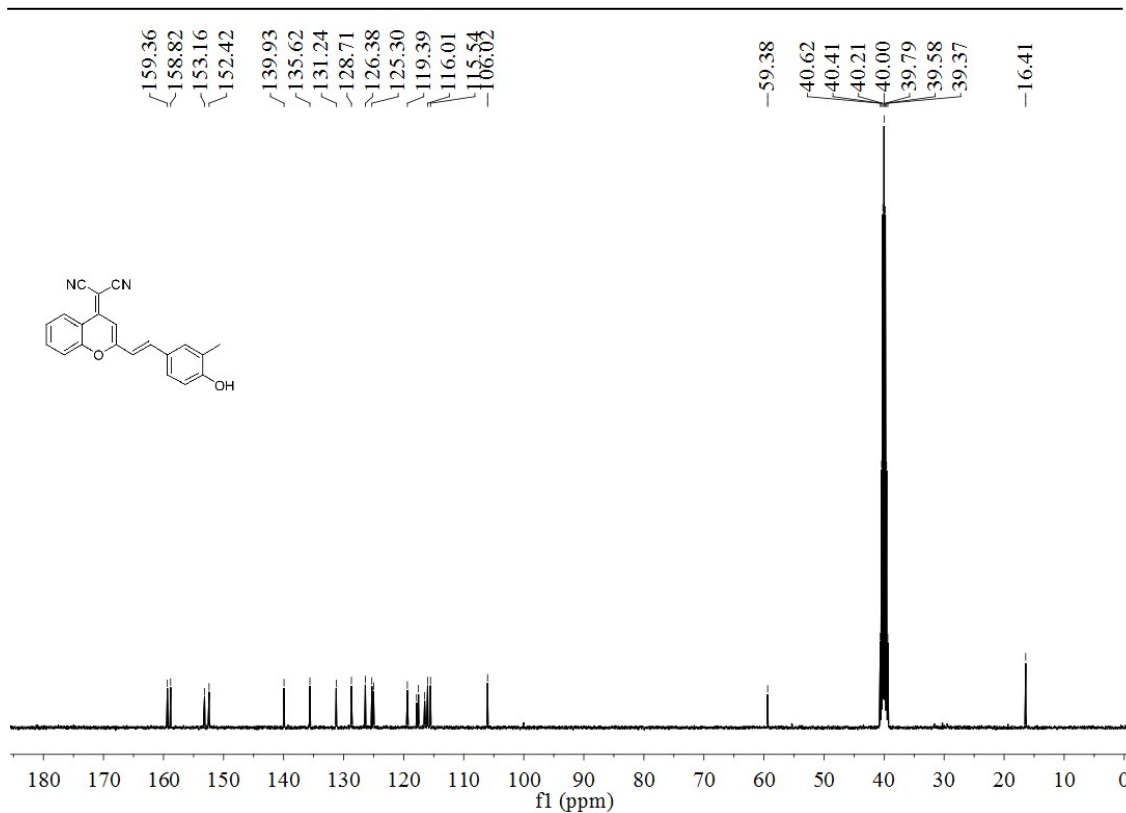


Fig. S54. ¹³C-NMR spectrum of **3e** (100 MHz, DMSO-*d*₆).

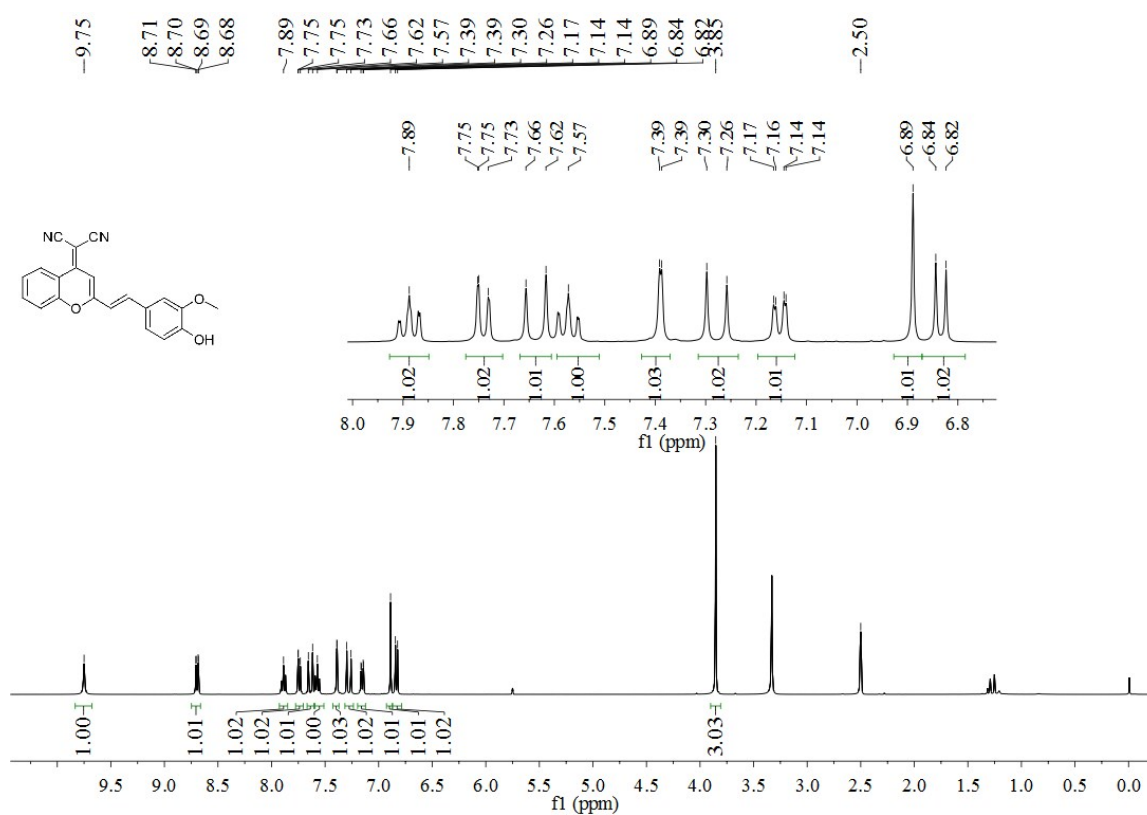


Fig. S55. ¹H-NMR spectrum of **3f** (400 MHz, DMSO-*d*₆).

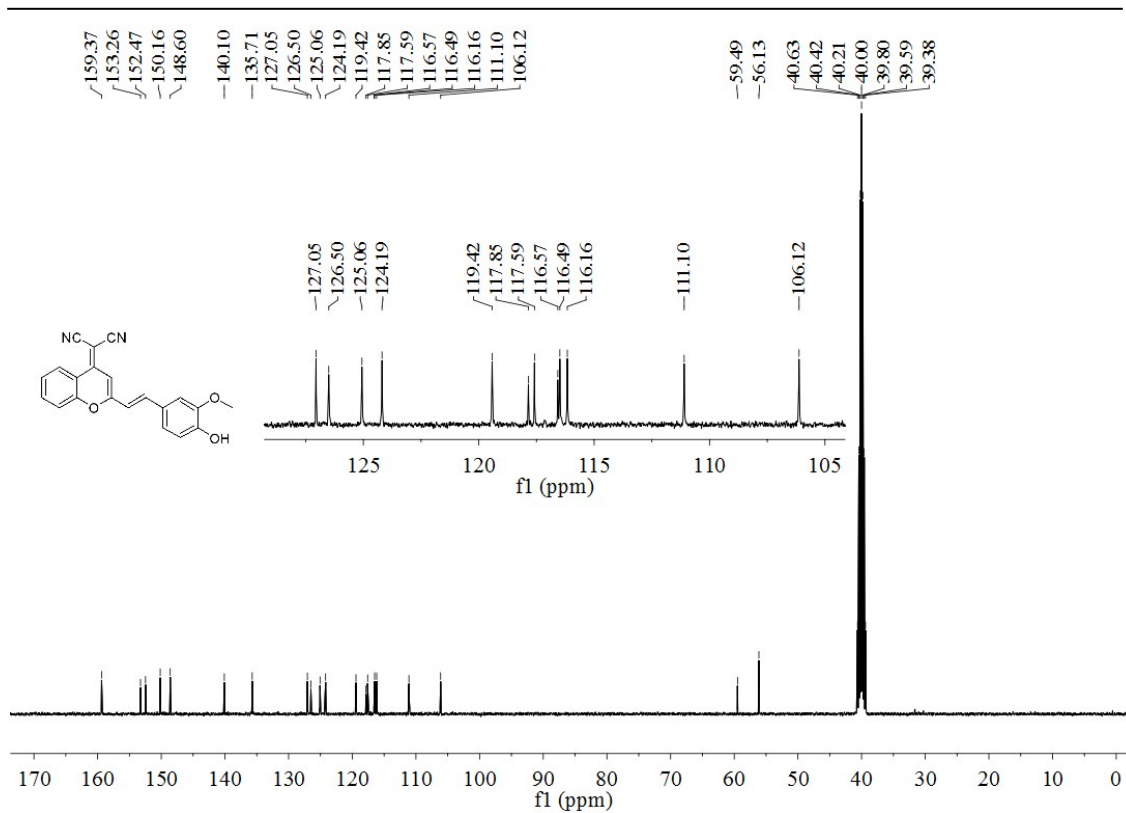


Fig. S56. ¹³C-NMR spectrum of **3f** (100 MHz, DMSO-*d*₆).

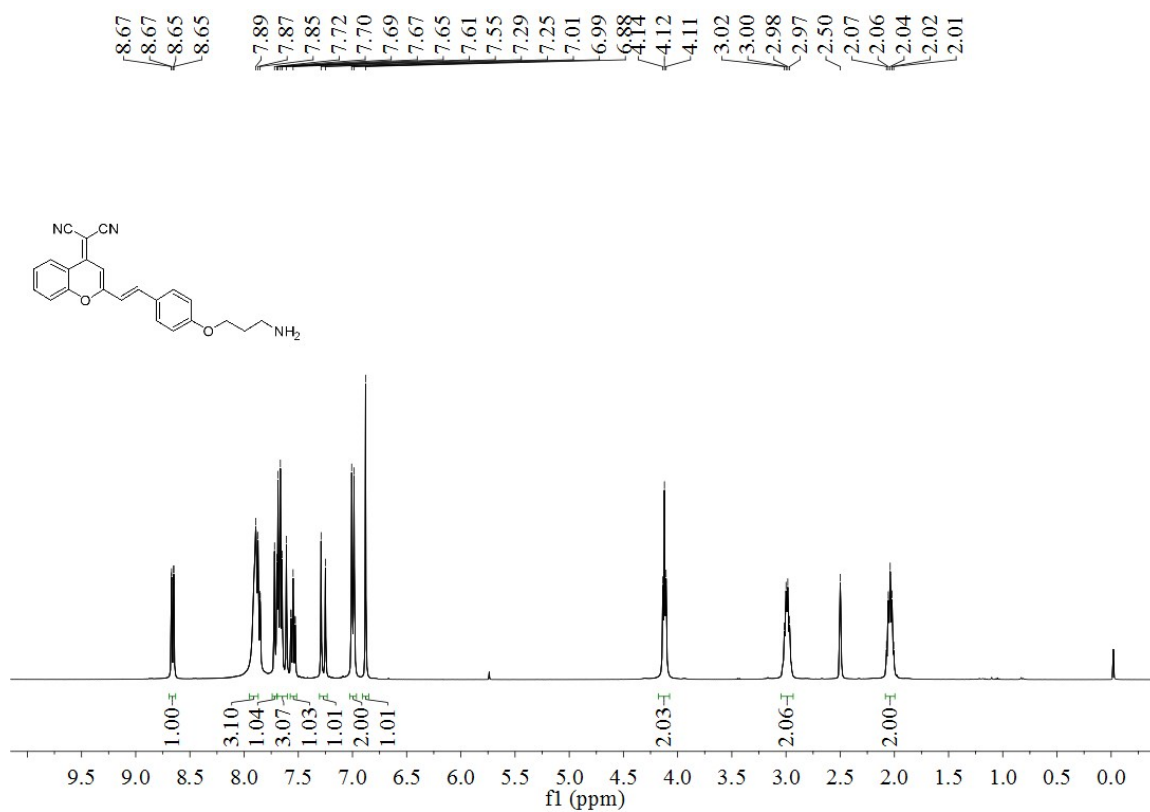


Fig. S57. ¹H-NMR spectrum of **probe 1** (400 MHz, DMSO-*d*₆).

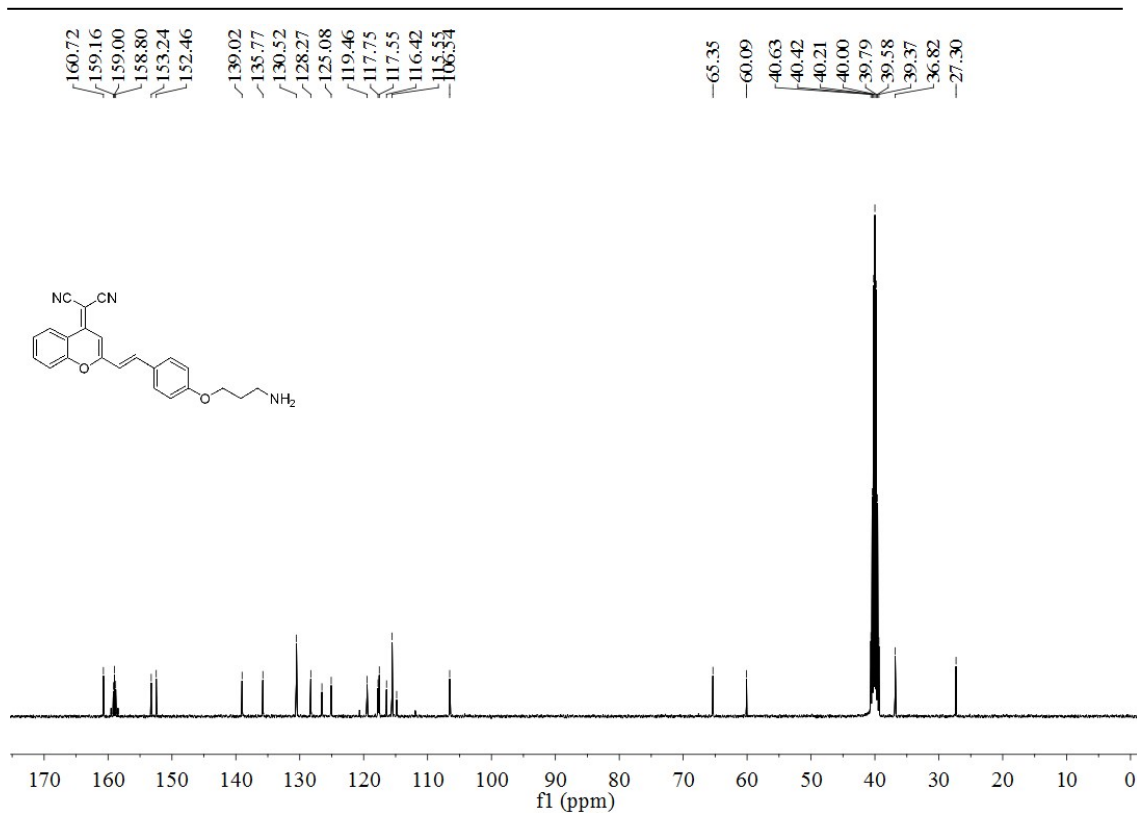


Fig. S58. ¹³C-NMR spectrum of probe 1 (100 MHz, DMSO-*d*₆).

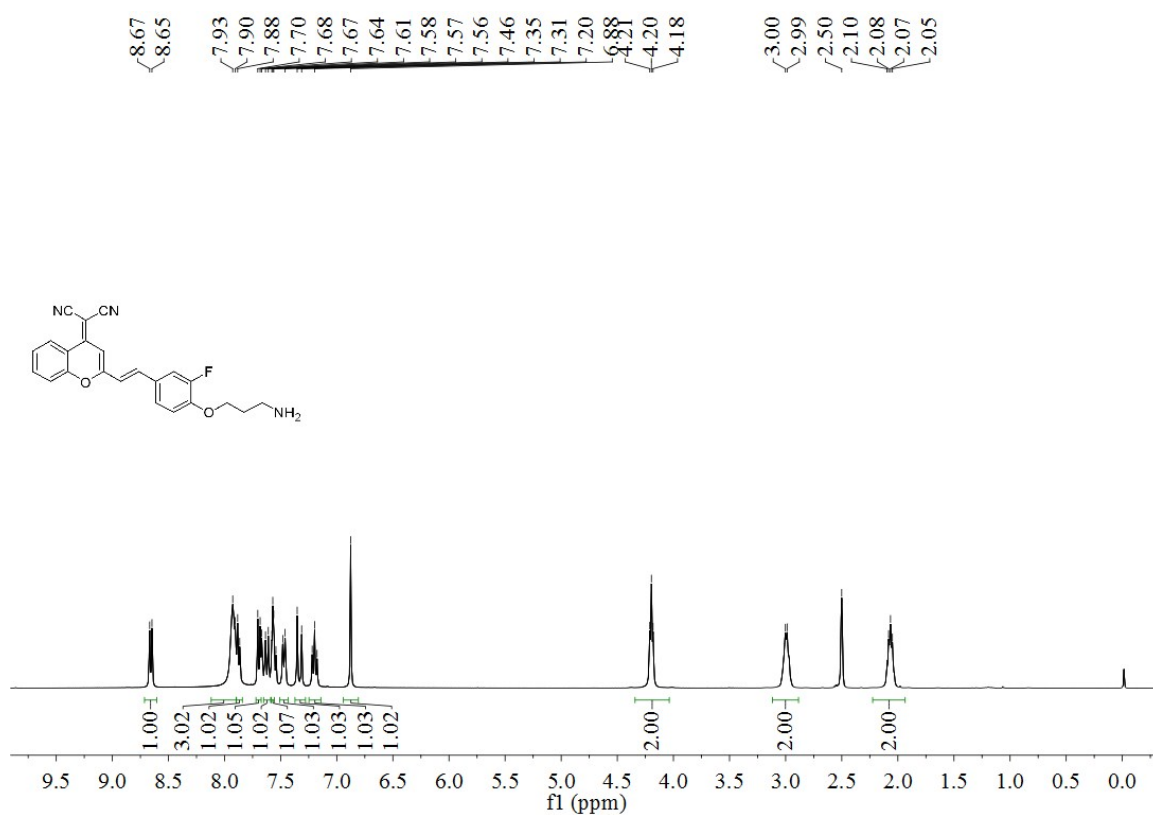


Fig. S59. ¹H-NMR spectrum of probe 2 (400 MHz, DMSO-*d*₆).

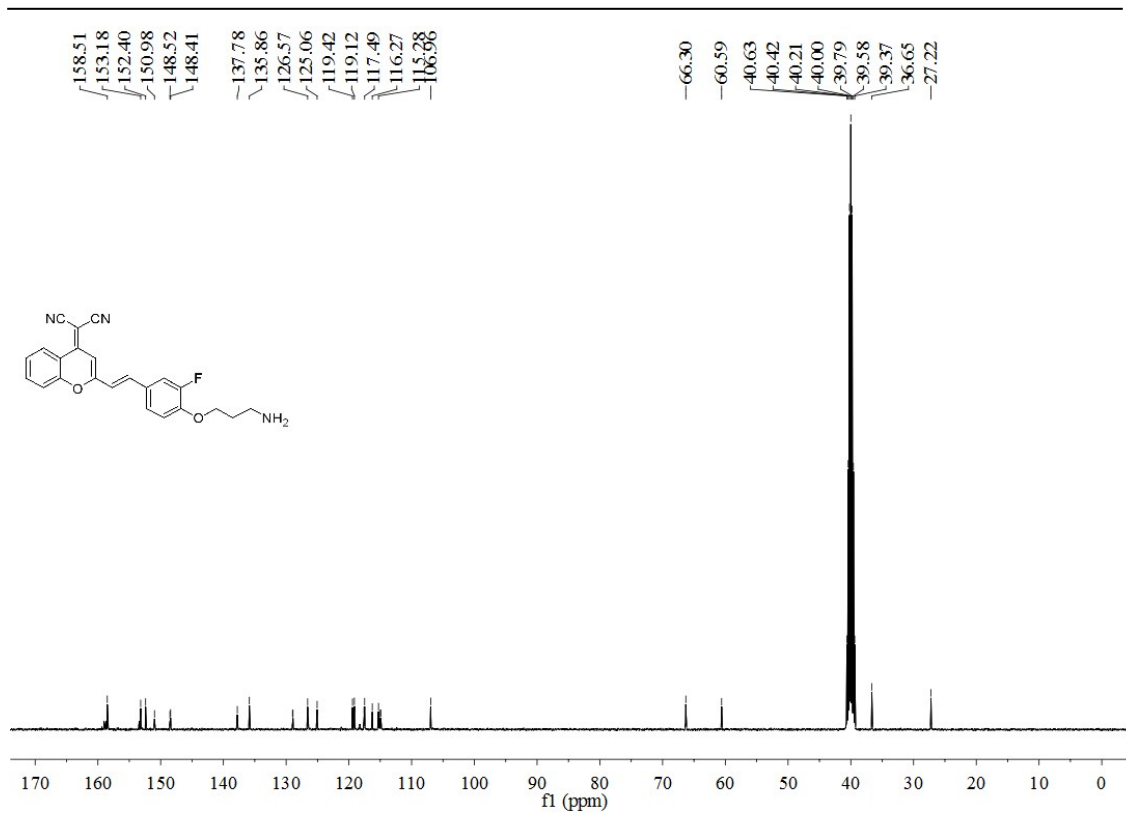


Fig. S60. ¹³C-NMR spectrum of probe 2 (100 MHz, DMSO-*d*₆).

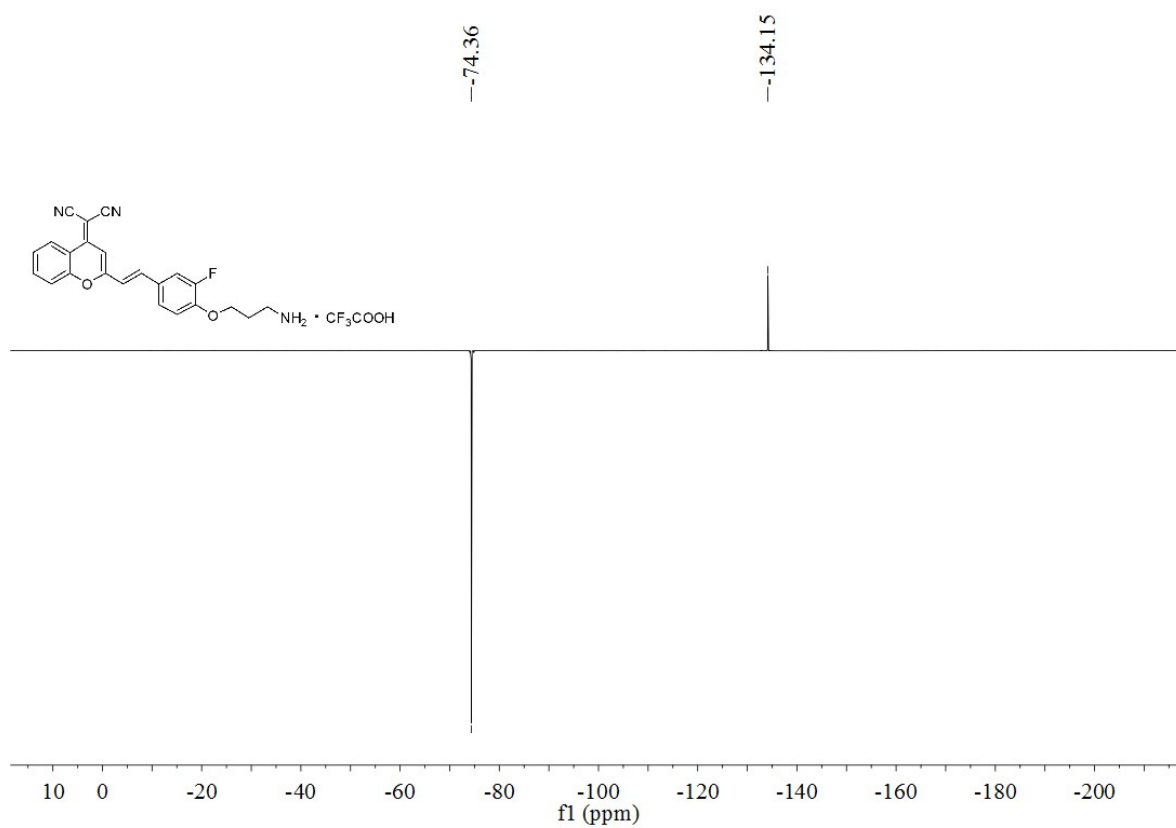


Fig. S61. ¹⁹F-NMR spectrum of probe 2 (400 MHz, DMSO-*d*₆).

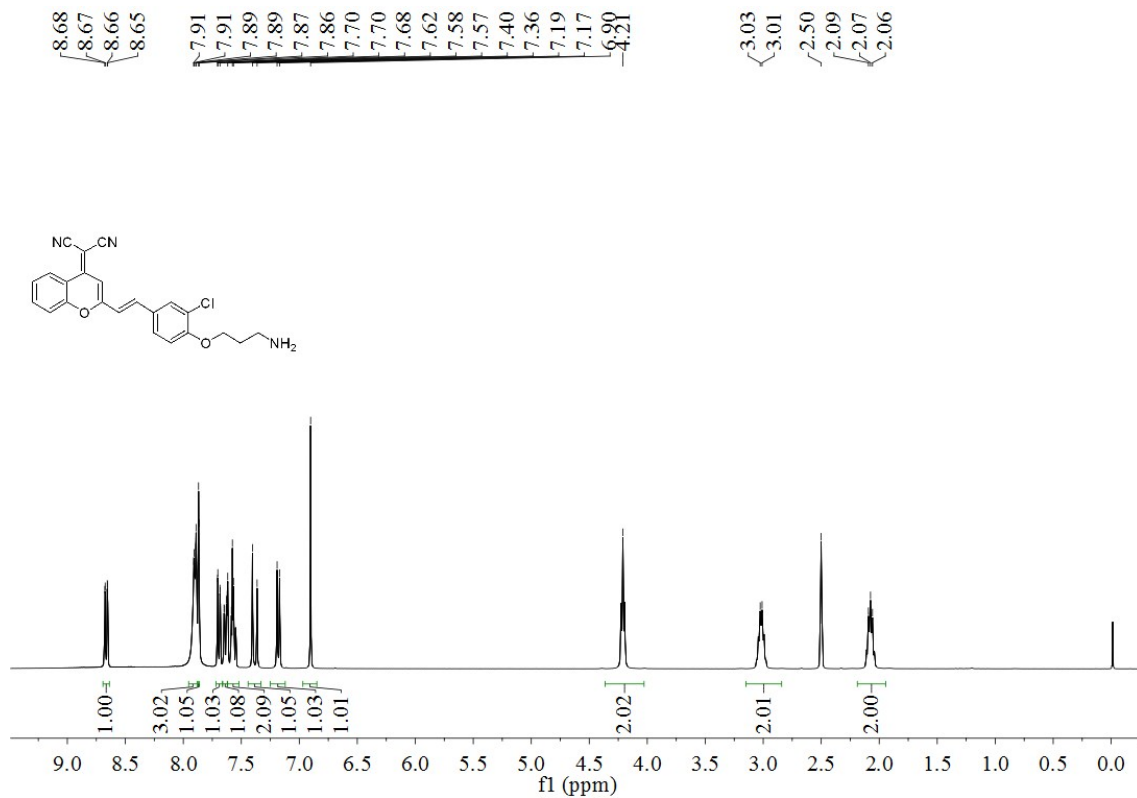


Fig. S62. ¹H-NMR spectrum of probe 3 (400 MHz, DMSO-*d*₆).

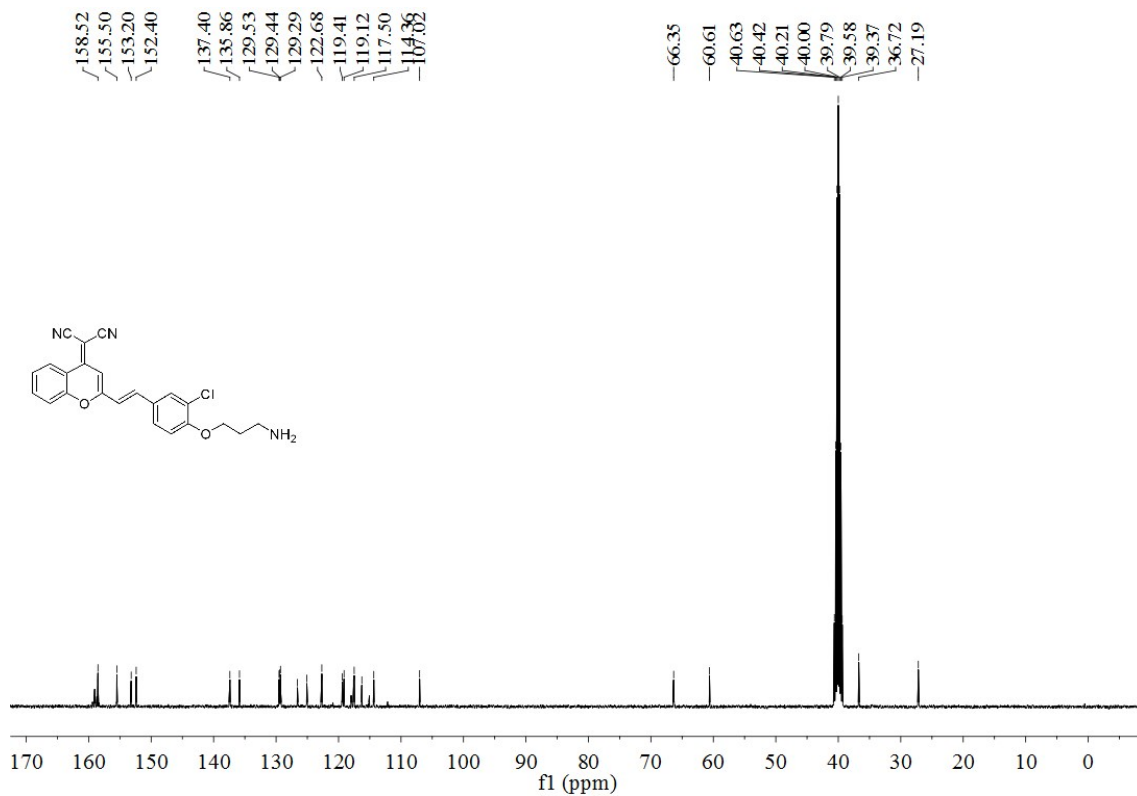


Fig. S63. ¹³C-NMR spectrum of probe 3 (100 MHz, DMSO-*d*₆).

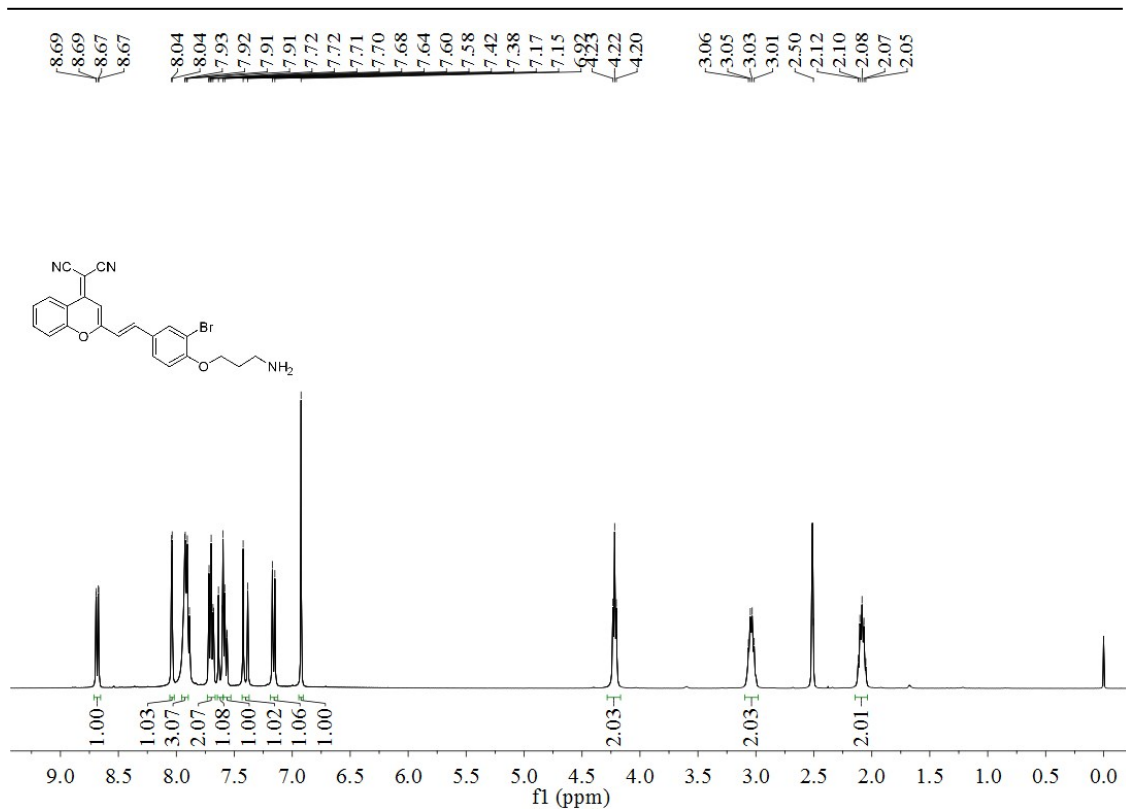


Fig. S64. ¹H-NMR spectrum of probe 4 (400 MHz, DMSO-*d*₆).

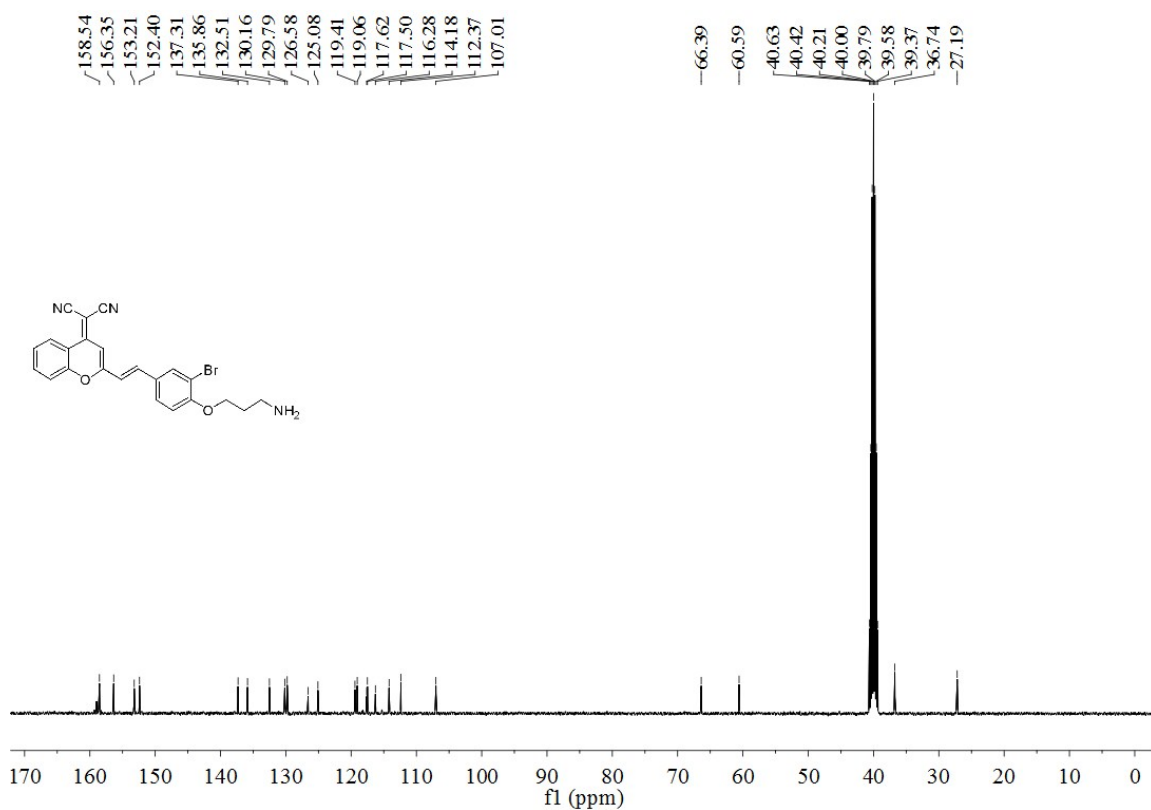


Fig. S65. ¹³C-NMR spectrum of probe 4 (100 MHz, DMSO-*d*₆).

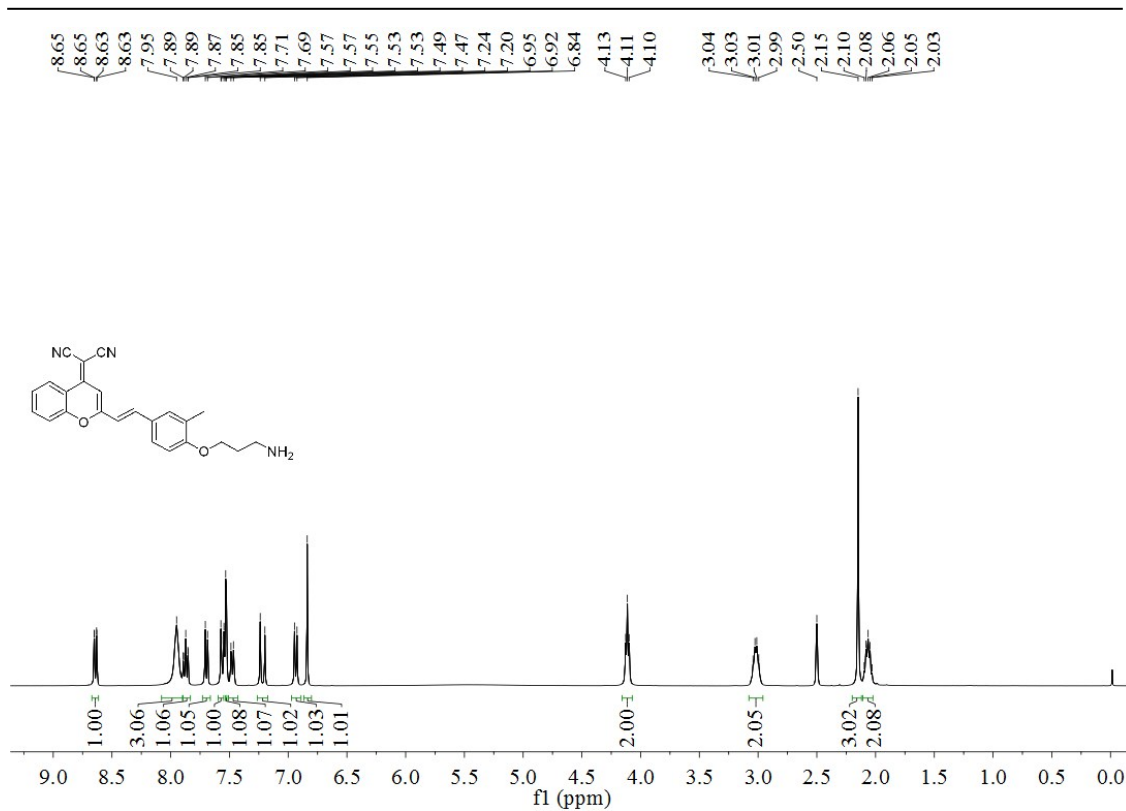


Fig. S66. ¹H-NMR spectrum of probe 5 (400 MHz, DMSO-*d*₆).

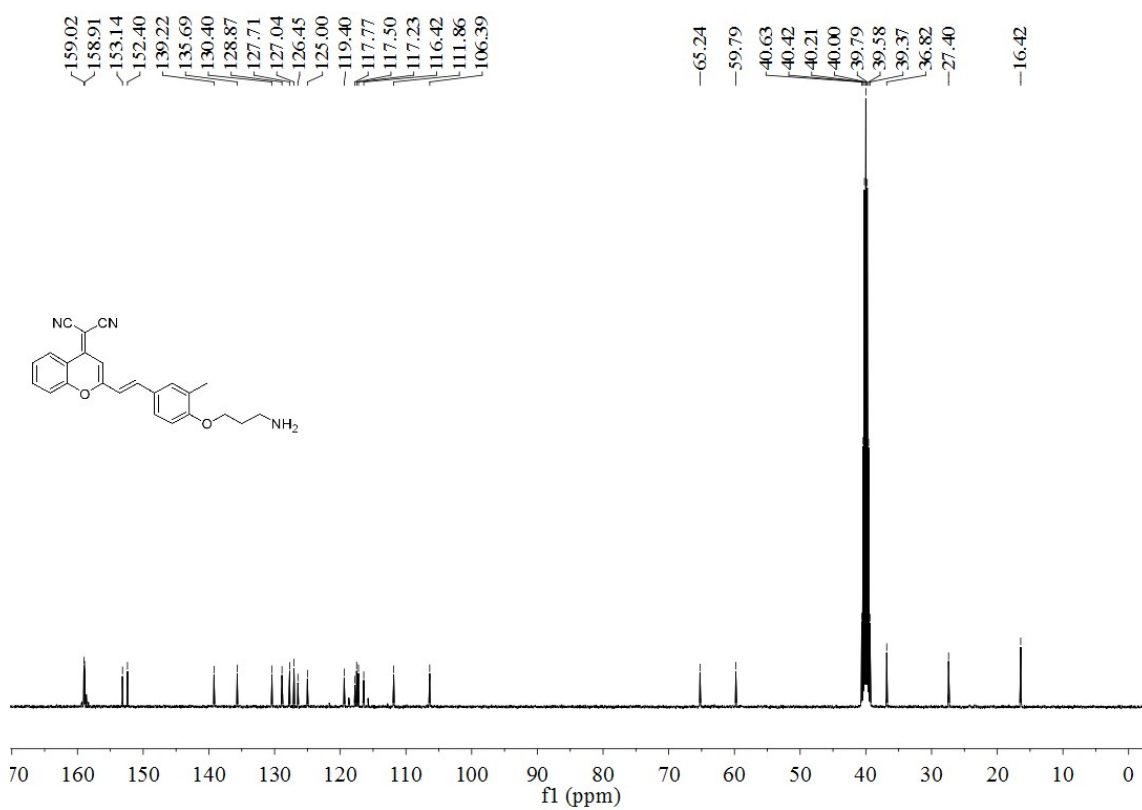


Fig. S67. ¹³C-NMR spectrum of probe 5 (100 MHz, DMSO-*d*₆).

References

1. Z. Li, X. H. Gao, Y. Y. Zhang, W. Shi, H. M. Ma, *Anal. Chem.* 2013, **85**, 3926-3932.
2. a) M. J. Frisch, G. W. Trucks, H. B. Schlegel, G. E. Scuseria, M. A. Robb, J. R. Cheeseman, G. Scalmani, V. Barone, G. A. Petersson, H. Nakatsuji, X. Li, M. Caricato, A. V. Marenich, J. Bloino, B. G. Janesko, R. Gomperts, B. Mennucci, H. P. Hratchian, J. V. Ortiz, A. F. Izmaylov, J. L. Sonnenberg, Williams, F. Ding, F. Lipparini, F. Egidi, J. Goings, B. Peng, A. Petrone, T. Henderson, D. Ranasinghe, V. G. Zakrzewski, J. Gao, N. Rega, G. Zheng, W. Liang, M. Hada, M. Ehara, K. Toyota, R. Fukuda, J. Hasegawa, M. Ishida, T. Nakajima, Y. Honda, O. Kitao, H. Nakai, T. Vreven, K. Throssell, J. A. Montgomery Jr, J. E. Peralta, F. Ogliaro, M. J. Bearpark, J. J. Heyd, E. N. Brothers, K. N. Kudin, V. N. Staroverov, T. A. Keith, R. Kobayashi, J. Normand, K. Raghavachari, A. P. Rendell, J. C. Burant, S. S. Iyengar, J. Tomasi, M. Cossi, J. M. Millam, M. Klene, C. Adamo, R. Cammi, J. W. Ochterski, R. L. Martin, K. Morokuma, O. Farkas, J. B. Foresman, D. J. Fox, *Gaussian 16 Rev. A.03*, Wallingford, CT, 2016. b) Y. Zhao, D. G. Truhlar, *Theor. Chem. Acc.*, 2008, **120**, 215. c) F. Weigend, R. Ahlrichs, *Phys. Chem. Chem. Phys.*, 2005, **7**, 3297. d) L. Yuan, W. Lin, S. Zhao, W. Gao, B. Chen, L. He, S. Zhu, *J. Am. Chem. Soc.*, 2012, **134**, 13510.
3. W. Zhou, M. P. Valley, J. Shultz, E. M. Hawkins, L. Bernad, T. Good, D. Good, T. L. Riss, D. H. Klaubert, K. V. Wood, *J. Am. Chem. Soc.*, 2006, **128**, 3122.
4. A. E. Albers, K. A. Rawls, C. J. Chang, *Chem. Commun.*, 2007, **44**, 4647.
5. X. F. Li, H. T. Zhang, Y. S. Xie, Y. Hu, H. Y. Sun, Q. Zhu, *Org. Biomol. Chem.*, 2014, **12**, 2033.
6. S. Long, L. Chen, Y. Xiang, M. Song, Y. Zheng, Q. Zhu, *Chem. Commun.*, 2012, **48**, 7164.
7. D. Kim, S. Sambasivan, H. Nam, K. H. Kim, J. Y. Kim, T. Joo, K. H. Lee, K. T. Kim, K. H. Ahn, *Chem. Commun.*, 2012, **48**, 6833.
8. Y. Zhang, Y. Xu, S. Tan, L. Xu, X. Qian, *Tetrahedron Lett.*, 2012, **53**, 6881.
9. Y. Xiang, B. He, X. Li, Q. Zhu, *Rsc. Adv.*, 2013, **3**, 4876.
10. X. Li, J. Yu, Q. Zhu, L. Qian, L. Li, Y. Zheng, S. Q. Yao, *Analyst*, 2014, **139**, 6092.
11. L. Li, C. W. Zhang, G. Y. J. Chen, B. W. Zhu, C. Chai, Q. H. Xu, E. K. Tan, Q. Zhu, K. L. Lim, S. Q. Yao, *Nat. Commun.* 2014, **5**, 3176.
12. L. L. Li, K. Li, Y. H. Liu, H. R. Xu, X. Q. Yu, *Sci. Rep-uk.*, 2016, **6**, 31217.
13. R. Wang, X. Han, J. You, F. Yu, L. Chen, *Anal. Chem.*, 2018, **90**, 4054.
14. W. Shen, J. Yu, J. Ge, R. Zhang, F. Cheng, X. Li, Y. Fan, S. Yu, B. Liu, Q. Zhu, *ACS Appl. Mater. Inter.*, 2015, **8**, 927.
15. X. Wu, L. Li, W. Shi, Q. Gong, X. Li, H. Ma, *Anal. Chem.*, 2016, **88**, 1440.
16. X. F. Wu, S. Wen, X. H. Li, H. M. Ma, *Angew. Chem. Int. Ed.*, 2017, **56**, 15319.